EXHAUST GAS CLEANING BY THREE WAY CATALYTIC CONVERTERS

A THESIS SUBMITTED TO
THE GRADUATE SCHOOL OF NATURAL AND APPLIED SCIENCES
OF
MIDDLE EAST TECHNICAL UNIVERSITY

BY

ZUHAL KARAKOÇ YILDIZ

IN PARTIAL FULLFILLMENT OF THE REQUIREMENTS
FOR
THE DEGREE OF MASTER OF SCIENCE
IN
CHEMICAL ENGINEERING

FEBRUARY 2013

Approval of the thesis:

EXHAUST GAS CLEANING BY THREE WAY CATALYTIC CONVERTERS

submitted by **ZUHAL KARAKOÇ YILDIZ** in partial fulfillment of the requirements for the degree of **Master of Science in Chemical Engineering Department, Middle East Technical University** by,

Prof. Dr. Canan Özgen _____
Dean, Graduate School of **Natural and Applied Sciences**

Prof. Dr. Deniz Üner _____
Head of Department, **Chemical Engineering**

Prof. Dr. Işık Önal _____
Supervisor, **Chemical Engineering Dept., METU**

Examining Committee Members:

Assist. Prof. Görkem Külah _____
Chemical Engineering Dept., METU

Prof. Dr. Işık Önal _____
Chemical Engineering Dept., METU

Assoc. Prof. Dr. Ayşen Yılmaz _____
Chemical Engineering Dept., METU

Assist. Prof. Serkan Kıncal _____
Chemical Engineering Dept., METU

Dr. Derya Düzenli _____
General Directorate of Mineral Research and Exploration

Date: 25 / 02 / 2013

I hereby declare that all information in this document has been obtained and presented in accordance with academic rules and ethical conduct. I also declare that, as required by these rules and conduct, I have fully cited and referenced all material and results that are not original to this work.

Name, Last name :

Signature :

ABSTRACT

EXHAUST GAS CLEANING BY THREE WAY CATALYTIC CONVERTERS

KARAKOC YILDIZ, Zuhal
M.S., Department of Chemical Engineering
Supervisor : Prof. Dr. Isık Onal

February 2013, 101 Pages

In this study, powder catalysts slurries are washcoated on cordierite monoliths. CeO_2-ZrO_2 (CZO) and CeO_2-ZrO_2-Al_2O_3 (CZAO) mixed oxides are synthesized by co-precipitation. Pd and Rh metals are used as a nobel metals in these supports. Metal loaded CZO is mixed with gamma phase alumina. Powder catalysts are characterized by XRD, BET, ICP-MS and the monolithic catalysts are imaged by SEM. Catalytic activities of monolithic catalysts are tested in dynamic test system which is computerized and basically composed of gas flow control and conditioning units, split furnace, quartz reactor, mass spectrometer and CO analyzer. Gas mixture containing CO, C_3H_6, C_3H_8, NO, H_2, O_2, CO_2, SO_2, H_2O and N_2 is used to simulate the exhaust gas automotive. O_2 is oscillated at 1 Hz frequency around the stoichiometric condition. Monolithic catalyst in the reactor is heated between 150 ºC and 600 ºC at a rate of 5 ºC/min and then cooled. Gas composition data from mass spectrometer & CO analyzer and temperature data from thermocouple at the monolith entrance, are converted to conversion versus temperature graphs. Catalyst containing co-impregnated support material with metals, showed the lowest loss of catalytic performance after exposure to SO_2 during activity tests. As a result, this catalyst has more resistant than Tofas commercial monolithic catalyst.

Keywords: Catalyst ,Three Way Catalytic Converters, Catalytic Activity

ÖZ

EGZOZ GAZLARININ ÜÇ YOLLU KATALİTİK KONVERTÖRLER İLE TEMİZLENMESİ

Karakoç YILDIZ, Zuhal
Yüksek Lisans, Kimya Mühendisliği Bölümü
Tez Yöneticisi : Prof. Dr. Işık Önal

Şubat 2013, 101 Sayfa

Bu çalışmada, toz katalizörlerin sulu karışımı kordierit monolitlerin üzerine kaplanmıştır. CeO_2-ZrO_2 (CZO) ve CeO_2-ZrO_2-Al_2O_3 (CZAO) karışık oksitleri beraber çöktürme yöntemiyle sentezlenmişlerdir. Pd ve Rh soy metalleri kullanılmıştır. Metal yüklenmiş CZO, gama fazındaki alumina ile karıştırılmıştır. Toz katalizörler XRD, BET, ICP-MS ile karakterize edilmiş ve monolitik katalizörler SEM ile görüntülenmiştir. Monolitik katalizörlerin katalitik aktiviteleri, bilgisayarla donatılmış ve temel olarak gaz akış kontrolü ve şartlandırma üniteleri, split fırın, kuvars reaktör, kütle spektrometresi ve CO analizöründen oluşan test sisteminde test edilmiştir. CO, C_3H_6, C_3H_8, NO, H_2, O_2, CO_2, SO_2, H_2O ve N_2 içeren gaz karışımı benzinli araçların egzoz gazını simule etmek için kullanılmıştır. O_2 gazı stokiometik durum etrafında 1 Hz frekansında salınım yapmıştır. Reaktör içindeki monolitik katalizör 150 ºC ve 600 ºC arasında 5 ºC/dk ile ısıtılıp ve soğutulmuştur. Kütle spektrometre ve CO analizöründen gaz kompozisyon verileri ve monolit girişindeki sıcaklık ölçerden sıcaklık verileri, dönüşüme karşılık sıcaklık grafiklerine dönüştürülmüştür. Beraber çöktürme yöntemiyle soy metal içeren katalizör, aktivite testleri süresince SO_2'ye maruz kaldıktan sonra en düşük katalitik performans kaybını göstermiştir. Bu katalizörler, uygulanan prosedürlere ticari katalizörden daha fazla direnç göstermişlerdir.

Anahtar Sözcükler: Katalizör, Egzos, Üç Yollu Katalitik Konvertörler, Katalitik Aktivite

To My Husband

ACKNOWLEDGEMENT

The present study was carried out in the Department of Chemical Engineering at Middle East Technical University.

I would like to express my deepest gratitude to my supervisor Prof. Dr. Isık Onal for his guidance, advice, criticism, encouragements and insight throughout the research.

It is a pleasure to thank Ministry of Industry and Trade of Turkish Republic and Tofas Turk Otomobil Fabrikası A.S. since this study was funded as SAN-TEZ Project No:00207.STZ.2007-2.

I would like to acknowledge the technical services supported by TERRALAB A.S.

I would also like to thank Duygu Gerceker for her advice and help.

My parents deserve more than I can give in return for their all kinds of supports.

Finally I owe to my husband, Seyfettin, for his endless patience.

TABLE OF CONTENTS

ABSTRACT iv
ÖZ v
ACKNOWLEDGEMENT vi
TABLE OF CONTENTS viii
LIST OF TABLES x
LIST OF FIGURES xi
LIST OF SYMBOLS xiv
LIST OF ABBREVIATIONS xv
CHAPTERS 1
1. INTRODUCTION 1
1.1 Automotive Exhaust Gases 1
1.2 Three Way Catalytic Reactions 1
1.3 Air to Fuel Ratio 2
1.4 The Light – Off (T50) Temperature 2
1.5 Structure of Three Way Catalytic Converters in Automotive 2
1.6 Components of Three Way Catalyst 3
1.7 Objective of the Study 3
2. LITERATURE SURVEY 5
2.1 Support Material of Three Way Catalyst 5
2.2 Monolith Coating 5
2.3 Catalytic Activity Measurements of Three Way Catalyst 5
3. EXPERIMENTAL 9
3.1 Powder Catalyst Preparation 9
3.1.1 Support Materials Preparation 9
3.1.2 Impregnation of Nobel Metals 10
3.2 Monolith Coating 11
3.2.1 Preparation of Pseudoboehmite 11
3.2.2 Preparation of Washcoating Slurry 11
3.2.3 Preparation of Monolith Coating 12
3.2.4 Catalyst Characterizations 12
3.3 Catalyst Activity Tests in Dynamic Test System 12
3.3.1 Dynamic Test System Description 12
3.3.2 Catalytic Activity Test Description 15
3.3.3 The Effect of SO_2 During Catalytic Activity Tests 16
3.4 Calibrations 16
3.4.1 Mass Flow Controller Calibrations 17
3.4.2 Mass Spectrometer Calibrations 17
4. CHARACTERIZATIONS 19
4.1 Support Materials 19
4.1.1 Characterizations of CZO and CZAO Support Materials 19
4.2 Metal Loaded Catalyst Powders 20
4.2.1 Characterizations of Metal Loaded Catalyst 21
5. CATALYTIC ACTIVITY TESTS 25
6. CONCLUSIONS 59
REFERENCES 61
APPENDICES 65

A. CATALYST PREPARATION 65
A.1 Preparation of Ceria – Zirconia Mixed Oxide 65
A.2 Preparation of Pseudoboehmite 65
A.3 Addition of Metals 65
A.4 Preparation of Washcoating Slurry 66
B. CATALYTIC ACTIVITY TEST CALCULATIONS 67
B.1 Mass Simulated Exhaust Gas Flow Rate Calculation 67
B.2 Exhaust Gas Composition 68
B.3 Water Content in The Simulated Exhaust Gas Composition 71
B.4 Analysis of Catalytic Activity Test Data 72
B.4.1 Mass CO Analyzer Data Calculations 72
B.4.2 MS Data Calculations 72
C. CALIBRATIONS 75
C.1 Mass Flow Controller Calibrations 75
C.2 Mass Spectrometer Calibrations 81
C.2.1 Mass Spectrometer Calibration 81
D. CATALYTIC ACTIVITY TEST RESULTS 85
D.1 Catalytic Activity Tests Without SO2, Research Monolithic Catalyst 85
D.2 Catalytic Activity Tests With SO2, Research Monolithic Catalyst 89
D.3 Catalytic Activity Tests Without SO2, Tofas Commercial Monolithic Catalyst 92
D.4 Catalytic Activity Tests With SO2, Tofas Commercial Monolithic Catalyst 96
E. ESTIMATION OF PARTICLE SIZE AND XRD DIFFRACTOGRAMS 99
E.1 Particle Size 99
E.2 XRD Diffractograms of Fresh Powdered Slurries of Catalysts 100

LIST OF TABLES

Table 1. 1 The Three Way Catalytic Converters Reactions (Kaspar et al., 2003a) 2
Table 3. 1 Powder Catalysts List 10
Table 3. 2 Monolithic Catalysts List 12
Table 3. 3 Simulated Exhaust Gas Mixture Composition with SO_2 15
Table 3. 4 Simulated Exhaust Gas Mixture Composition without SO_2 16
Table 4. 1 BET Surface Areas of CZO and CZAO Support Materials 20
Table 4. 2 Powder Catalysts List 21
Table 4. 3 BET Surface Area of The Powder Catalysts 21
Table 4. 4 ICP-MS Results of The Powder Catalysts 22
Table 4. 5 Total Loaded Metal Content 22
Table 5. 1 Heating/Cooling Catalytic Activity Data of Research Monolithic Catalyst 26
Table 5. 2 Catalytic Activity Data of Research Catalyst During Test 1 30
Table 5. 3 Catalytic Activity Data of Tofas Commercial Monolith Catalyst During Test 1 34
Table 5. 4 Catalytic Activity Data of Tofas Commercial Monolith Catalyst & Research Monolithic Catalyst During Test1 37
Table 5. 5 Catalytic Activity Data of Research Monolith Catalyst During Test1 &Test4 39
Table 5. 6 Catalytic Activity Data of Tofas COM Monolith Catalyst During Test1 & Test 4 47
Table 5. 7 Catalytic Activity Data of Tofas COM1 and COM2 Monolithic Catalysts 55
Table B.2. 1 Simulated Exhaust Gas Mixture Composition 68
Table B.2. 2 Cylinder Compositions 69
Table B.2. 3 Flow Rates of Cylinders Gas Compositions for Reducing, Stoichiometric and Oxidizing Conditions 69
Table B.2. 4 Simulated Gas Mixture Composition for Reducing, Stoichiometric and Oxidizing Conditions 70
Table C1. 1 MFC Gas Correction Factors 75
Table C1. 2 Calibration Data for Mix MFC 76
Table C1. 3 Calibration Data for NO MFC 77
Table C1. 4 Calibration Data for SO_2 MFC 78
Table C1. 5 Calibration Data for O_2 MFC 79
Table C1. 6 Calibration Data for N_2 MFC 80
Table C2. 1 O_2 MS Calibration Data 81
Table C2. 2 NO MS Calibration Data 82
Table C2. 3 C_3H_6 MS Calibration Data 82
Table C2. 4 C_3H_8 MS Calibration Data 83
Table C2. 5 H_2 MS Calibration Data 84
Table C2. 6 Calibration Equations for MS Calibration 84

LIST OF FIGURES

Figure 1. 1 Diagram of a Typical Catalytic Converter (1) & Metallic Honeycomb Monolith(2) (Kaspar et al., 2003a)..... 3
Figure 3. 2 Dynamic Test System..... 14
Figure 4. 1 XRD patterns of CZO Support Material..... 19
Figure 4. 2 XRD patterns of CZAO Support Material..... 20
Figure 4. 3 SEM Images of Research Monolithic Catalyst..... 23
Figure 4. 4 SEM Images of Research Monolithic Catalyst..... 23
Figure 4. 5 SEM Images of Research Monolithic Catalyst..... 24
Figure 5. 1 C_3H_8 Catalytic Activity of (CZO-SI) / (AO-SI) Monolithic Catalyst..... 27
Figure 5. 2 C_3H_6 Catalytic Activity of (CZO-SI) / (AO-SI) Monolithic Catalyst..... 27
Figure 5. 3 NO Catalytic Activity of (CZO-SI) / (AO-SI) Monolithic Catalyst..... 28
Figure 5. 4 H_2 Catalytic Activity of Fresh (CZO-SI) / (AO-SI) Monolithic Catalyst..... 28
Figure 5. 5 O_2 Catalytic Activity of (CZO-SI) / (AO-SI) Monolithic Catalyst..... 29
Figure 5. 6 CO Catalytic Activity of (CZO-SI) / (AO-SI) Monolithic Catalyst..... 29
Figure 5. 7 CO Catalytic Activity of (CZO-SI) / (AO-SI) Monolithic Catalyst During Test1..... 30
Figure 5. 8 NO Catalytic Activity of (CZO-SI) / (AO-SI) Monolithic Catalyst During Test1..... 31
Figure 5. 9 C_3H_6 Catalytic Activity of (CZO-SI) / (AO-SI) Monolithic Catalyst During Test 1. 31
Figure 5. 10 C_3H_8 Catalytic Activity of (CZO-SI) / (AO-SI) Monolithic Catalyst During Test 132
Figure 5. 11 H_2 Catalytic Activity of (CZO-SI) / (AO-SI) Monolithic Catalyst During Test 1... 32
Figure 5. 12 O_2 Catalytic Activity of (CZO-SI) / (AO-SI) Monolithic Catalyst During Test 1 .. 33
Figure 5. 13 CO Catalytic Activity of Tofas COM Monolithic Catalyst During Test1..... 34
Figure 5. 14 NO Catalytic Activity of Tofas COM Monolithic Catalyst During Test1..... 35
Figure 5. 15 C_3H_6 Catalytic Activity of Tofas COM Monolithic Catalyst During Test 1 35
Figure 5. 16 C_3H_8 Catalytic Activity of Tofas COM Monolithic Catalyst During Test 1 36
Figure 5. 17 H_2 Catalytic Activity of Tofas COM Monolithic Catalyst During Test 1 36
Figure 5. 18 O_2 Catalytic Activity of Tofas COM Monolithic Catalyst During Test 1..... 37
Figure 5. 19 CO Catalytic Activity of (CZO-SI) / (AO-SI) Monolithic Catalyst During Tests 1, 2, 3 & 4..... 38
Figure 5. 20 CO Catalytic Activity of (CZO-SI) / (AO-SI) Monolithic Catalyst During Tests 1 & 4 39
Figure 5. 21 NO Catalytic Activity of (CZO-SI) / (AO-SI) Monolithic Catalyst During Tests 1, 2, 3 & 4 40
Figure 5. 22 NO Catalytic Activity of (CZO-SI) / (AO-SI) Monolithic Catalyst During Tests 1 & 4 41
Figure 5. 23 C_3H_6 Catalytic Activity of (CZO-SI) / (AO-SI) Monolithic Catalyst During Tests 1, 2, 3 & 4 41
Figure 5. 24 C_3H_6 Catalytic Activity of (CZO-SI) / (AO-SI) Monolithic Catalyst During Tests 1, & 4 42
Figure 5. 25 CO Catalytic Activity of (CZO-SI) / (AO-SI) Monolithic Catalyst During Tests 1, 2, 3 & 4 42
Figure 5. 26 CO Catalytic Activity of (CZO-SI) / (AO-SI) Monolithic Catalyst During Tests 1 & 4 43
Figure 5. 27 C_3H_8 Catalytic Activity of (CZO-SI) / (AO-SI) Monolithic Catalyst During Tests 1, 2, 3 & 4 43
Figure 5. 28 C_3H_8 Catalytic Activity of (CZO-SI) / (AO-SI) Monolithic Catalyst During Tests 1 & 4 44

Figure 5. 29 H_2 Catalytic Activity of (CZO-SI) / (AO-SI) Monolithic Catalyst During Tests 1, 2, 3 & 4 44
Figure 5. 30 H_2 Catalytic Activity of (CZO-SI) / (AO-SI) Monolithic Catalyst During Tests 1 & 4 45
Figure 5. 31 O_2 Catalytic Activity of (CZO-SI) / (AO-SI) Monolithic Catalyst During Tests 1, 2, 3 & 4 45
Figure 5. 32 O_2 Catalytic Activity of (CZO-SI) / (AO-SI) Monolithic Catalyst During Tests 1 & 4 46
Figure 5. 33 ΔT50 (˚C) of (CZO-SI) / (AO-SI) Monolithic Catalyst During Tests 1 & 4 46
Figure 5. 34 ΔT50 (˚C) of Tofas Monolithic Catalyst During Tests 1 & 4 48
Figure 5. 35 C_3H_8 Catalytic Activity of Tofas COM Monolithic Catalyst During Tests 1, 2, 3 & 4 48
Figure 5. 36 C_3H_8 Catalytic Activity of Tofas COM Monolithic Catalyst During Tests 1 & 4 49
Figure 5. 37 CO Catalytic Activity of Tofas COM Monolithic Catalyst During Tests 1, 2, 3 & 4 49
Figure 5. 38 CO Catalytic Activity of Tofas COM Monolithic Catalyst During 50
Figure 5. 39 C_3H_6 Catalytic Activity of Tofas COM Monolithic Catalyst During 50
Figure 5. 40 C_3H_6 Catalytic Activity of Tofas COM Monolithic Catalyst During 51
Figure 5. 41 NO Catalytic Activity of Tofas COM Monolithic Catalyst During 51
Figure 5. 42 NO Catalytic Activity of Tofas COM Monolithic Catalyst During 52
Figure 5. 43 H_2 Catalytic Activity of Tofas COM Monolithic Catalyst During 52
Figure 5. 44 H_2 Catalytic Activity of Tofas COM Monolithic Catalyst During 53
Figure 5. 45 O_2 Catalytic Activity of Tofas COM Monolithic Catalyst During 53
Figure 5. 46 O_2 Catalytic Activity of Tofas COM Monolithic Catalyst During 54
Figure 5. 47 CO Catalytic Activity of Tofas COM1 & Tofas COM2 Monolithic Catalyst 56
Figure 5. 48 NO Catalytic Activity of Tofas COM1 & Tofas COM2 Monolithic Catalyst 56
Figure 5. 49 C_3H_6 Catalytic Activity of Tofas COM1 & Tofas COM2 Monolithic Catalyst 57
Figure 5. 50 C_3H_8 Catalytic Activity of Tofas COM 1 & Tofas COM2 Monolithic Catalyst 57
Figure 5. 51 H_2 Catalytic Activity of Tofas COM1 & Tofas COM2 Monolithic Catalyst 58
Figure 5. 52 O_2 Catalytic Activity of Tofas COM1 & Tofas COM2 Monolithic Catalyst 58
Figure C.1. 1Calibration Graph for Mix MFC 76
Figure C.1. 2 Calibration Graph for NO MFC 77
Figure C.1. 3 Calibration Graph for SO_2 MFC 78
Figure C.1. 4 Calibration Graph for O_2 MFC 79
Figure C.1. 5 Calibration Graph for N_2 MFC 80
Figure C.2. 1 O_2 MS Calibration Graph 81
Figure C.2.2 NO MS Calibration Graph 82
Figure C.2. 3 C_3H_6 MS Calibration Graph 83
Figure C.2. 4 C_3H_8 MS Calibration Graph 83
Figure C.2. 5 H_2 MS Calibration Graph 84
Figure D.1.1 C_3H_8 Catalytic Activity of Research Monolithic Catalyst During Tests 1 & 4 85
Figure D.1. 2 C_3H_6 Catalytic Activity of Research Monolithic Catalyst During Tests 1 & 4 86
Figure D.1. 3 NO Catalytic Activity of Research Monolithic Catalyst During Tests 1 & 4 86
Figure D.1. 4 H_2 Catalytic Activity of Research Monolithic Catalyst During Tests 1 & 4 87
Figure D.1. 5 O_2 Catalytic Activity of Research Monolithic Catalyst During Tests 1 & 4 87
Figure D.1. 6 CO Catalytic Activity of Research Monolithic Catalyst During Tests 1 & 4 88
Figure D.2. 1 C_3H_8 Catalytic Activity of Research Monolithic Catalyst During Tests 2 & 3 89
Figure D.2. 2 C_3H_6 Catalytic Activity of Research Monolithic Catalyst During Tests 2 & 3 89
Figure D.2. 3 NO Catalytic Activity of Research Monolithic Catalyst During Tests 2 & 3 90
Figure D.2. 4 H_2 Catalytic Activity of Research Monolithic Catalyst During Tests 2 & 3 90
Figure D.2. 5 O_2 Catalytic Activity of Research Monolithic Catalyst During Tests 2 & 3 91
Figure D.2. 6 CO Catalytic Activity of Research Monolithic Catalyst During Tests 2 & 3 91
Figure D.3. 1 C_3H_8 Catalytic Activity of Tofas COM Monolithic Catalyst During Tests 1 & 4 92
Figure D.3. 2 C_3H_6 Catalytic Activity of Tofas COM Monolithic Catalyst During Tests 1 & 4 93

Figure D.3. 3 NO Catalytic Activity of Tofas COM Monolithic Catalyst During 93
Figure D.3. 4 H_2 Catalytic Activity of Tofas COM Monolithic Catalyst During Tests 1 & 4 ... 94
Figure D.3. 5 O_2 Catalytic Activity of Tofas COM Monolithic Catalyst During Tests 1 & 4 ... 94
Figure D.3. 6 CO Catalytic Activity of Tofas COM Monolithic Catalyst During Tests 1 & 4 ... 95
Figure D.4. 1 C_3H_8 Catalytic Activity of Tofas COM Monolithic Catalyst During Tests 2 & 3 96
Figure D.4. 2 C_3H_6 Catalytic Activity of Tofas COM Monolithic Catalyst During Tests 2 & 3 96
Figure D.4. 3 NO Catalytic Activity of Tofas COM Monolithic Catalyst During Tests 2 & 3 ... 97
Figure D.4. 4 H_2 Catalytic Activity of Tofas COM Monolithic Catalyst During Tests 2 & 3 97
Figure D.4. 5 O_2 Catalytic Activity of Tofas COM Monolithic Catalyst During Tests 2 & 3 98
Figure D.4. 6 CO Catalytic Activity of Tofas COM Monolithic Catalyst During Tests 2 & 3 ... 98
Figure E.2. 1 XRD Diffractograms of (CZO-SI) / (AO-SI) Monolithic Catalyst 100
Figure E.2. 2 XRD Diffractogram of Tofas Commercial Monolithic Catalyst 101

LIST OF SYMBOLS

Symbol	Definition	Units
A, B, C	Antoine Equation Constants	-
C_{A_0}	İnitial Concentration	ppm
C_A	İnstant Concentration	ppm
P^{sat}	Saturation Pressure	torr
S	Stoichiometric Number	-
T	Temperature	ºC
V_{eff}	Effective Volume	cm^3
T50	Light-off Temperature	ºC
X	Conversion	%
γ	Gamma Phase	-
ν_0	Flow Rate	mL/min

LIST OF ABBREVIATIONS

AO	Aluminum Oxide
A/F	Air to Fuel Ratio
CZAO	Cerium Zirconium Aluminum Oxide
CZO	Cerium Zirconium Oxide
GHSV	Gas Hourly Space Velocity
HC	Hydrocarbon
HDPE	High Density Polyethylene
MFC	Mass Flow Controller
MS	Mass Spectrometer
NOx	Nitrogen Oxides
OSC	Oxygen Storage Capacity
TWC	Three Way Catalyst
w/o	Without

CHAPTER 1

INTRODUCTION

1.1 Automotive Exhaust Gases

Air pollution occurs due to the combustion of fuels in automotive engines. After burning of hydrocarbon (HC), water and carbon dioxide are formed. However, high temperatures and non-perfect combustion cause high amounts of pollutants in the exhaust gases. Automotive exhaust gases contain unburned carbon monoxide, hydrocarbons and nitrogen oxides, mostly NO, water, hydrogen, nitrogen, oxygen, etc. Due to the world attention on air pollution and environmental legislations, harmful compounds limits in exhaust gases become more tight (Kaspar et al., 2003) [15]. Thus, three way catalytic converters (TWCs) are designed. Harmful HCs, CO and NOx are converted simultaneously and efficiently into partially harmless CO_2, H_2O and N_2 by TWCs (Ulla, 2003) [29].

1.2 Three Way Catalytic Reactions

Exhaust gases from the gasoline vehicles have harmful effects on the environment. These compounds are originated by incomplete combustion of fuel. The major exhaust pollutants are nitrogen oxides, carbon monoxide and hydrocarbons. Moreover, it includes combustion products as nitrogen, water, oxygen, hydrogen and carbon dioxide and sulphur oxides from the sulphur in the fuel (Kaspar et al., 2003a; Ulla, 2003) [16, 29]. Three way catalytic converters can play an important role to convert destructive CO, NOx and HCs into non-destructive CO_2, N_2 and H_2O (Ulla, 2003) [29].
Both the reduction and oxidation reactions occurs in the catalytic converter as many other side reactions. General three way catalytic reactions on the three way catalytic converter are given in Table 1.1.

Table 1. 1 The Three Way Catalytic Converers Reactions (Kaspar et al., 2003a) [16]

Oxidation	$2CO + O_2 \rightarrow 2CO_2$ $4C_mH_n + (4m+n)\ O_2 \rightarrow 4mCO_2 + 2nH_2O$ $2H_2 + O_2 \rightarrow 2HO_2$
Reduction	$2CO + 2NO \rightarrow 2CO_2 + N_2$ $4C_mH_n + (8m+2n)\ NO \rightarrow (4m+n)N_2 + 4mCO_2 + 2nH_2O$ $2H_2 + 2NO \rightarrow 2H_2O + N_2$
Water Gas Shift	$CO + H_2O \rightarrow CO_2 + H_2$
Steam Reforming	$4\ C_mH_n + 4mH_2O \rightarrow 2mCO_2 + (4m+n)H_2$

1.3 Air to Fuel Ratio

Air to fuel ratio (A/F) determines emissions from automobiles. Under fuel lean conditions NOx emissions are reduced due to the lower combustion temperatures. On the other hand, under fuel rich conditions contain higher amounts of fuel and higher power is obtained. Higher A/F ratios cause higher HC emissions. High conversion rates of pollutants is achieved at 14.6 which is called as stoichiometric condition (Kaspar et al., 2003a; Fornasiero et al., 2008) [16, 10]. O_2 sensor is used to control A/F ratio in the engine. Oscillation of oxygen is around the stoichiometric window at a frequency of 0.5 or 1 Hz (Farrauto & Heck, 1999) [8].

1.4 The Light – Off (T50) Temperature

The temperature at which a reactant conversion is 50% is defined as light-off temperature (Noh et al., 1999) [21]. A typical light –off behavior of a three way catalyst (TWC) is plotted as conversion vs. temperature curves (Kaspar & Fornasiero, 2003) [15, 10]. The performance of TWC is determined by the light-off temperature. Higher TWC activity and performance is at lower light-off temperature (Di Monte et al., 2002; Yucai, 2006) [7, 32].

1.5 Structure of Three Way Catalytic Converters in Automotive

TWC includes a stainless steel container and a honeycomb cordierite monolith. The efficiency of catalytic converters is determined by honeycomb monolith. TWC work at strong heat and mass transfer conditions to get high conversion. TWC are made of either ceramic or metal cordierite. The metal monoliths have advantages with low heat capacity, thinner wall thickness and high thermal conductivity. On the other hand, ceramic monoliths are porous, easy washcoating and lower production cost. The monolith is coated by dipping into the washcoating slurry. The excess washcoat materials are carried out with air. Lastly, the

washcoated monolith is calcined to obtaine the three way catalyst. (Kaspar et al., 2003a) [16].

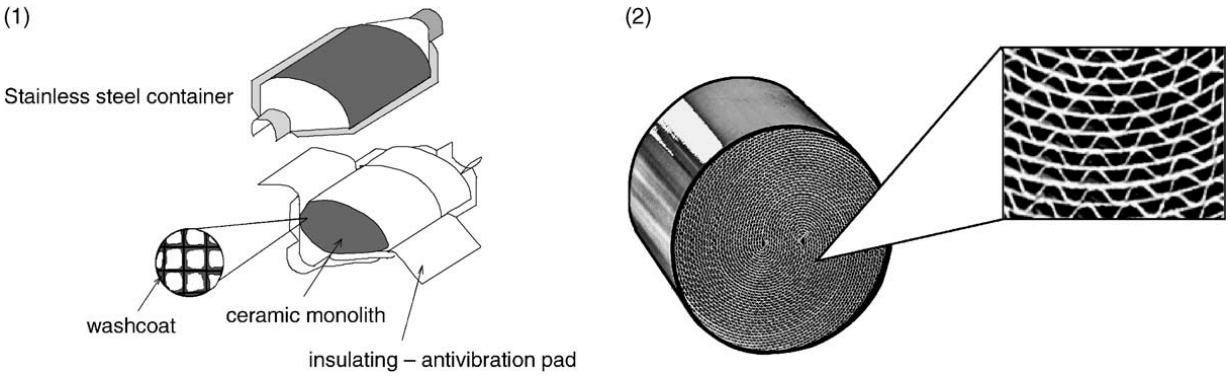

Figure 1. 1 Diagram of a Typical Catalytic Converter (1) & Metallic Honeycomb Monolith(2) (Kaspar et al., 2003a) [16]

1.6 Components of Three Way Catalyst

TWCs mainly include CZO, noble metals, stabilizers and □-alumina,. □-alumina is used to increase surface area of honeycomb monolith for dispersing of noble metals. Moreover, □-alumina provides high stability against the hydrothermal conditions. Stabilizers also increase the surface stability (Kaspar et al., 2003a) [16]. Cerium oxide provides oxygen storage capacity (OSC), increases the thermal stability of alumina support, stabilizes the noble metal dispersion, promotes the water-gas shift and steam reforming reactions at low temperatures and (Kaspar et al., 2003a; Yao et al., 1997) [16, 30]. Zirconium oxide is used to increase the thermal stability of cerium oxide, low temperature catalytic activity and OSC (Yingying et al., 2007) [31].

1.7 Objective of the Study

The aim of this study is to improve TWCs which have low light-off temperatures. The light-off temperatures of the catalysts are determined by performing using simulated exhaust gas in the dynamic catalytic activity tests system. Many powder catalysts are produced with different noble metal combinations and coated on cordierite monoliths to get monolithic catalysts. In the dynamic test system, the catalytic activities of the monolithic catalysts are evaluated. Aim of synthesizing different monolithic catalysts is to analyze impregnation of noble metal position and evaluate the importance of physical separation of noble metals on catalytic activity according to dynamic test data. During the dynamic test the effect of SO_2 on monolithic catalysts is also analyzed. This dynamic test program is also applied on Tofas commercial monolithic catalyst. The data are evaluated with developed research catalysts.

CHAPTER 2

LITERATURE SURVEY

2.1 Support Material of Three Way Catalyst

It is proved that noble metals can process the highest conversions of harmful pollutants with the OSC of TWC by Kaspar and Fornasiero (2003) [10]. The main oxygen storage/release components are CeO_2-ZrO_2 mixed oxides. However, OSC property is lost at high temperature by sintering of CeO_2-ZrO_2 mixed oxides. So oxygen storage components with high thermal stability are needed. Therefore, TWCs contain CeO_2-ZrO_2 mixed oxides because of their ability of highest pollutant conversions and high thermal stability.

It is stated that the ZrO_2 doped CeO_2 has high OSC and catalytic activity by Di Monte et al. (1998) [7]. CeO_2-ZrO_2 mixed oxides have high oxygen mobility in the bulk of the solid solution.

$Ce_xZr_{1-x}O_2$ mixed oxides have high thermal stability which are with "x" value larger than 0.5 indicated by Rossignol et al. (1999a) [24]. In addition to this, the $Ce_{0.75}Zr_{0.25}O_2$ mixed oxide has improved thermal stability and promoted OSC by Rossignol et al. (1999b) [25].

2.2 Monolith Coating

The three way catalyst converters are mostly placed in ceramic monoliths which are made of cordierite ($2MgO.2Al_2O_3.5SiO_2$). Cordierite monoliths have ability of mechanical strength and low thermal expansion coefficient. Thus, the cordierites are resistant against high temperatures and high temperature differences. Density of monolith is up to 900 cells/in^2. They are washcoated with slurry of powder catalyst by dipcoating. After dipcoating, cordierite monolith is shaken and cleaned by pressurized air. Then monolith is dried and calcined to have a stable coating. To fix coating binding agents are used. The amount of binder in the slurry is nearly 10 wt% and the total solid content is 40-50 wt% in the slurry (Nijhuis et al., 2001) [20].

2.3 Catalytic Activity Measurements of Three Way Catalyst

The pellet size of catalysts are measured for isothermal activity and light-off temperature by Beck et al. (1994) [3]. The feed-stream compositions are simulated the exhaust gases compositions. Propylene represents the hydrocarbons in emission gases because in the exhaust gases the abundant hydrocarbon species are alkenes. Firstly, the simulated exhaust gases are stabilized with nitrogen at 600 ºC, then it is cooled up to 100 ºC at a rate of 20 ºC/min for evaluating catalytic activity of catalysts.

Gonzales-Velasco et al. (2001) [13] measured the pellet size catalysts by performing four different activity measurement around the stoichiometric windows and evaluated performance of steam reforming and the water gas shift. The steam was taken out from product gases and the remaining product gases were analyzed. Before starting the light-off

tests, the gas compositions are subject to N_2 flow at 100 ºC for 4h. Then the sample gases are heated up to 600 ºC with a rate of 3 ºC/min. During the cycled light-off tests, the feed stream is between the oxidizing and reducing conditions around the stoichiometric condition. For the stoichiometric window, A/F ratio is changed and the nitrogen containing compounds conversions and selectivity are measured at 500 ºC. At each conditions, the conversion is measured up to 500 ºC.

Agrafiotis et al.(2001) [2] studied coated honeycombs. Activity tests were performed in a tubular oven which was heated up to 700 ºC at a rate of 3 ºC/min, then the activity tests were performed at 700 ºC for 30 min. The simulated gas mixture contained toluene, methane, ethylene, ethane, pentane and benzene. Lastly, the product gases were analyzed.

Lambrou et al.(2004) [17] determined the effects of aging of a commercial Pd-Rh (9:1, w/w) TWC, OSC and the redox properties of washcoating supports. A lot of fresh and aged commercial TWCs were used. The samples were cut out from the up and down monolith of a Ford Cougar 2.5 V6. It was determined that the OSC of the TWC decreases with catalyst aging in the 0–56,000 km range at 500–750 ºC. The fresh commercial three way catalytic activities were analyzed with the compositions of 20 ppm SO_2 or 10% CO_2 in 1.5% O_2/He gas mixture.

Shinjoh et al. (2004) [26] studied on NOx reduction behavior of Pt, Pd, and Rh containing catalysts. Catalytic activities were evaluated on a fixed bed flow reactor from 200 ºC to 500 ºC. The product gas was sent to condenser to move the water vapor, then they were analyzed. CO and CO_2 were analyzed by nondispersive infrared, HCs were analyzed by flame ionization, SO_2 was analyzed by flame photometry, O_2 was analyzed by magnetic susceptibility and NOx was analyzed by chemiluminescence. Catalytic activity of Pt, Pd, and Rh containing three way catalysts were mainly measured as a temperature and O_2 concentration.

Lassi et al. (2004) [18] considered deactivation of Pd/Rh monoliths. The catalysts contained Pd, Rh supported on □-Al_2O_3. The washcoat also included CeO_2, La_2O_3 and $Ce_XZr_{(1-X)}O_2$ mixed oxides as stabilizers and promoters. The catalysts were dried at 100–150 ºC and then calcined at 300–550 ºC. Pd/Rh monoliths were aged at 800– 1200 ºC temperatures in the exhaust gas streams.

Rajasree et al. (2004) [23] studied the kinetics of CO oxidation by O_2. Pd-TWCs also contained alumina. Experiments were performed in a fixed bed reactor at 573 K with and without H_2O and CO_2 in the feed. The feed compositions were changed periodically between 1 vol% CO in He and 0.5 vol% O_2 in He with a frequency of 1/30 Hz. Presence of H_2O experiments were carried out 14 vol% water as a real exhaust gas compositions. The reaction rate was increased with presence of water, but it was restricted by CO_2. According to the experimental results, the transient kinetic model of this catalyst was improved. It was determined that bulk diffusion of oxygen in ceria becomes important, when the rate is improved by water. Lower amount of oxygen-storage site inhibits CO_2 oxidation.

Granados et al. (2005) [14] used fixed bed flow reactors for commercial TWCs.The concentration of O_2, CO and H_2 were cycled at 1 Hz. The feed concentrations were 10% v/v H_2O, 10% v/v CO_2, 900 ppm NO, 900 ppm C_3H_6 and H_2, CO, O_2 concentrations were oscillated between 0.13–0.53%, v/v H_2, 0.4–1.6%, v/v CO and 0.77–1.37%,v/v O_2. Experiments were performed out up to 700 ºC at a rate of 5 ºC/min. The product gases were evaluated by quadrupole mass spectrometer for C_3H_6 , H_2 and O_2,by dispersive infrared detectors for CO and CO_2, and by paramagnetic detector for O_2, by chemiluminescence detector for NO.

Pt-Rh coated catalysts were analyzed under stoichiometric windows by Suopanki et al. (2005) [27]. The gas composition was 125 ppm C_3H_8, 1500 ppm NO, 1% CO, 375 ppm C_3H_6,

0.65% O_2 (0.22% at 1 Hz), 10% H_2O, 10% CO_2, balance N_2.The fresh catalyst experiment was carried out up to 400 ºC at a rate of 11.5 ºC/min. Then, catalysts were aged in a muffle furnace at atmospheric pressure for 3h at 1000 ºC or 900 ºC. It was stated that the highest oxidation activity for fresh catalysts was achieved with Pt and Rh catalysts. Pt-Rh TWCs had the highest activity in carbonmonoxide and hydrocarbon oxidation and nitrogen oxide reduction reactions after ageing.

CHAPTER 3

EXPERIMENTAL

In this study, experimental part is divided into the two sections. In the first section, powder catalysts are synthesized and characterized. After choosing active powder catalyst according to characterization results, these catalysts are washcoated on cordierite monoliths. In the second section, monolithic catalysts' activities are characterized by Dynamic Test System as a fresh without SO_2 composition and with SO_2 composition in the feed stream.

3.1 Powder Catalyst Preparation

In this first section, powder catalysts are prepared and characterized. Firstly, powder catalysts are prepared using support materials and precious metal. Secondly, slurry of powder catalysts are prepared with binder material and nitric acid. Preparation of powder catalysts, support and binder material, addition of precious metal and washcoating monolith are described below in more details.

3.1.1 Support Materials Preparation

3.1.1.1 Ceria-Zirconia Mixed Oxide (CZO) Preparation

Ceria-zirconia mixed oxide (CZO) solid solution with composition $Ce_{0.8}Zr_{0.2}O_2$ are prepared by co-precipitation technique defined by Gernnari's et al. (2008) [12]. In the co-precipitation technique, ceria- zirconia mixed oxides with Ce/Zr atomic ratio of 4/1 are synthesized with an aqueous solution of and zirconyl nitrate hexahydrate ($N_2O_7Zr.aq$) (Fluka, ~ 27% Zr (gravimetric)) and cerium (III) nitrate hexahydrate ($CeN_3O_9.6H_2O$) (Aldrich, 99%)). For the complete cerium oxidation reaction, hydrogen peroxide (H_2O_2 (J. T. Baker, 30% v/v)) is added and hold on vigorous stirring for 1h. The mixture is added drop wisely into the excess ammonium hydroxide solution (NH_4OH) (Aldrich, 33% NH_3) and hold 12h for complete precipitation. The solution is filtered, and suspended into iso-propanol ($CH_3CHOHCH_3$) (J. T. Baker). Later, the solution is stirred and refluxed for 6h. Finally, the product is dried at 150 °C for 12h, grounded and calcined in an oven in dry air for 3h at 500 °C with a heating rate of 5°C/min.

3.1.1.2 Ceria-Zirconia-Alumina Mixed Oxide (CZAO) Preparation

Firstly, CZO is synthesized by co-precipitation technique. The mixed oxide is milled for 8h at 275 rpm. For milling mixed oxide, 3 mm alumina mills are added 33 vol% mixture. Secondly, CZO is mixed with gamma phase aluminum oxide (γ-Al_2O_3) (AO) in deionized water as 40% solid content. Ce is 19 wt% of the total and pseudoboehmite is 10 wt% γ-Al_2O_3 . Aluminum oxide (γ-Al_2O_3)(AO) is milled for 8h at 275 rpm as CZO. These two solution is mixed and milled for 3h at 275 rpm. Lastly, the mixture is dried at 150 °C for 12h, grounded and calcined in an oven in dry air for 3h at 500 °C with a heating of 5 °C/min.

3.1.2 Impregnation of Nobel Metals

Impregnation method is used to add metal to support materials which are synthesized by co-precipitation (CZO), (CZAO), or gamma phase aluminum oxide (AO).

In the beginning of the study, impregnation of different metal combinations on support are tested. The ceria-zirconia mixed oxide (CZO), the ceria-zirconia-alumina mixed oxide (CZAO) or gamma phase aluminum oxide (γ-Al_2O_3) (AO) is impregnated with only Pt, only Pd, combination of Pt-Rh and Pd-Rh metals.

The impregnation ratio of only Pt or Pd is 0.65 wt% and Rh is 0.1 wt%, Pt/Rh or Pd/Rh is 6.5 (as Pt is 0.65 wt% and Rh is 0.1 wt% or Pd is 0.65 wt% and Rh is 0.1 wt%). Metal sources are Platinum (II) chloride solution (Aldrich, $PtCl_2$, 5 wt% solution in 10 wt% HCl) , palladium (II) chloride solution (Aldrich, Pd_2Cl, 5 wt% solution in 10 wt% HCl) and rhodium (III) nitrate solution (Aldrich, $Rh(NO_3)_3$ ~ 10 wt% Rh in > 5 wt% nitric acid ($HNO_{3)}$). The first step of impregnation metal is determining the water capacity of support materials. Therefore, water capacity of 1 g support sample is measured by adding water drop wisely until sample is saturated to water. This amount of water is recorded as a mL water/g sample. The second step is dissolving nobel metal with 1.5 times of water of support sample water capacity. Before mixing with support material, nobel metal-water is mixed for 30 min in rotary vacuum evaporator without vacuum and heating for taking homogenous mixture. The third step is adding ceria-zirconia mixed oxide in balon joje. Metals are impregnated homogeneously on support material by rotation under vacuum (-850 mbar ,130 rpm) in the 80 °C water bath until all water evaporating. Then, sample is dried at 150 °C for 12h. The last step of impregnation of metal is grounding and calcination in an oven with dry air at 550°C for 1h.

In this study, only Pt, only Pd, Pt-Rh and Pd-Rh are impregnated on support. Pt-Rh and Pd-Rh are impregnated on support together on ceria-zirconia-alumina mixed oxide support or separate ceria-zirconia mixed oxide and gamma alumina oxides support. Co–impregnated support materials are mainly defined as CZAO-Cl and separate impregnated support materials are defined as CZAO-SI, CZO / AO-SI, (CZO-SI) / (AO-SI), CZO-SI + AO . All synthesized powder catalysts list is given in more details in Table 3.1.

Table 3. 1 Powder Catalysts List

ID	CATALYST POWDER
CZAO-SI	Pt + (CZAO)
CZO / AO-SI	(CZO) / (Pd + AO)
CZAO-SI	Pd + (CZAO)
(CZO-SI) / (AO-SI)	(Rh + CZO) / (Pt + AO)
CZAO-CI	(Pt + Rh) + (CZAO)
(CZO-SI) / (AO-SI)	(Rh + CZO) / (Pd + AO)
CZAO-CI	(Pd + Rh) + (CZAO)
CZO-SI + AO	(CZO + Rh) / (CZO + Pd) + AO

3.2 Monolith Coating

3.2.1 Preparation of Pseudoboehmite

Pseudoboehmite (AlO(OH)) is used as a binder in washcoating slurry. Nguefack et al.(2003) [19] described the method of synthesize pseudoboehmite. Aluminum-tri-sec-butoxide (Al(OC4H9)3) is hydrolyzed with deionized water. Al(OC4H9)3 is 12 wt% of total mixture. The mixture is stirred 2h at 60 °C. Then HCl is added for peptization of Al(OC4H9)3 and the mixture is stirred 1h at 80 °C. The product is dried 48h at 150 °C. Lastly, the powder is grounded and calcinated in an oven with dry air for 5h at 300 °C with a heating rate of 5 °C/min.

3.2.2 Preparation of Washcoating Slurry

In this study, after characterization of powder catalyst washcoating slurry samples are decided. According to characterization results, one metal impregnated powder catalysts are not used to washcoat monolith.

The kinds of washcoating slurry depend on impregnation place of metal on support, co-impregnation and separate impregnation. Gamma alumina is used in washcoating slurry to improve catalytic performance and provide apparent catalytic activity. Under rich fuel gamma alumina produces oxygen. At above 600 °C gamma alumina surface area decreases. This sintering washcoat slurry also decreases catalytic activity and metal dispersion. In addition to this, pseudoboehmite is used as a binder in washcoating slurry. Pseudoboehmite promotes adhesion of interparticles between ionizable compounds and aluminum oxide during drying and heat treating. Pseudoboehmite binding activity depends on pH of washcoating slurry. The activity of pseudoboehmite is high at pH of washcoating slurry to below 7, especially below 5. Nitric acid is used to adjust to pH value of washcoating slurry. The viscosity of washcoating slurry is lowered to enough to easily coat a monolith surface by Beck et al . (1994) [3].

In this study two kinds of preparation method is used to compare binding effect of pseudoboehmite in washcoating slurry.

The first washcoating slurry preparation method is with binder (using pseudoboehmite). Separate impregnated cerium-zirconium mixed oxide catalyst powders and co-impregnated ceria-zirconia mixed oxide catalyst powders are mixed with gamma phase aluminum oxide (AO). Pseudoboehmite is added to powder catalysts as 10 wt% of γ-Al_2O_3. Weight percentages of Ce are adjusted to19 % of total catalyst powder. These catalyst powders are mixed with deionized water. Moreover, the washcoating slurry solid content is adjusted 40 wt % with deionized water with 3 mm alumina bills which are made of high density polyethylene (HDPE). The washcoating slurry is ball milled at 275 rpm for 30 min before adding HNO_3. pH of slurry is adjusted with HNO_3 and then the washcoating slurry is ball milled for 3h at 275 rpm.

The second washcoating slurry preparation method is without binder. The catalyst powders, CZAO-CI, are directly used to prepare slurry. Moreover, they are not mixed with γ-Al_2O_3 due to already containing it.

3.2.3 Preparation of Monolith Coating

In monolith coating process, the washcoating slurry is used. In this study, dipcoating technique is used to washcoat monoliths. Physical properties of monoliths are 22 mm in diameter , 13 mm in height and monolith also have 600 cells/in^2. Firstly, monoliths bare are weighted after heating for 30 min at 150 °C. The monoliths are dipped into the slurry and waited 1 or 2 seconds in the slurry. The monoliths are turned down on slurry for homogeny coating. Then, they are removed from the slurry and monolith is shaken. Furthermore, monoliths are blown out with pressurized air to extract excess liquid in monolith channel. Moreover, excess coating on outer surface of monolith is cleaned. The monoliths is dried for 30 min at 150 °C and weighted. After monoliths are weighted, they are dried in the oven at 150°C for 12h. They are calcinated at oven 500°C for 3h. Lastly, coating amount is calculated as g/ft^3. In Table 3.2 all washcoated monolithic catalysts list is given.

Table 3. 2 List of Monolithic Catalysts

ID	MONOLITHIC CATALYST
(CZO-SI) / (AO-SI)	(Rh + CZO) / (Pt + AO)
(CZO-SI) / (AO-SI)	(Rh + CZO) / (Pd + AO)
CZAO-CI	(Pd + Rh) + (CZAO)
CZO-SI + AO	(CZO + Rh) / (CZO + Pd) + AO

3.2.4 Catalyst Characterizations

In this study, the BET, XRD, ICP-MS and SEM characterizations tests are done to analyze three way catalysts performance. Powder catalysts are analyzed by the BET, XRD, ICP-MS. Catalysts surface areas are evaluated by using “Quantachrome Corporation, Autosorb-6” instrument. XRD technique is used to specify crystal structure of catalysts using Cu X-ray radiation at 40 kV and 40 mA with scan speed of 2 degrees/min. “Perkin Elmer DRC II” model inductively coupled plasma mass-spectrometer (ICP-MS) is used to identify noble metals contents in catalysts. The washcoated monolith channels are monitored by QUANTA 400F” model field emission scanning electron microscope (SEM) to get information about catalyst binding on channels.

3.3 Catalyst Activity Tests in Dynamic Test System

3.3.1 Dynamic Test System Description

Activity tests of monolithic catalysts are used to evaluate them as a three way catalyst or not. Therefore, monolithic catalysts activity tests are done under a similar automotive conditions. Monolithic catalyst are exposured the simulated automotive exhaust gases. In addition to this, the temperature changes in automotive exhaust are also simulated by controlling a thermocouple. The product gases of monolithic catalyst are analyzed dynamically by CO analyzer and mass spectrometer. Lastly, graphs data of monolithic catalyst activity are achieved for each gas species.

In this study, dynamic test system is used, which is shown in Figure 3.1. This dynamic system is designed to control and measure all variables. The system elements are a quartz reactor, a split furnace, a Teledyne model 7600 infrared CO Analyzer and a Hiden HPR-20

Q/C Mass Spectrometer (MS).The simulated exhaust gas is provided by five gas cylinder. They are mixed with a defined ratio to get simulated exhaust gas composition. The first cylinder contains mixture of C_3H_6 (0.33%), C_3H_8 (0.11%), CO_2 (2.04%), , CO (8.87%), and H_2 (88.65%). The second cylinder contains mixture of NO (50%), N_2 (50%). The third cylinder contains 100 ppm SO_2 in N_2. The other two cylinder contains pure O_2 and pure N_2, separately. The gas pipes are 1/8 in inch Teflon. The gases flow rate is controlled by five mass flow controllers. In addition to this, the oxygen oscillation is provided directly to reactor inlet by separate gas pipe. The gas flow is controlled by solenoid valve opening with a frequency of 1 Hz and flow rate is reduced by flow reducer. 10% water vapor in exhaust gas is provided by nitrogen gas. Nitrogen controlled by MFC5 is gone to water bath at 54 °C to carry water vapor to system. In the manifold all the gases are mixed and saturated nitrogen are added to them at the exit of manifold. To obstruct water vapor condensation all pipes are heated . The system is purge by the VTP6 and the VTP7 valves. The other main element of dynamic system is the quartz reactor. The height of the reactor is 80 cm. The quartz reactor is divided into two sections. The first section is composed of pipes, flat pipe and spiral pipe. The thermocouple is placed in quartz flat pipe and reaches the monolith top surface. Thus monolith temperature is measured and the oven temperature is adjusted according the thermocouple measurements. The spiral quartz pipe is 27.5 cm long and 4 cm diameter. The feed stream enters into monolithic catalyst surface through this way. The first section also covers the second section. The second section has a quartz cup to place monolithic catalyst. This quartz cup is placed 30 cm from the top of the reactor. The monolithic catalyst samples are prepared on cordierite substrates with 600 cells/in^2 and the cordierite monoliths' dimensions are 2.2 cm in diameter and 1.3 cm in height. To prevent impurities a quartz filter is located under the monolithic catalyst. The product gas is carried from the reactor by the 4mm diameter quartz stripe of cup. Only 1L product gases is sent to MS and CO Analyzer, and . The product gases volume are regulated by rotameter and also conditioned to remove water vapor. The MAS-SOFT program is used to collect data from MS and CO Analyzer.

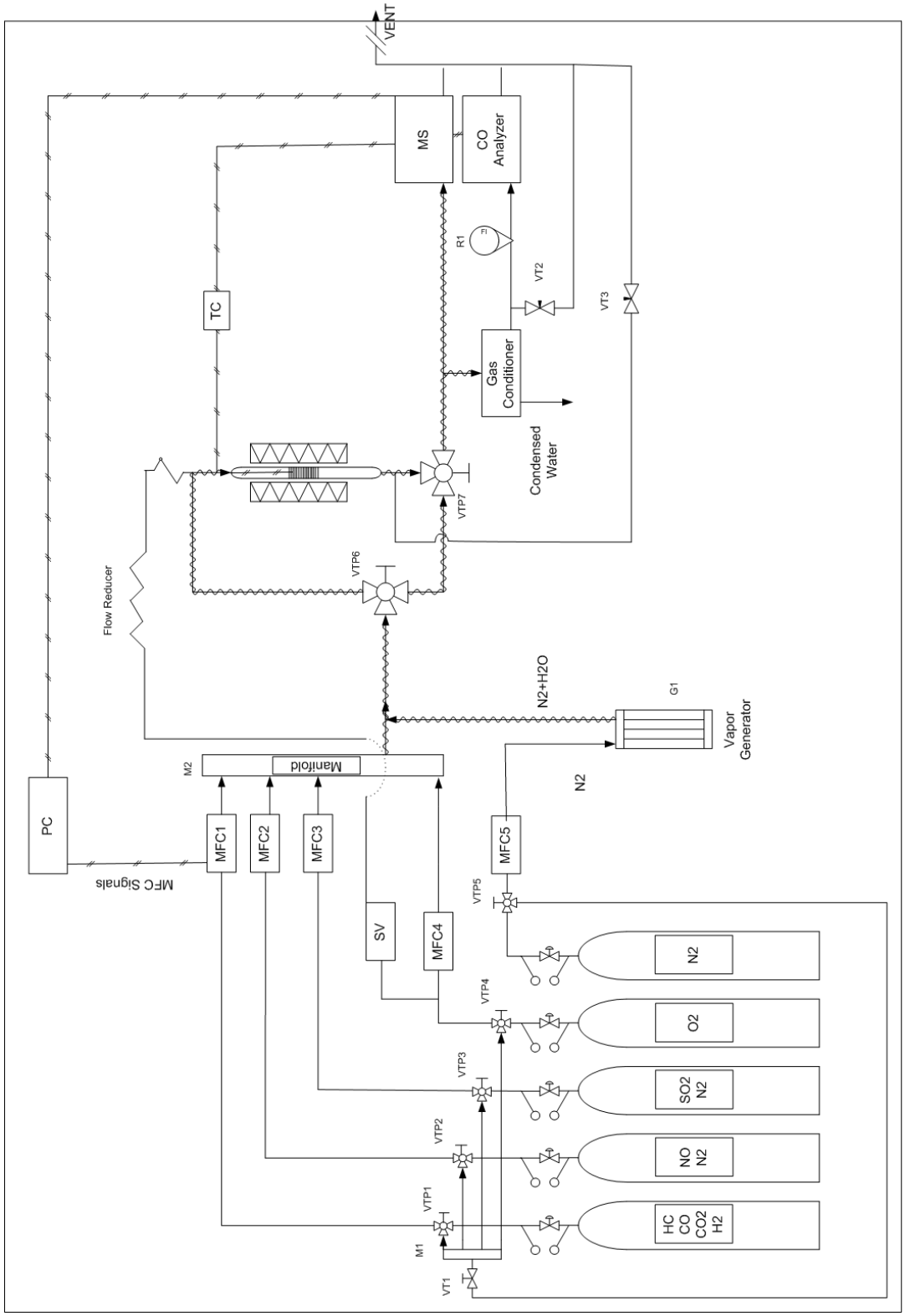

Figure 3. 2 Dynamic Test System

3.3.2 Catalytic Activity Test Description

The catalytic activity test is started with locating the catalytic monolith in quartz cup of reactor. The thermocouple is placed in the flat quartz pipe. Then the oven is heated to 150 °C. When the monolith temperature is stable at 150 °C, the simulated exhaust gas compositions are flown by-pass reactor. The simulated exhaust gas hourly space velocity is adjusted to 50,000 h^{-1}. In the Table 3.3 and Table 3.4 gas compositions are given for catalytic activity test with SO_2 and without SO_2. When each species MS and CO Analyzer data are stabilized, this data are used as initial concentrations, zero data. In addition to this, using valve VTP6 and VTP7 the simulated exhaust gases are flown through monolith. Data are collected in every 40 seconds in the MAS-SOFT computer program via CO Analyzer and MS. The oven temperature is started to heat at a rate of 5 °C/min from 150 °C to 600 °C, and then cooled to 150°C. O_2 is oscillated around the stoichiometric feed stream by solenoid valve opening with a frequency of 1 Hz. The MAS-SOFT computer program data are used for conversion versus temperature graphs for each species. To calculate conversion of species the initial concentration of species and MS calibration equations are used. All calculations are given in Appendix C.

Table 3. 3 Simulated Exhaust Gas Mixture Composition with SO_2

Species	Gas Mixture Composition (%)		
	Reducing	**Stoichiometric**	**Oxidizing**
C_3H_6	0.037	0.037	0.037
C_3H_8	0.012	0.012	0.012
CO	1.002	1.001	0.999
H_2	0.231	0.230	0.230
CO_2	10.018	10.000	9.981
NO	0.150	0.150	0.150
SO_2	0.002	0.002	0.002
O_2	0.585	0.767	0.949
N_2	Balance	Balance	Balance

Table 3. 4 Simulated Exhaust Gas Mixture Composition without SO_2

Species	Gas Mixture Composition (%)		
	Reducing	**Stoichiometric**	**Oxidizing**
C_3H_6	0.037	0.037	0.037
C_3H_8	0.012	0.012	0.012
CO	1.002	1.001	0.999
H_2	0.231	0.230	0.230
CO_2	10.018	10.000	9.981
NO	0.150	0.150	0.150
SO_2	0.000	0.000	0.000
O_2	0.585	0.767	0.949
N_2	Balance	Balance	Balance

3.3.3 The Effect of SO_2 During Catalytic Activity Tests

The addition of SO_2 to the feed stream affects HCs conversion activities of the three way catalyst. This is caused by the poisoning of the support catalytic sites. Besides, CeO_2 and ZrO_2 are adsorb SO_x species. Reduced and oxidized CeO_2 has a capability to adsorb SO_2 with both surface and bulk-type of sulphates. In reducing conditions H_2 eliminates sulphates as H_2S with the help of noble metals. CO also assists the sulphates reduction to reduced oxy-sulphur species.

The presence of SO_2 affects the OSC of CeO_2. ZrO_2 is added to increase CeO_2 to sulphur poisoning resistance. This may be related with the higher OSC efficiency of the CZOs.

In this study four tests are carried out to analyze the effect of SO_2 during the catalytic activity tests. Test 1 is carried out with the gas composition without SO_2, the composition is given in Table 3.1. Throughout Test 2 and Test 3, SO_2 is added into simulated exhaust gas, given in Table 3.2. Lastly, Test 4 is performed is without SO_2 as Test 1. As a result, the catalytic activity differences between Test 2 - Test 3 and Test 1 - Test 4 show the effect of SO_2 on monolithic catalyst. All catalytic activity test graphics are given in Appendix D.

3.4 Calibrations

The system accuracy is obtained by calibration of system elements. In this dynamic test system MFCs and MS are calibrated.

3.4.1 Mass Flow Controller Calibrations

In this study dynamic test system, all flow rates of the gases are controlled by using MFCs. MFC accuracy depends on the actual flow and the input flow. Thus, calibration is used to obtain the correlation between actual and input flow.

Calibration of MFC is done with nitrogen gas. Gas correction factor is used according to each gas MFC in dynamic test system. Each gas species has a special gas correction factor. Moreover, for mixture gas cylinders correction factor is the highest concentration gas correction factor or an average of gases correction factors. Actual flow rate is measured with soup bubble, and input flow rate is set in MFC computer program. Then, actual flow rate is multiplied with the gas correction factor. Lastly, graph of the set flow rate values vs. the measured flow rate values are plotted. Calibration calculations for MFCs are shown in Appendix C.

3.4.2 Mass Spectrometer Calibrations

MS data are determined as gas pressure in the system. This data accuracy are obtained by calibration of MS according to the simulated exhaust gas concentrations. CO analyzer gives directly CO concentration as ppm unit. Therefore, MS calibration is not done for CO.

During the MS calibration, total flow rate of calibration gas mixture is same as the catalytic activity test flow rate. Calibration gas mixture is flow through the by-pass line. Calibration gas mixture contains calibration gas, nitrogen and water vapor. Three lines of system are used for MS calibration. First line is for calibration gas. Second line is for nitrogen which carries water vapor and the third line is for nitrogen. Calibration gas is flown through first line with different flow rates. Nitrogen flow rate in second line is constant to carry constant water vapor. Third line low rate is adjusted according to flow rate of calibrated gas. At the end, the graph of concentration of the calibrated gas vs. the MS data curves are drawn and calibration equations are obtained. MS calibration data are tabulated in Appendix C.

CHAPTER 4

CHARACTERIZATIONS

4.1 Support Materials

In this study, all support materials are synthesized by co-precipitation method. Ce/Zr ratio is constant at 4/1 either ceria-zirconia mixed oxide (CZO) or ceria-zirconia alumina mixed oxide (CZAO) to synthesize $Ce_{0.8}Zr_{0.2}O_2$. Gamma phase aluminum oxide is added to compare thermal stability of CZO with CZAO. The catalytic activity test results are used to decide the most effective support.

4.1.1 Characterizations of CZO and CZAO Support Materials

4.1.1.1 X-Ray Diffraction Studies

Powder X-ray diffraction (XRD) patterns of ceria-zirconia mixed oxides ($Ce_{0.8}Zr_{0.2}O_2$) are recorded in the 25–90° 2θ range in the scan mode (0.03°,1s) using Cu X-ray radiation at 40 kV and 40 mA . In Figure 4.1 XRD patterns of CZO is given.

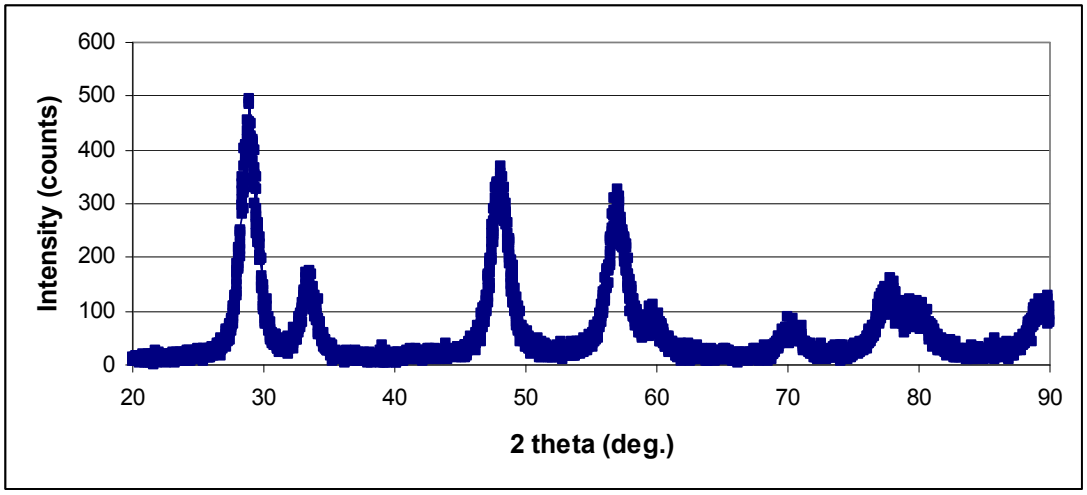

Figure 4. 1 XRD patterns of CZO Support Material

In Figure 4.2 XRD patterns of ceria-zirconia alumina mixed oxide is given. XRD pattern of CZAO are recorded in the 25–90° 2θ range in the scan mode (0.03°,1s). XRD patterns of CZO and CZAO are quite similar.

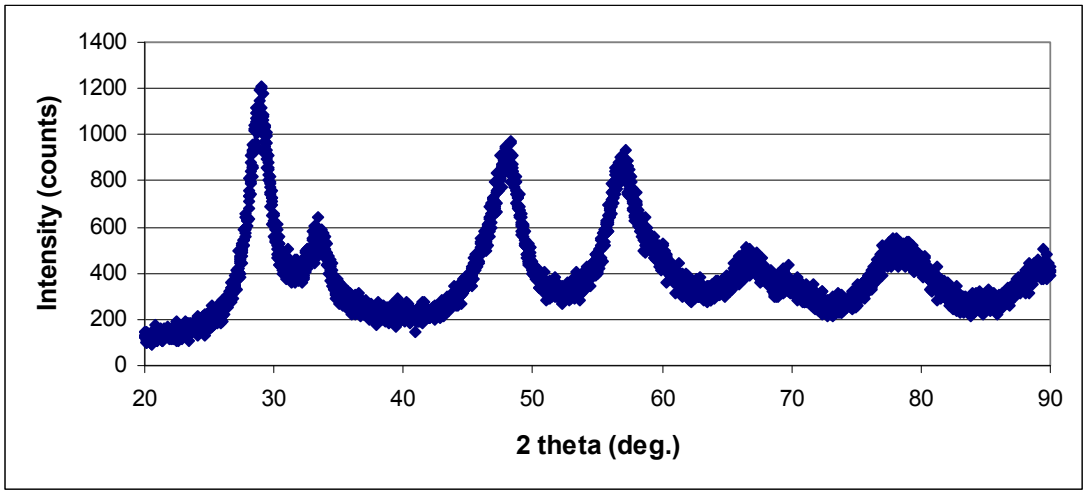

Figure 4. 2 XRD patterns of CZAO Support Material

4.1.1.2 BET Surface Area Studies

Nitrogen adsorption isotherms are recorded at liquid nitrogen temperature (-196.15 °C) using a Quantachrome Corporation, Autosorb-6" instrument. Prior to determination of an adsorption isotherm, the sample was degassed at 139.85 °C. In Table 4.1 BET surface areas of ceria-zirconia mixed oxide and ceria-zirconia alumina mixed oxide are given. The BET surface area of CZAO is higher than CZO. This shows that gamma alumina has strong effect of increasing surface area of catalyst powder.

Table 4. 1 BET Surface Areas of CZO and CZAO Support Materials

Catalyst	CZO	CZAO
BET Surface Area (m^2/g)	145.3	320.6

4.2 Metal Loaded Catalyst Powders

In this study, support materials of CZO and CZAO are synthesized by co-precipitation method. By using these support materials different type powder catalysts are synthesized according to the noble metal co-impregnation surface. Only Pt, only Pd, Pt-Rh and Pd-Rh are impregnated on support material. Pt-Rh and Pd-Rh are impregnated on support together on CZAO support, CZO or separate CZO and gamma alumina oxides support. Co–impregnated support materials are mainly defined as CZAO-CI and separate impregnated support materials are defined as CZAO-SI, CZO / AO-SI, (CZO-SI) / (AO-SI), CZO-SI + AO.

The CZAO-CI powders are also synthesized by co-impregnation of Pt, Pd, Rh on CZAO support. The impregnation content ratio of only Pt or Pd is 0.65 wt% and Pt/Rh or Pd/Rh is 6.5 in all kinds of catalyst powders. In Table 4.2 synthesized powder catalysts list is given.

Table 4. 2 Powder Catalysts List

ID	CATALYST POWDER
CZAO-SI	Pt + (CZAO)
CZO/AO-SI	(CZO) / (Pd + AO)
CZAO-SI	Pd + (CZAO)
(CZO-SI) / (AO-SI)	(Rh + CZO) / (Pt + AO)
CZAO-CI	(Pt + Rh) + (CZAO)
(CZO-SI) / (AO-SI)	(Rh + CZO) / (Pd + AO)
CZAO-CI	(Pd + Rh) + (CZAO)
CZO-S I+ AO	(CZO + Rh) / (CZO + Pd) + AO

4.2.1 Characterizations of Metal Loaded Catalyst

4.2.1.1 BET Surface Area Studies

The three- way catalyst activity also depends on the surface area of catalysts. BET surface area is effected by calcination temperature and calcination time. In Table 4.3 BET surface area of the powder catalysts are given. As seen in the Table 4.3, CZO surface area is decreased from 145.3 m^2/g to nearly 80.0 m^2/g. This can be explained due to one more calcination for noble metal impregnations on support material. CZAO surface area is also decreased from 320.6 m^2/g to 83.3 m^2/g.

Table 4. 3 BET Surface Area of The Powder Catalysts

Powder Catalyst	BET Surface Area (m^2 / g)
Pt + (CZAO)	80.61
(CZO) / (Pd + AO)	83.30
(Rh + CZO) / (Pt + AO)	83.38
(Rh + CZO) / (Pd + AO)	83.73
(Pd + Rh) + (CZAO)	81.16
(CZO + Rh) / (CZO + Pd) + AO	-

This observation is consistent with the effect of sintering. The sintering of support material leads to pore volume increase. To control sintering effect gamma alumina is used during preparing catalyst powders. □-Al_2O_3 provides thermal stabilization. Moreover, the thermal stability of three way catalyst is increased by addition ZrO_2. The effect of thermal stability effect of ZrO_2 on three way catalyst should be analyzed by pore size diameter .

4.2.1.2 ICP-MS Studies

The contents of metal on catalyst powders are important for activity of catalyst. Because, the metal contents affect the monolithic catalysts' activity, and they are active on catalytic activity reactions. By ICP-MS method the metal contents of powder catalysts are analyzed. Total metal content on monolithic catalysts are calculated as g metal/ft^3 via using ICP-MS analysis result. The synthesized powder catalysts noble metal contents are given in Table 4.4. The targeted noble metal contents are Pt, Pd is 0.65 wt% and Rh is 0.1 wt%. According to ICP-MS result, noble metal amounts are higher than target values. This error can be experimental as during the preparation of powder catalyst, or calculation error of catalyst weight.

Table 4. 4 ICP-MS Results of The Powder Catalysts

Powder Catalyst / Nobel Metal	Pt Content	Pd Content (%)	Rh Content (%)
Pt + (CZAO)	0.621±0.009 (%)		
(CZO) / (Pd + AO)		0.593±0.012	
(Rh + CZO) / (Pt + AO)	0.54±0.009 (%)		0.086±0.001
(Rh + CZO) / (Pd + AO)		0.614±0.009	0.092±0.002
(Pd + Rh) + (CZAO)		0.593±0.016	0.085±0.002
(CZO + Rh) / (CZO + Pd) + AO	-	-	-
TOFAS COM	24.37±0.48 (mg/kg)	0.145±0.002	0.0191±0.0005

The catalysts activity depends on metal contents on monolithic catalysts. To observe this effect, the metal content on washcoated catalyst is calculated by ICP-MS results or powder catalysts. Thus, total metal content on monolithic catalysts is expressed as g/ft^3. The total metal contents of monolithic catalysts are given in Table 4.5.

Table 4. 5 Total Loaded Metal Content

Monolithic Catalyst	Total Loaded Metal Content (g/ft^3)
(Rh + CZO) / (Pt + AO)	34.5
(Rh + CZO) / (Pd + AO)	22.9
(Pd + Rh) + (CZAO)	35.5
(CZO + Rh) / (CZO + Pd) + AO	32.6
TOFAS COM	30.0

The difference between total metal content on monolithic catalysts are due to washcoating amount of monoliths.

4.2.1.3 SEM Images

To characterize monolithic catalyst SEM images are also used. Because, washcoating process is as important process as preparing the powder catalysts. Cordierite monolith cells are sometimes closed due to deposit of catalyst during washcoating process. Layer is formed on honeycomb monolith and the thickness of layer is increased as increasing amount of coating thus corners of monoliths are filled. To observe monolith cell status is analyzed with SEM. In Figure 4.3, Figure 4.4 and Figure 4.5 SEM monolithic catalysts are shown.

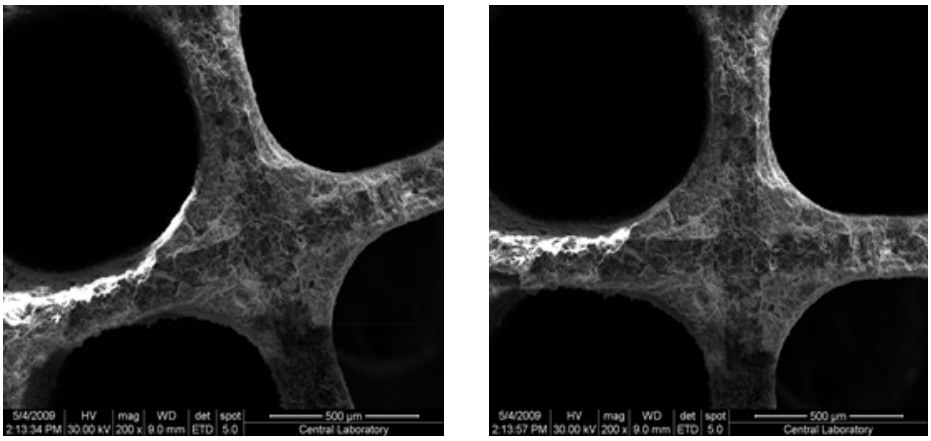

Figure 4. 3 SEM Images of Research Monolithic Catalyst

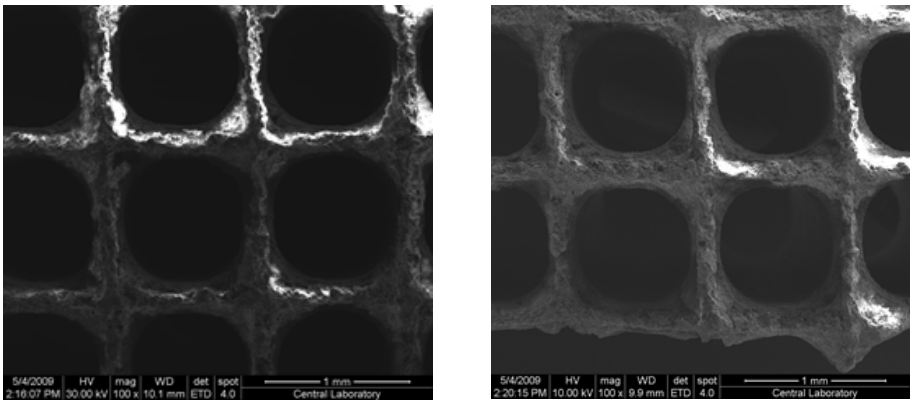

Figure 4. 4 SEM Images of Research Monolithic Catalyst

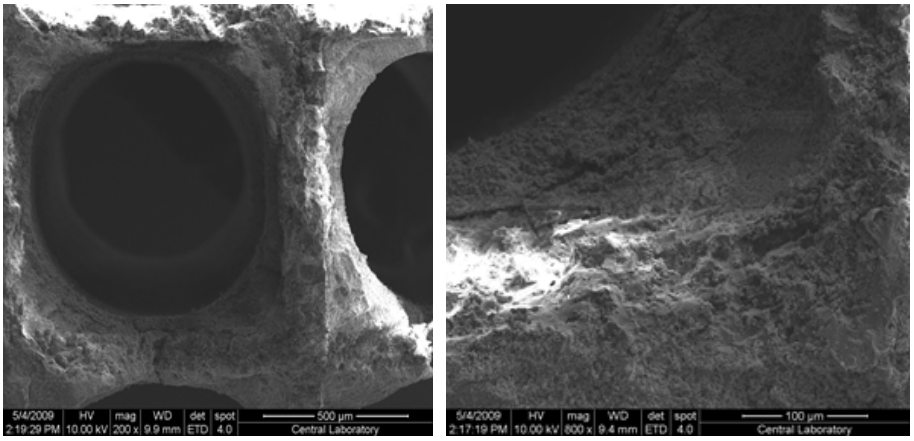

Figure 4. 5 SEM Images of Research Monolithic Catalyst

As seen in SEM images, the layers of catalyst powders do not fill the monolith cells corners. The shape of the cells are protected. The amount of washcoat is not too high. The monolithic catalysts are convenient for gas flow.

CHAPTER 5

CATALYTIC ACTIVITY TESTS

The monolithic catalysts are characterized for three-way catalytic performance in a laboratory reactor under simulating the operation of the catalyst in an automotive. The tests are conducted with the concentration of SO_2 in the simulated exhaust feed stream set at 20 ppm. The activity tests are performed without SO_2 and with SO_2 to evaluate the effect of sulphur on HC, CO and NOx activity.

In this study simulated exhaust gas includes C_3H_6 as an olefins and C_3H_8 as an paraffin. Automotive exhaust gas includes 200 different hydrocarbons as olefins, paraffins, aromatics and oxygenates. The conversion of olefins are easier than paraffin by TWCs.

TWCs have ability of high conversion of NO, CO and HCs. To improve this ability noble metals are impregnated on support materials. The high activity of rhodium for removal of NO. To remove CO, Pd or Pt is impregnated on $Ce_{0.8}Zr_{0.2}O_2$ mixed oxides. For hydrocarbon oxidation reactions Pd is used. Especially, for propylene oxidation Pd is catalytically more active than Rh. In addition to this, Rh is much more resistant against sulphur than Pd, and Rh has ability to recover the lost activity rapidly but Pd has not. This is result of Pd sensitivity against the sulphur. Sulphur migrates into Pd bulk. As a result, the conversions of CO and C_3H_6 are done by Pd. When Pd is poisoned by sulphur, CO and C_3H_6 conversion are decreased. Therefore, Rh is also used in the three way catalysts to remove poisoning effect of Pd.

To increase thermal stability of $Ce_{0.8}Zr_{0.2}O_2$ mixed oxides γ-Al_2O_3 are added. In addition to this co-impregnation of metals on γ-Al_2O_3 is lead to high thermal stabilities. According to the catalytic activity tests results the monolithic catalysts are evaluated as a three way catalyst or not.

In this study four catalytic activity tests of monolithic catalysts are performed. During the Test 1 the fresh monolithic catalysts activities are evaluated. The simulated exhaust gas mixture during the Test 1 does not contain SO_2. After Test 1, SO_2 is added into the simulated gas mixture during the Test 2 and the Test 3. Lastly, the monolithic catalyst are tested with simulated exhaust gas without SO_2, Test 4. By this test program the effect of SO_2 is analyzed.

The monolithic catalyst's activities are evaluated for species of CO, NO, H_2 O_2 , C_3H_8 and C_3H_6 according to conversion versus temperature graphs. The catalytic activities are analyzed according to the light-off temperature, the maximum conversion and the corresponding temperature (T_{max}). The highest catalytic activity is the highest conversion at the lowest T_{50}. The catalytic activity tests data are given in Table 5.1 as T_{50}, maximum conversion and T_{max} data. In Figure 5.1, 5.2, 5.3, 5.4, 5.5 and 5.6 the conversion versus temperature graph of research monolith catalyst are given. These test data are for fresh catalyst during the Test 1. In Figure 5.1, 5.2, 5.3, 5.4, 5.5 and 5.6 the conversion versus temperature graphs are drawn during heating and cooling steps. When heating step is

compared with cooling step, it is observed that the maximum conversion of species are reached at lower temperature during the cooling step. This situation can be understood more clearly from the shift between the heating and cooling activity curves of the species given in Figures. The cooling step catalytic activity curves shifts toward left, through lower temperatures. The catalyst is reduced and thus the monolithic catalyst activity is improved during the cooling step. The reductive pretreatment improves the conversion of NO and lowers CO and HCs' light-off temperatures was reported by Di Monte et al. (1998) [6]. Moreover, during the heating step, some oscillations are observed. This oscillations are caused from increasing the oven temperature unlinearly at low temperatures. On the other hand, during the cooling step regular "S" shape curves are obtained. Therefore, the cooling steps activity data are considered for the evaluation of the catalysts catalytic activity.

Table 5. 1 Heating/Cooling Catalytic Activity Data of (CZO-SI) / (AO-SI) Monolithic Catalyst During Test 1

Species	Heating			Cooling		
	T50 (˚C)	Max. Con. (%)	Tmax (˚C)	T50 (˚C)	Max. Con. (%)	Tmax (˚C)
CO	217	100	464	200	100	478
NO	274	96.5	579	242	96	579
C_3H_6	220	100	572	220	100	475
C_3H_8	273	100	594	264	100	553
H_2	-	100	360	162	100	241
O_2	219	91.5	459	198	92	580

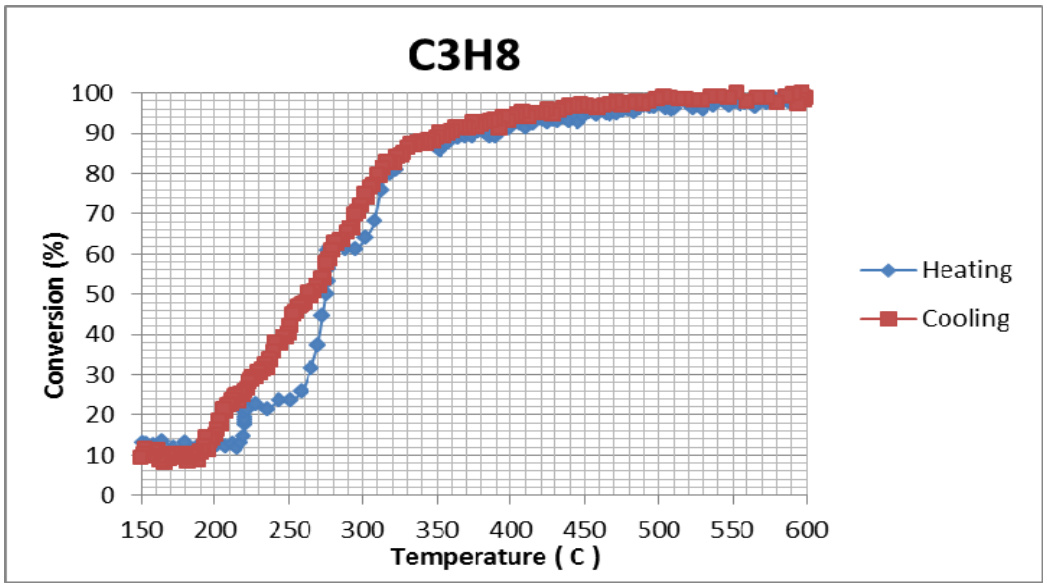

Figure 5. 1 C_3H_8 Catalytic Activity of (CZO-SI) / (AO-SI) Monolithic Catalyst

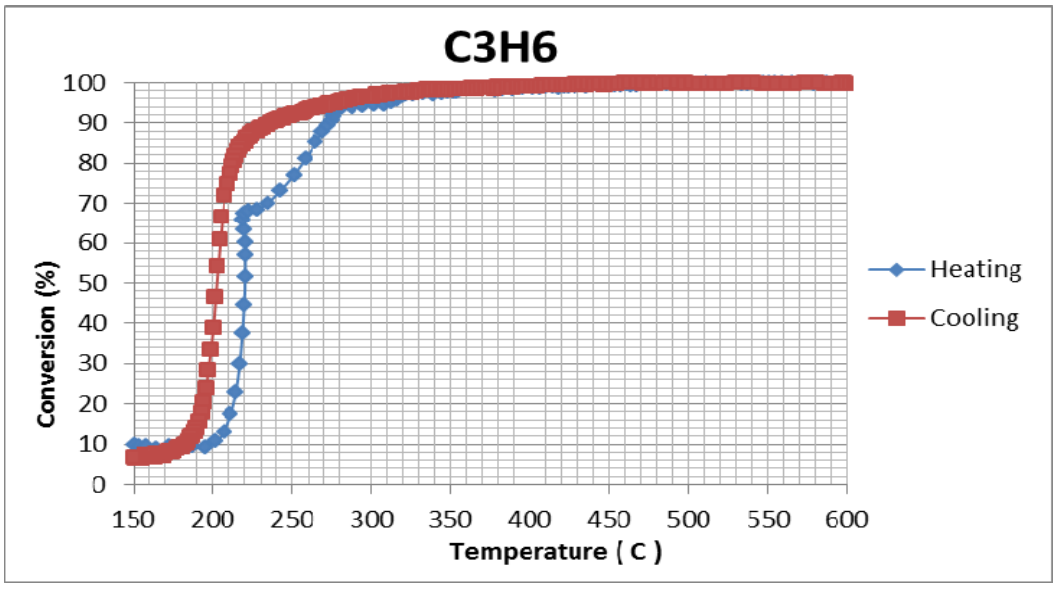

Figure 5. 2 C_3H_6 Catalytic Activity of (CZO-SI) / (AO-SI) Monolithic Catalyst

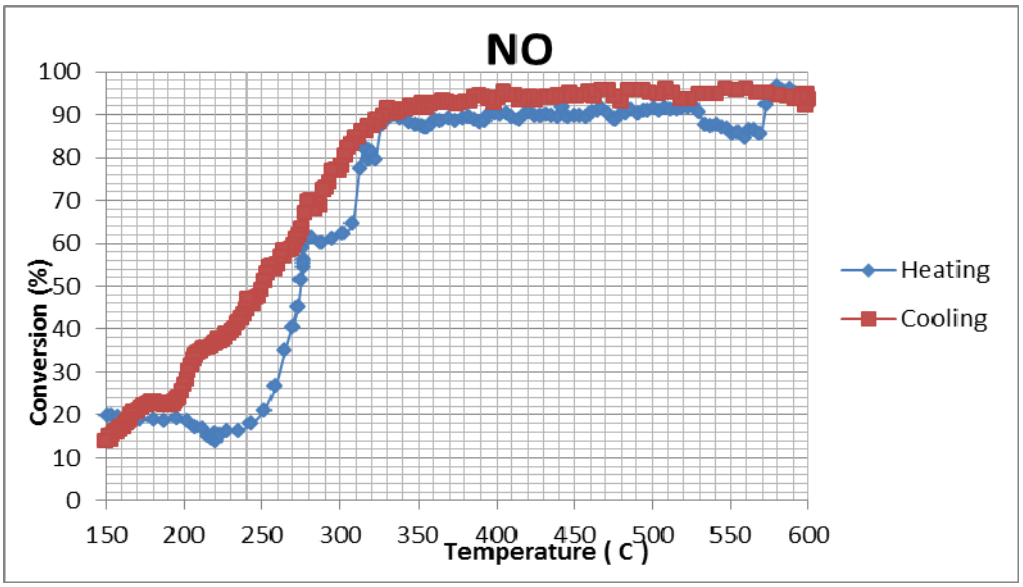

Figure 5. 3 NO Catalytic Activity of (CZO-SI) / (AO-SI) Monolithic Catalyst

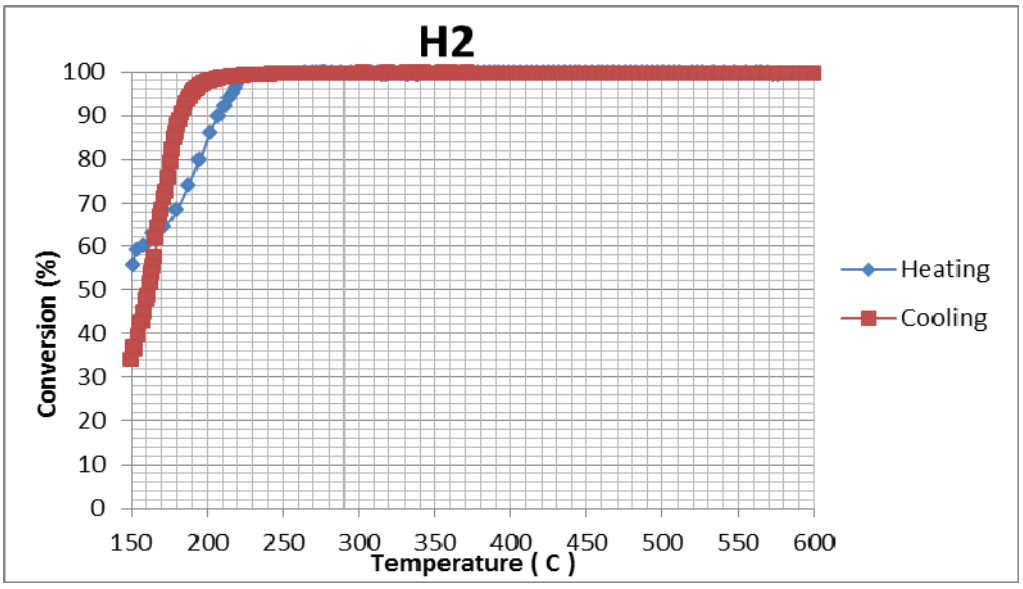

Figure 5. 4 H_2 Catalytic Activity of Fresh (CZO-SI) / (AO-SI) Monolithic Catalyst

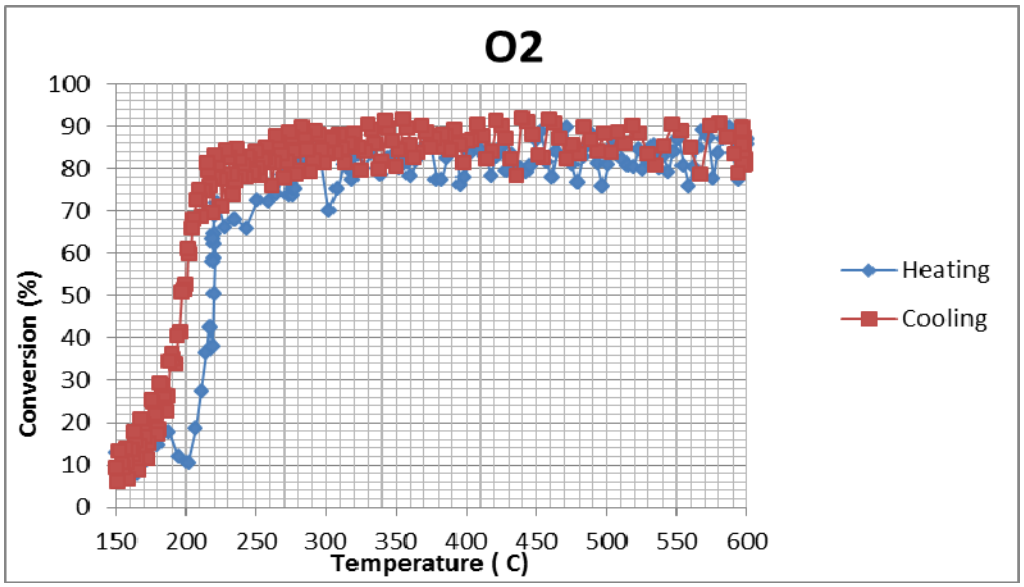

Figure 5. 5 O_2 Catalytic Activity of (CZO-SI) / (AO-SI) Monolithic Catalyst

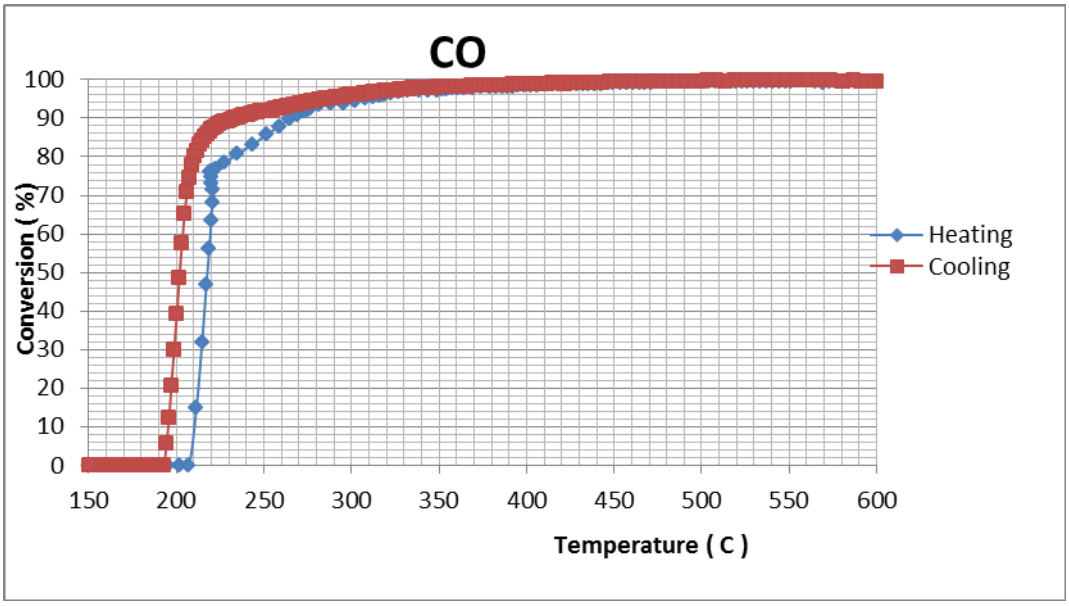

Figure 5. 6 CO Catalytic Activity of (CZO-SI) / (AO-SI) Monolithic Catalyst

The catalytic activity tests data of fresh catalyst are given in Table 5.2 as T_{50}, maximum conversion and T_{max} data. In Figure 5.7, 5.8, 5.9, 5.10, 5.11 and 5.12 the conversion versus temperature graph of research monolith catalyst are given. The Test 1 data are for fresh catalyst during the cooling steps.

Table 5. 2 Catalytic Activity Data of (CZO-SI) / (AO-SI) Catalyst During Test 1

Species	Fresh		
	T50 (˚C)	Maximum Conversion (%)	Tmax (˚C)
CO	200	100	478
NO	242	96	579
C_3H_6	220	100	475
C_3H_8	264	100	553
H_2	162	100	241
O_2	198	92	580

According to the conversion versus temperature graphs of CO, H_2, C_3H_6, O_2 the light off curves appears as “S” shapes. The conversions of C_3H_8, NO depend on temperature. Their conversion increases with the temperature. The catalytic activity sensivity of C_3H_8 is higher than C_3H_6 for research catalyst. Ulla et al. (2003) [29] stated that after the light off temperature was reached, CO oxidation reactions typically start first, followed then by HC oxidation. However, NO requires higher reduction temperatures.

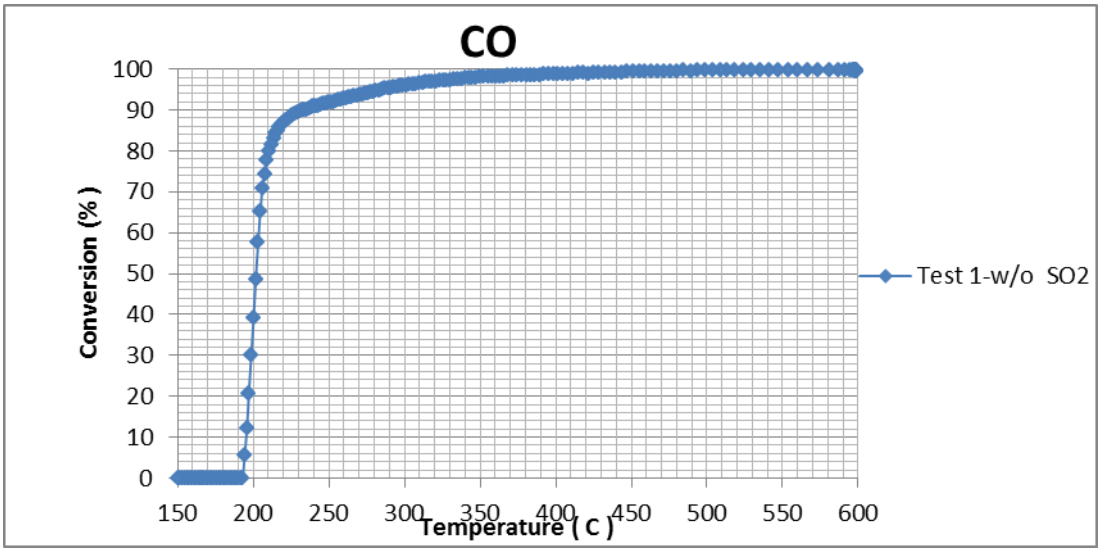

Figure 5. 7 CO Catalytic Activity of (CZO-SI) / (AO-SI) Monolithic Catalyst During Test1

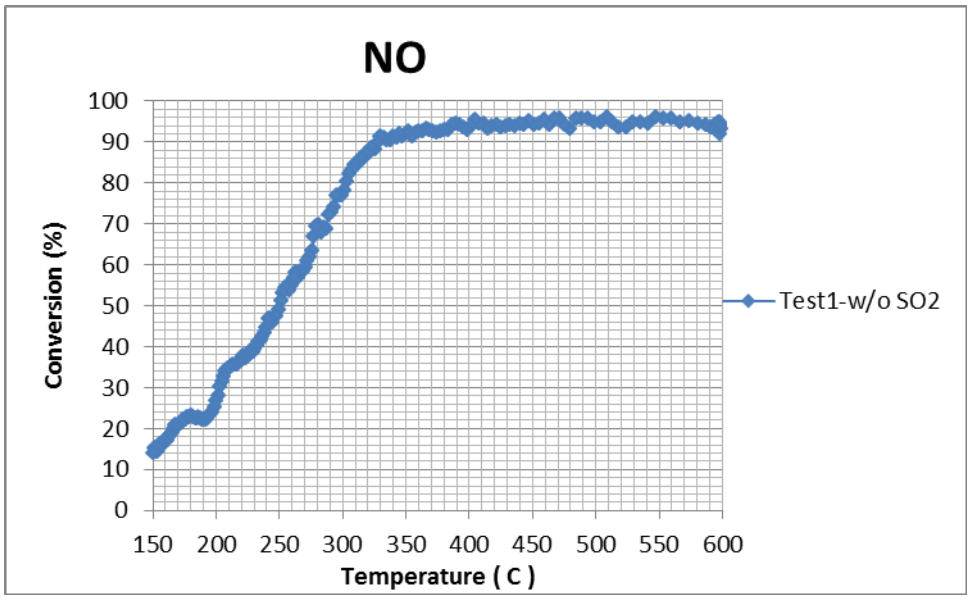

Figure 5. 8 NO Catalytic Activity of (CZO-SI) / (AO-SI) Monolithic Catalyst During Test1

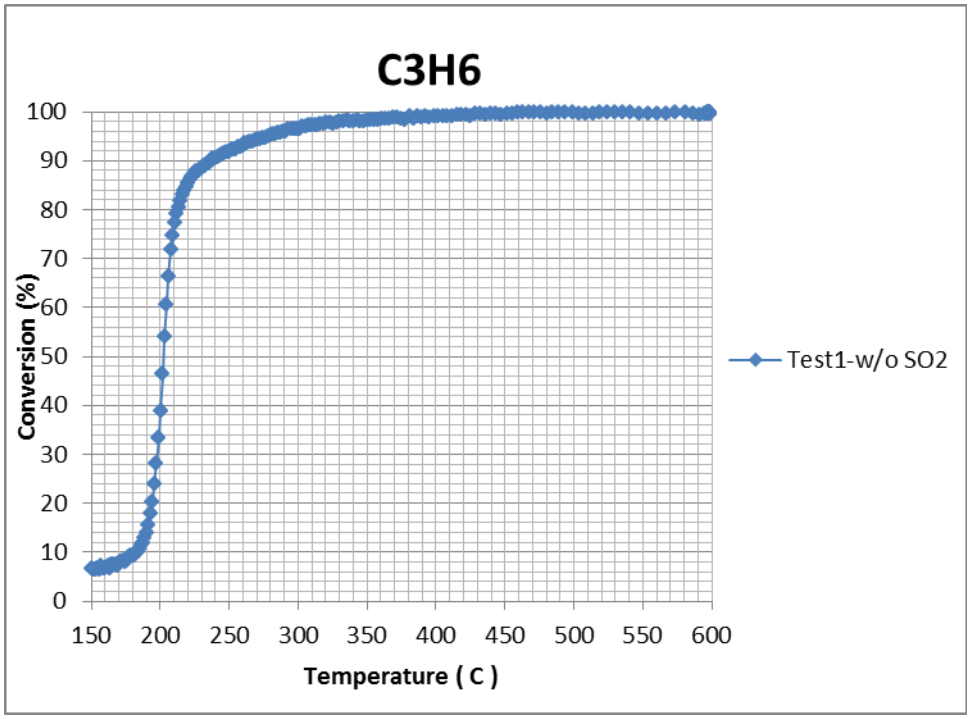

Figure 5. 9 C_3H_6 Catalytic Activity of (CZO-SI) / (AO-SI) Monolithic Catalyst During Test 1

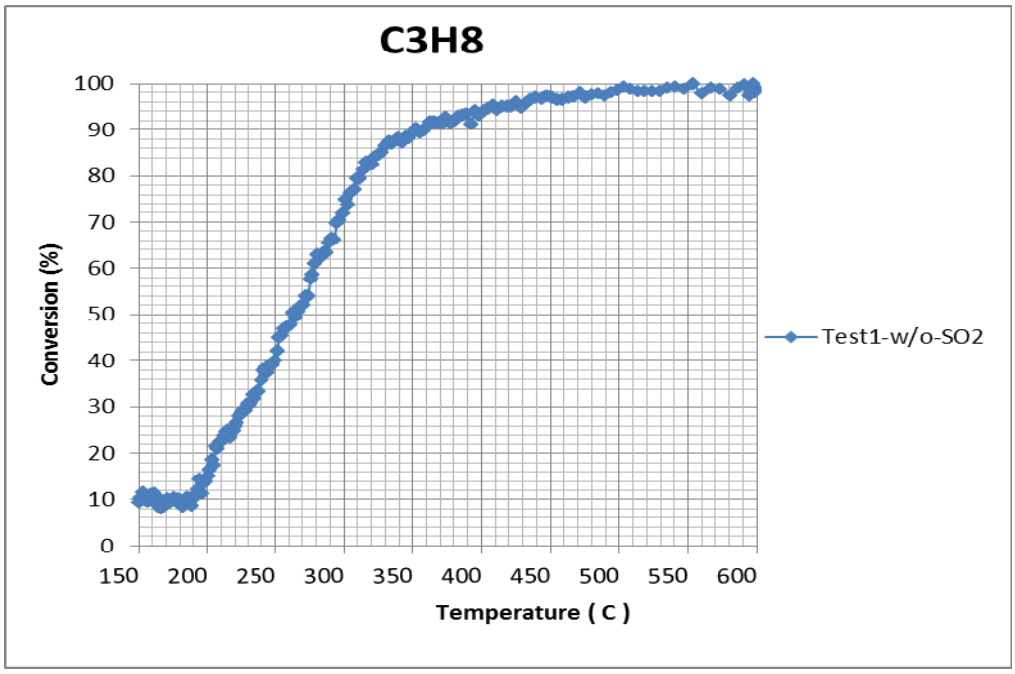

Figure 5. 10 C_3H_8 Catalytic Activity of (CZO-SI) / (AO-SI) Monolithic Catalyst During Test 1

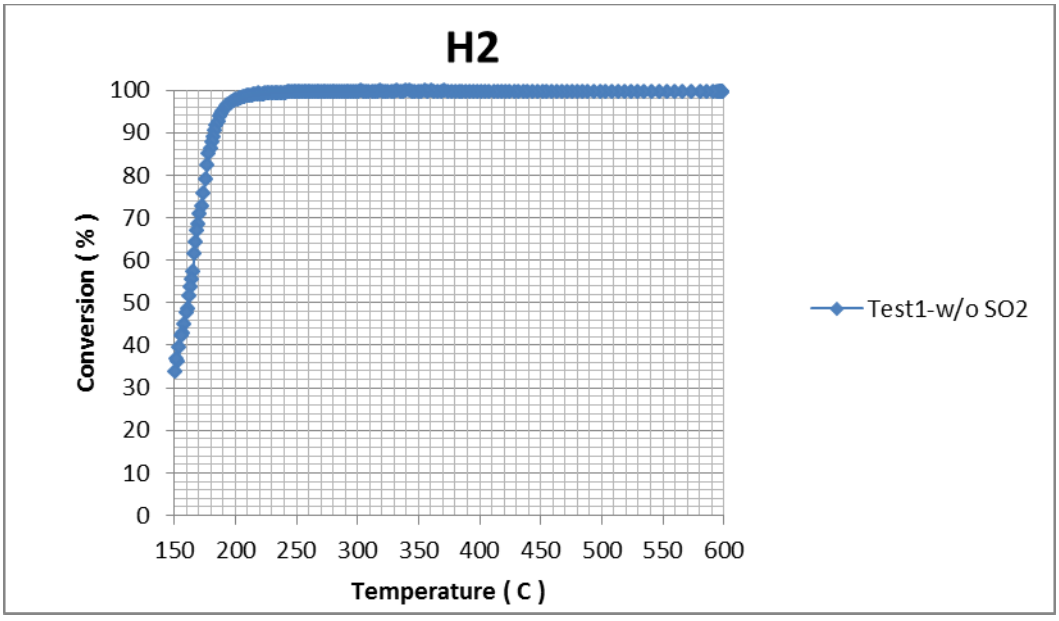

Figure 5. 11 H_2 Catalytic Activity of (CZO-SI) / (AO-SI) Monolithic Catalyst During Test 1

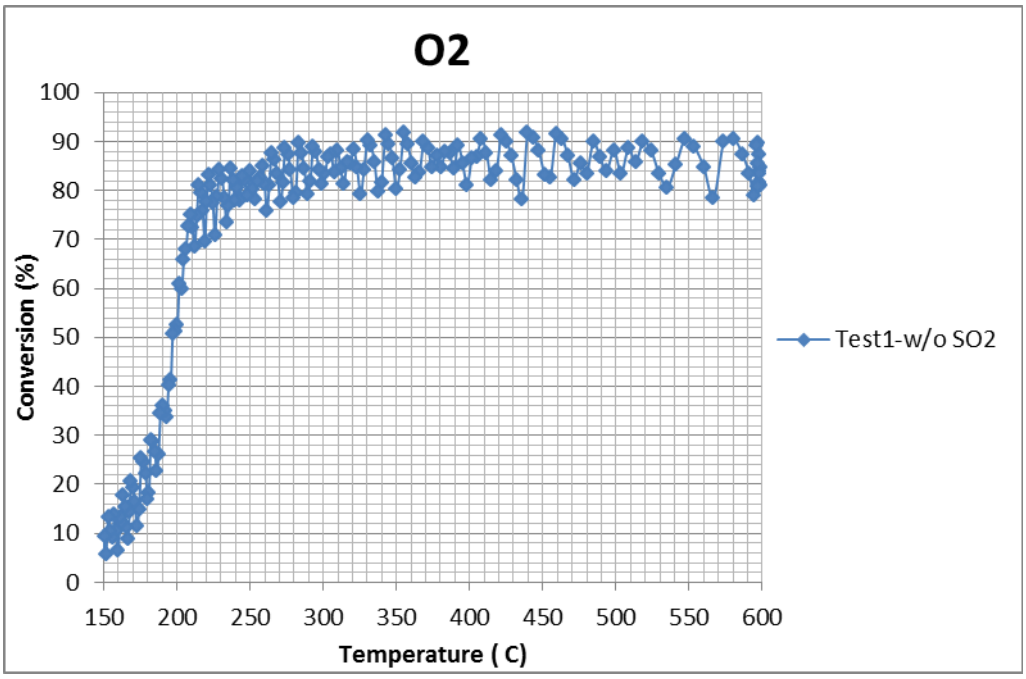

Figure 5. 12 O_2 Catalytic Activity of (CZO-SI) / (AO-SI) Monolithic Catalyst During Test 1

Catalytic activities of monolithic catalysts depend on the washcoat amount, homogeneity and total metal content. Thus, all monolithic catalysts performances are unique. To get correct catalytic activity of monolithic catalysts more than five monoliths are coated with one type catalyst powder and the activity tests are performed for each one. According to catalytic activity tests monolithic catalyst performance is analyzed.

In this study, Tofas commercial monolithic catalysts are also analyzed as a reference. Pd and Rh nobel metals are used in commercial monolith. Pd/Rh ratio of commercial monolith is 6.5 and the total metal content is 30.0 g/ft^3. It is assumed that commercial monolith is washcoated homogeneously. The volume of Tofas commercial monolith is nearly 200 times bigger than laboratory scale monolith so it would be washcoated more homogenously and more identical. It is cut as a laboratory scale and then tested in the dynamic test system. Catalytic activity tests of Tofas commercial monolith are performed with the simulated exhaust gas compositions. The catalytic activity data are tabulated in Table 5.3 and all curves for each species are plotted in Figures 5.13, 5.14, 5.15, 5.16 , 5.17 and 5.18.

Table 5. 3 Catalytic Activity Data of Tofas Commercial Monolith Catalyst During Test 1

Species	Tofas Commercial Monolith Catalyst		
	T50 (C)	Maximum Conversion (%)	Tmax (C)
CO	154	100	209
NO	232	89	408
C_3H_6	224	100	300
C_3H_8	265	98	600
H_2	-	100	150
O_2	-	95	525

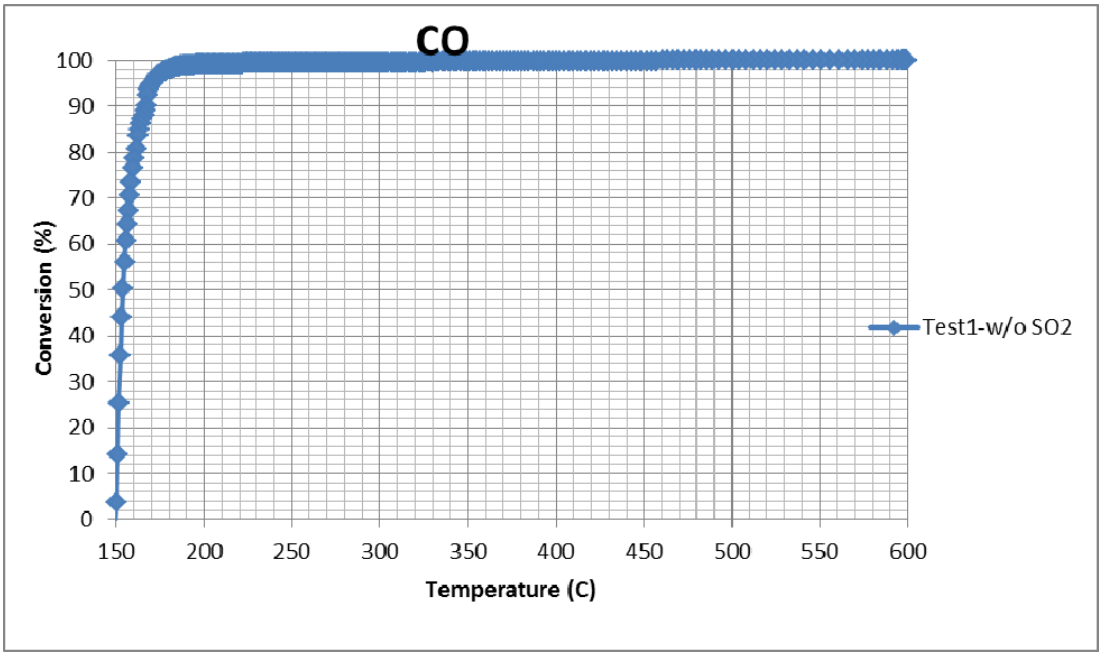

Figure 5. 13 CO Catalytic Activity of Tofas COM Monolithic Catalyst During Test1

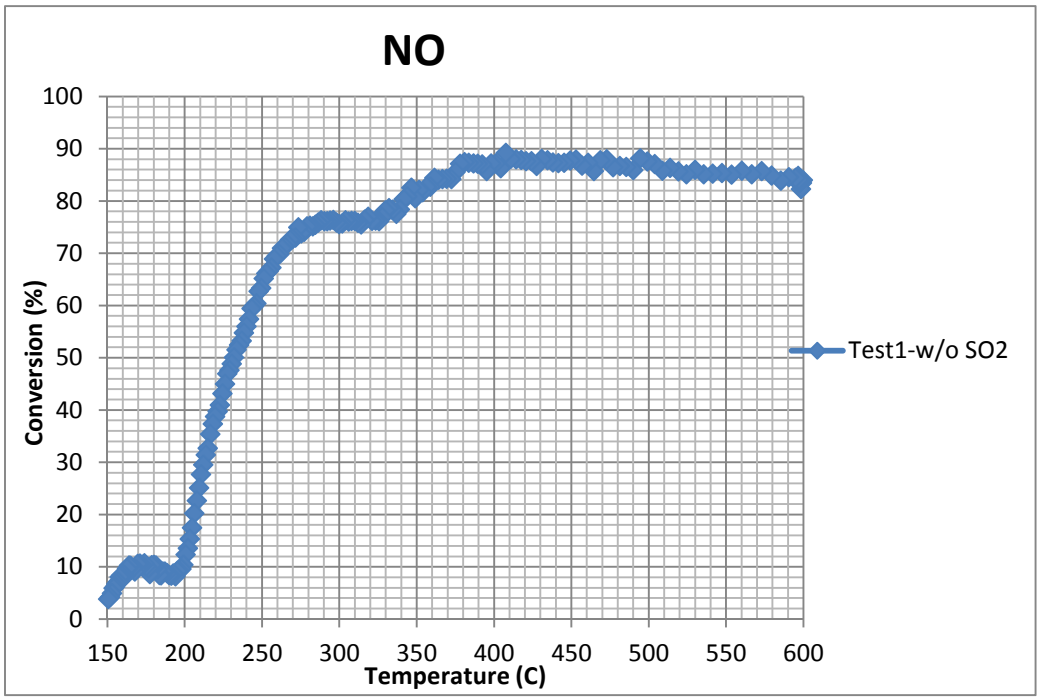

Figure 5. 14 NO Catalytic Activity of Tofas COM Monolithic Catalyst During Test1

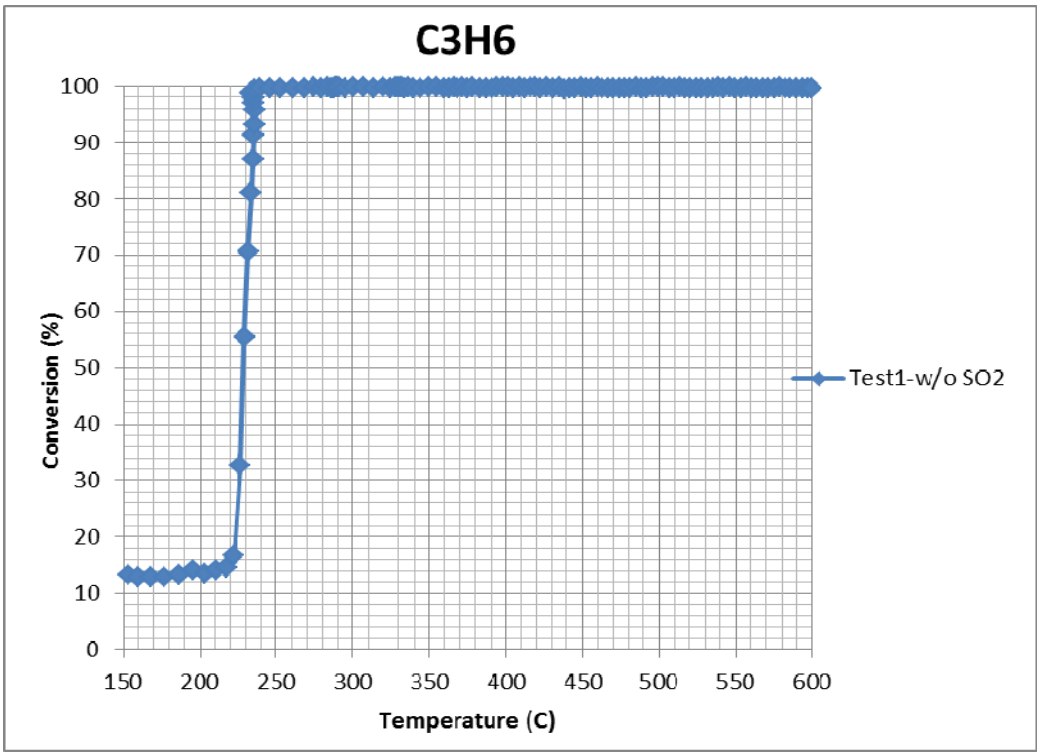

Figure 5. 15 C_3H_6 Catalytic Activity of Tofas COM Monolithic Catalyst During Test 1

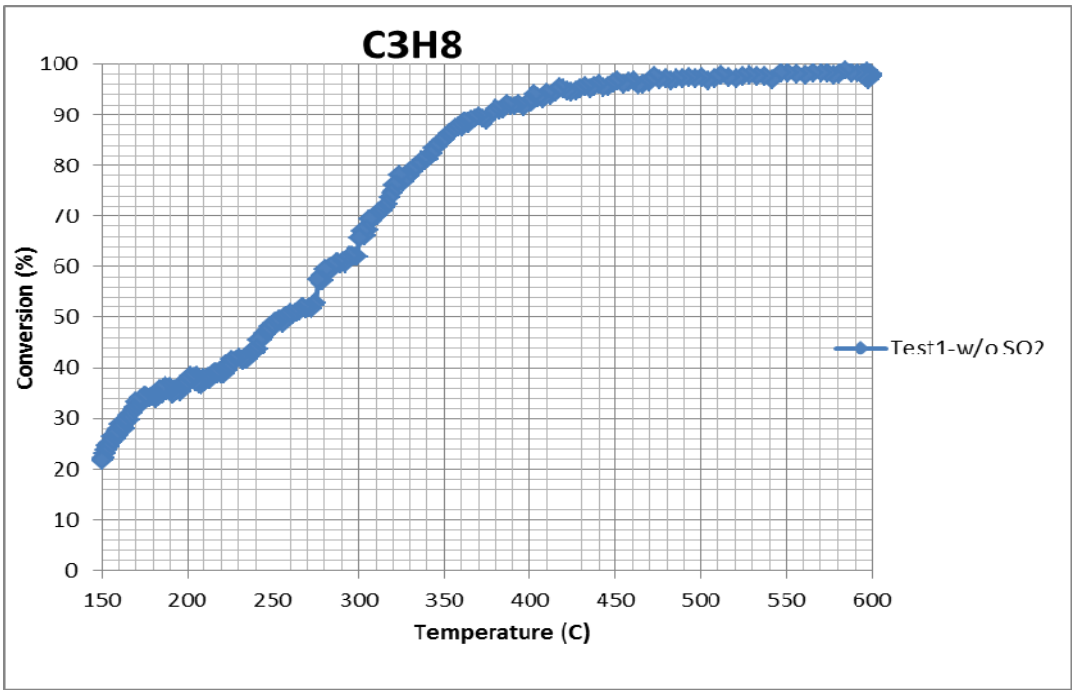

Figure 5. 16 C_3H_8 Catalytic Activity of Tofas COM Monolithic Catalyst During Test 1

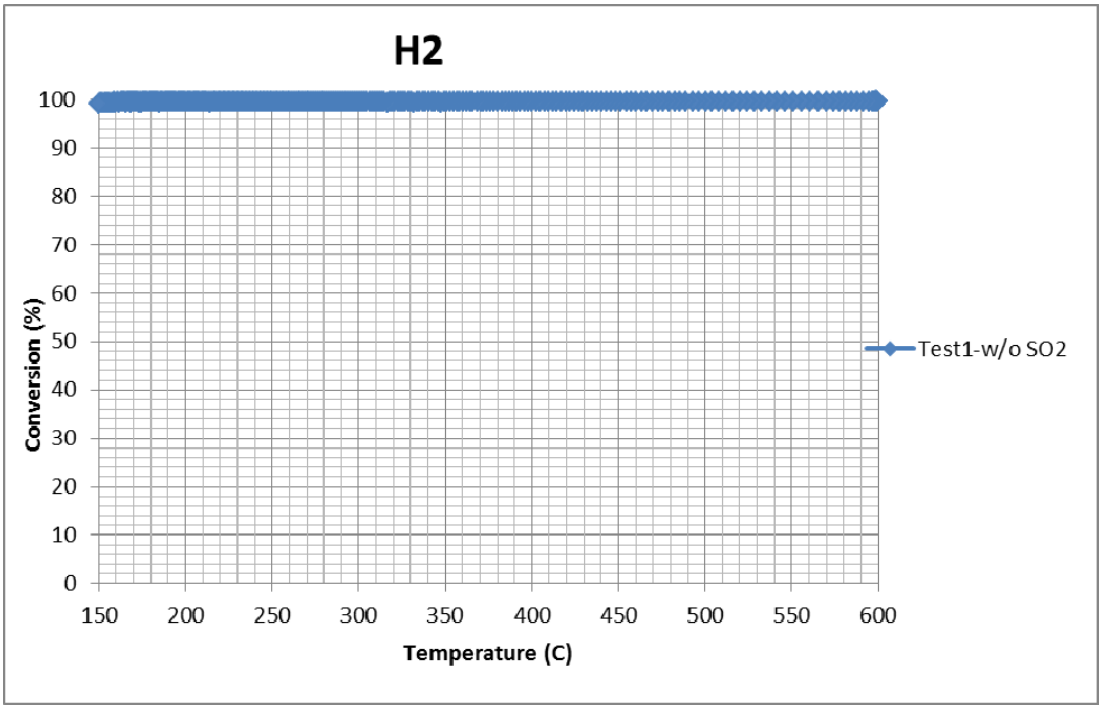

Figure 5. 17 H_2 Catalytic Activity of Tofas COM Monolithic Catalyst During Test 1

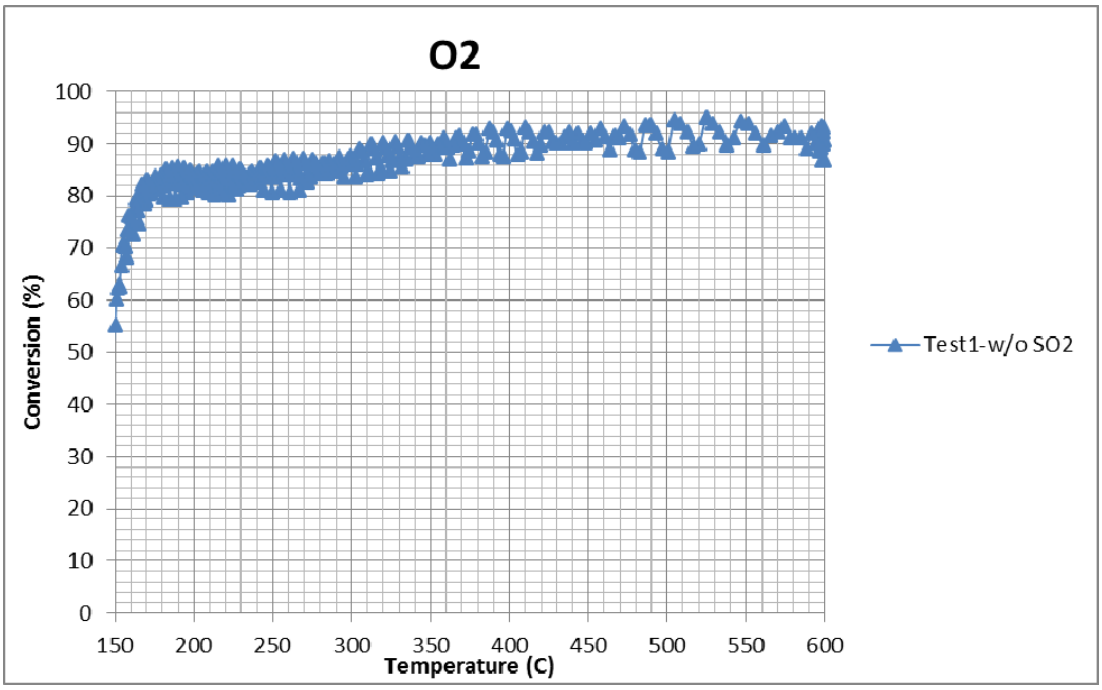

Figure 5. 18 O_2 Catalytic Activity of Tofas COM Monolithic Catalyst During Test 1

Table 5. 4 Catalytic Activity Data of Tofas Commercial Monolith Catalyst & (CZO-SI) / (AO-SI) Monolithic Catalyst During Test1

Species	Tofas Commercial Monolith Catalyst			Research Monolithic Catalyst		
	T50 (C)	Maximum Conversion (%)	Tmax (C)	T50 (C)	Maximum Conversion (%)	Tmax (C)
CO	154	100	209	200	100	478
NO	232	89	408	242	96	579
C_3H_6	224	100	300	220	100	475
C_3H_8	265	98	600	264	100	553
H_2	-	100	150	162	100	241
O_2	-	95	525	198	92	580

According to Table 5.4 , 100% conversion of CO, C_3H_6 and H_2 are achieved by the research monolithic catalyst and the commercial monolith catalyst. 100% conversion of C_3H_8 is also achieved by the research monolithic catalyst. Moreover, NO reduction ability of the research monolithic catalyst is higher than the commercial monolith catalyst.

The four catalytic activity tests of research monolithic catalyst are shown on the same graph in Figure 5.19 for CO, in Figure 5.21 for NO, in Figure 5.23 for C_3H_6, in Figure 5.25 for CO, in Figure 5.27 for C_3H_8, in Figure 5.29 for H_2 and in Figure 5.31 for O_2 . As seen in the graph, the catalytic activity during the Test 2 and Test 3 are decreased due to SO_2 effects. After Test 3 , the Test 4 is performed without SO_2. However, the catalytic activity during Test 4 is lower than the Test 1. There is a increase in the light off temperature of the catalyst during Test 4. This higher temperatures is caused from the loss in catalytic performance. The SO_2 effect on catalytic activity performance during the Test 1 and Test 4 is plotted in Figure 5.20, 5.22, 5.24, 5.26, 5.28, 5.30, 5.32.

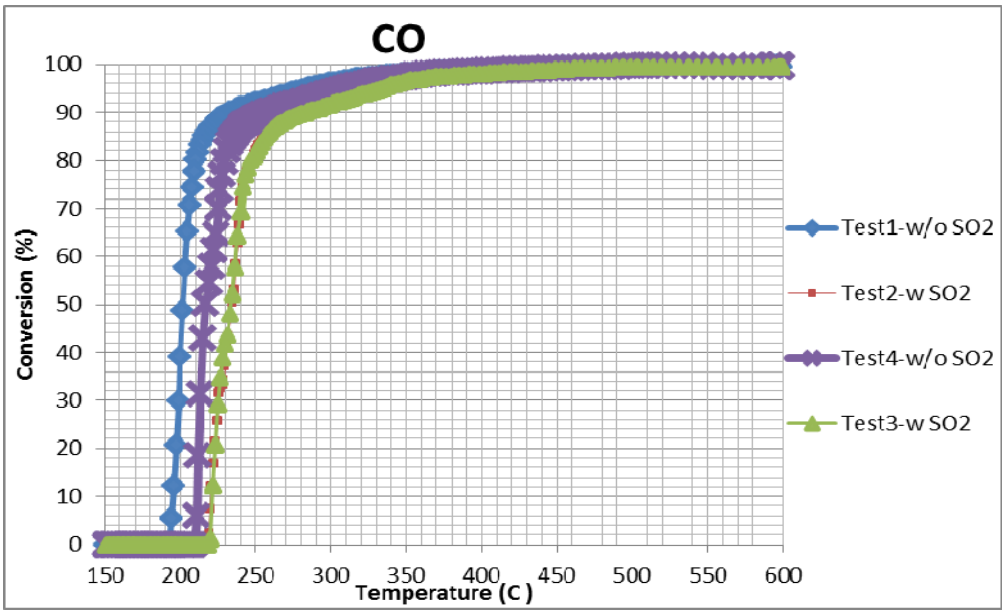

Figure 5. 19 CO Catalytic Activity of (CZO-SI) / (AO-SI) Monolithic Catalyst During Tests 1, 2, 3 & 4

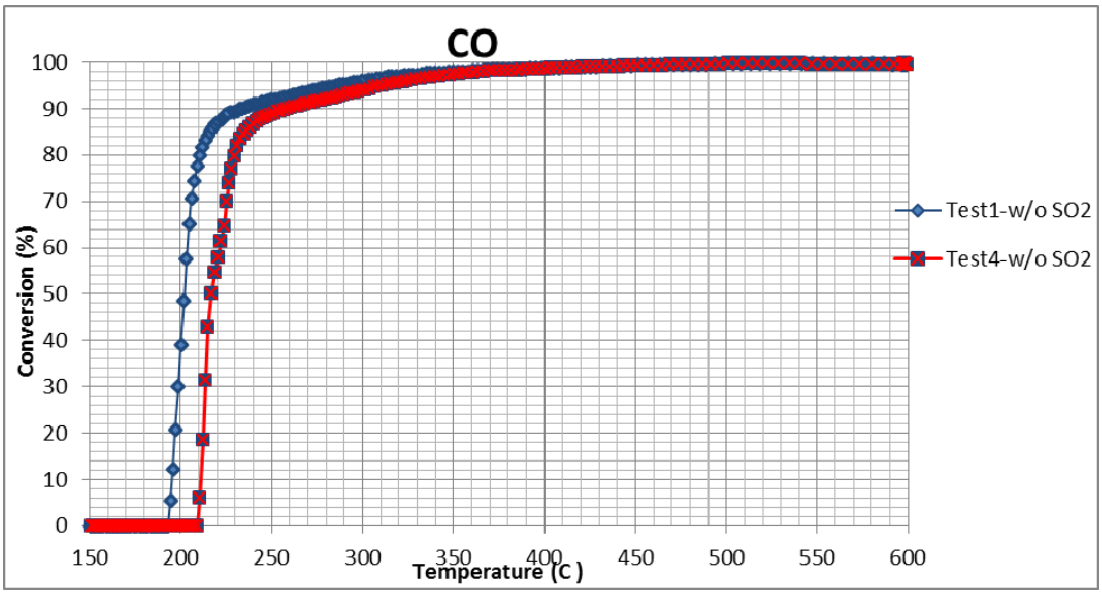

Figure 5. 20 CO Catalytic Activity of (CZO-SI) / (AO-SI) Monolithic Catalyst During Tests 1 & 4

The catalytic behavior of species are determined with comparison of T_{50}. The T_{50} values of research monolithic catalyst during the Test 1 and Test 4 are tabulated in Table 5.5. T_{50} and T_{max} values of monolithic catalyst are different from each other, while the maximum conversions are nearly same for the two tests. According to Test 1 & Test 4 result comparisons, the catalytic activity for NO and C_3H_6 is increased during SO_2 exposure. The effect SO_2 on C_3H_8 conversion is temporary, T50 of C_3H_8 is constant at Test 1 and Test 4. Other species conversions are reduced during SO_2 exposure.

Table 5. 5 Catalytic Activity Data of (CZO-SI) / (AO-SI) Monolith Catalyst During Test1 &Test4

Species	Test1			Test4		
	T50 (C)	Max. Con. (%)	Tmax (C)	T50 (C)	Max. Con. (%)	Tmax (C)
CO	200	100	478	217	100	512
NO	242	96	579	239	95.8	506
C_3H_6	220	100	475	218	100	534
C_3H_8	264	100	553	264	98	580
H_2	162	100	241	184	100	386
O_2	198	92	580	212	91	464

The four catalytic activity tests of research monolithic catalyst are shown on the same graph in Figure 5.21 for NO, in Figure 5.23 for C_3H_6, in Figure 5.25 for CO, in Figure 5.27 for C_3H_8, in Figure 5.29 for H_2 and in Figure 5.31 for O_2 . The SO_2 effect on catalytic activity performance during the Test 1 and Test 4 is plotted in Figure 5.20, 5.22, 5.24, 5.26, 5.28, 5.30, 5.32 below.

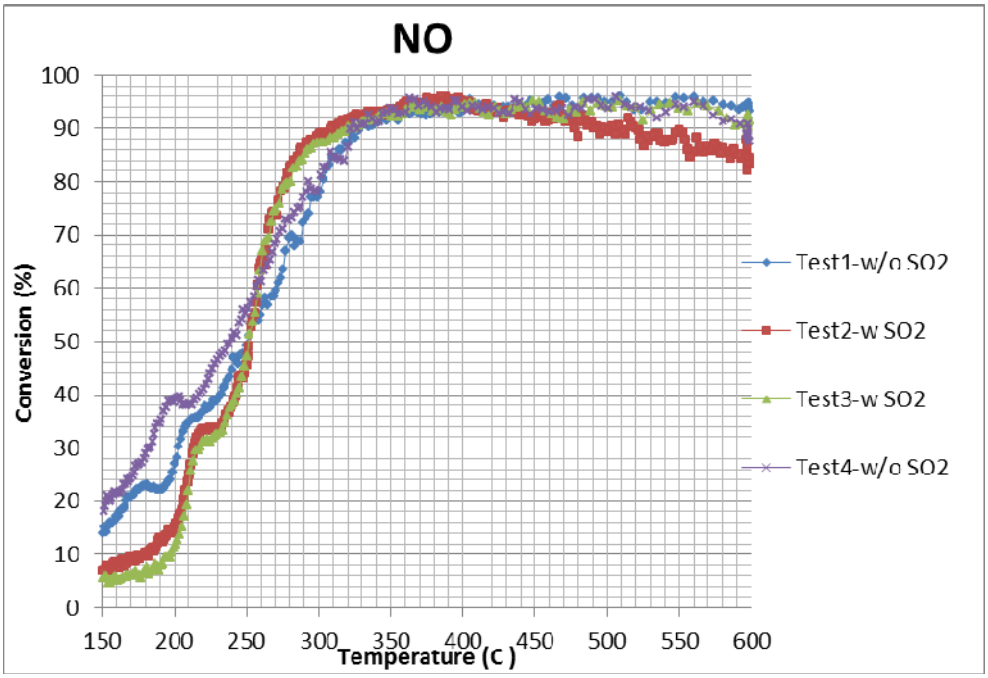

Figure 5. 21 NO Catalytic Activity of (CZO-SI) / (AO-SI) Monolithic Catalyst During Tests 1, 2, 3 & 4

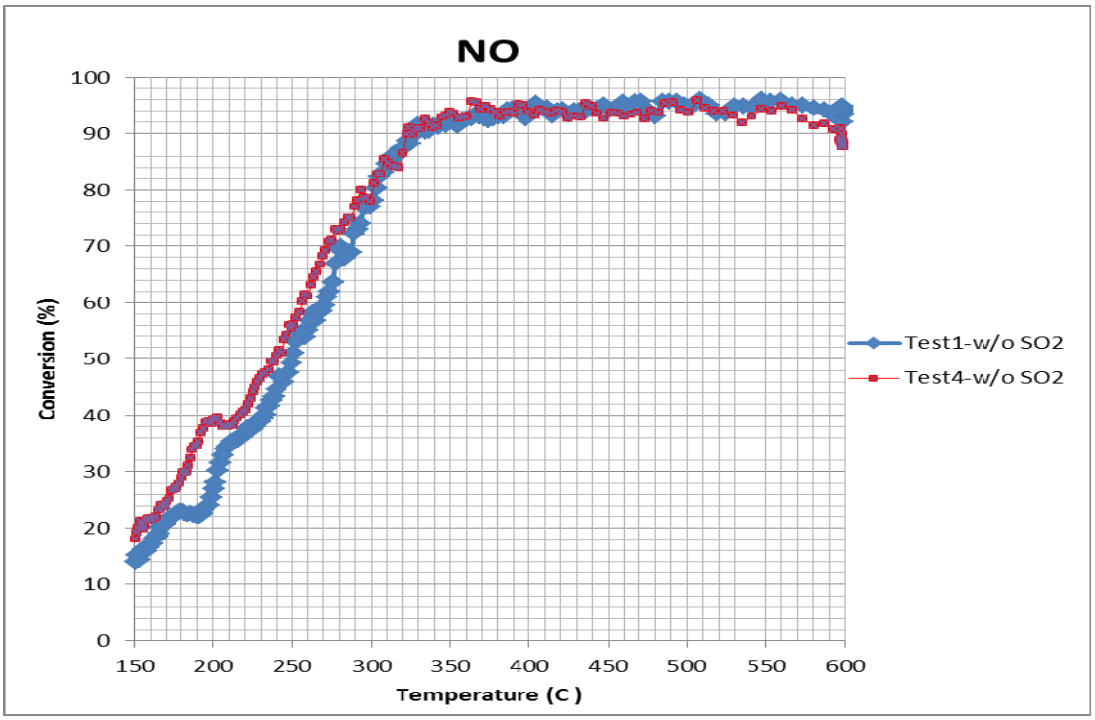

Figure 5. 22 NO Catalytic Activity of (CZO-SI) / (AO-SI) Monolithic Catalyst During Tests 1 & 4

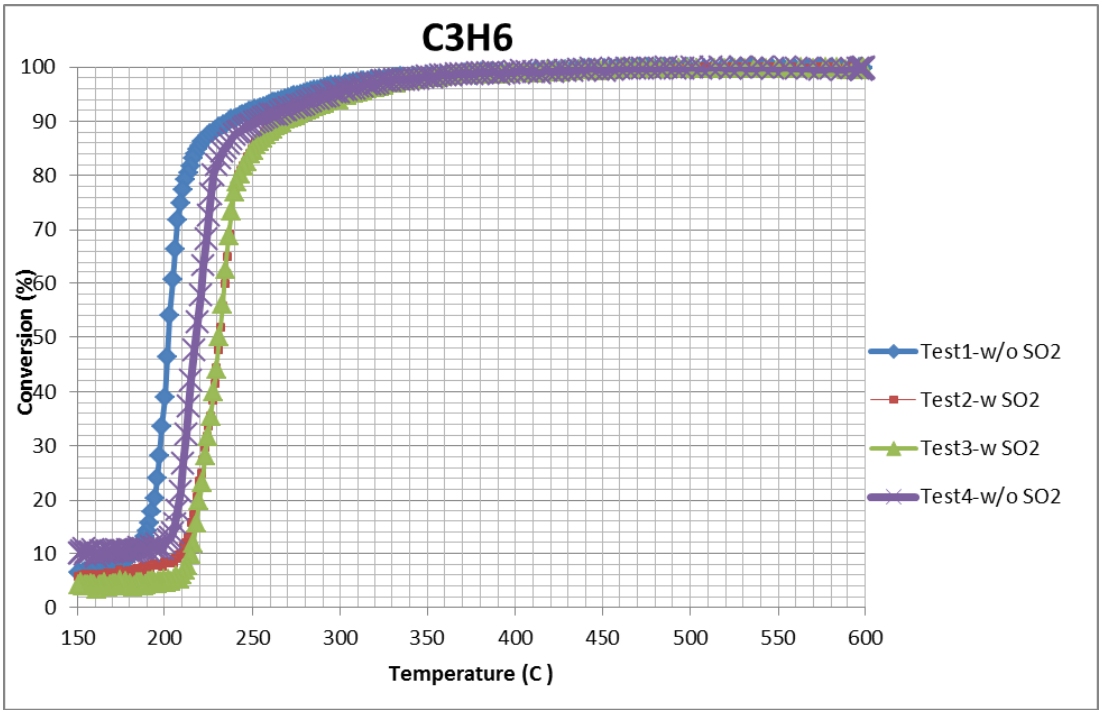

Figure 5. 23 C_3H_6 Catalytic Activity of (CZO-SI) / (AO-SI) Monolithic Catalyst During Tests 1, 2, 3 & 4

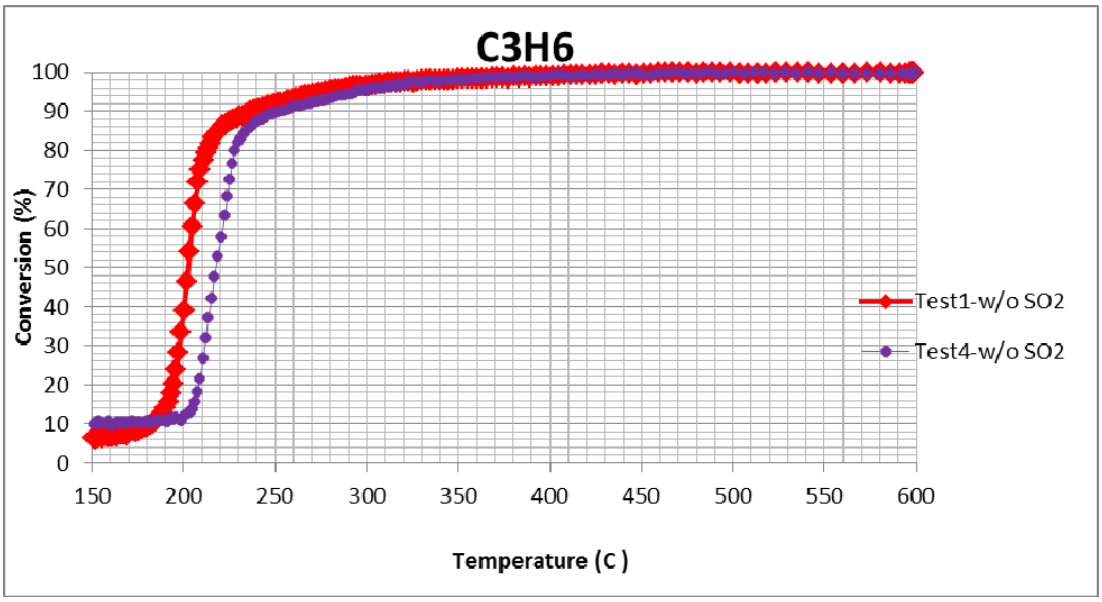

Figure 5. 24 C_3H_6 Catalytic Activity of (CZO-SI) / (AO-SI) Monolithic Catalyst During Tests 1, & 4

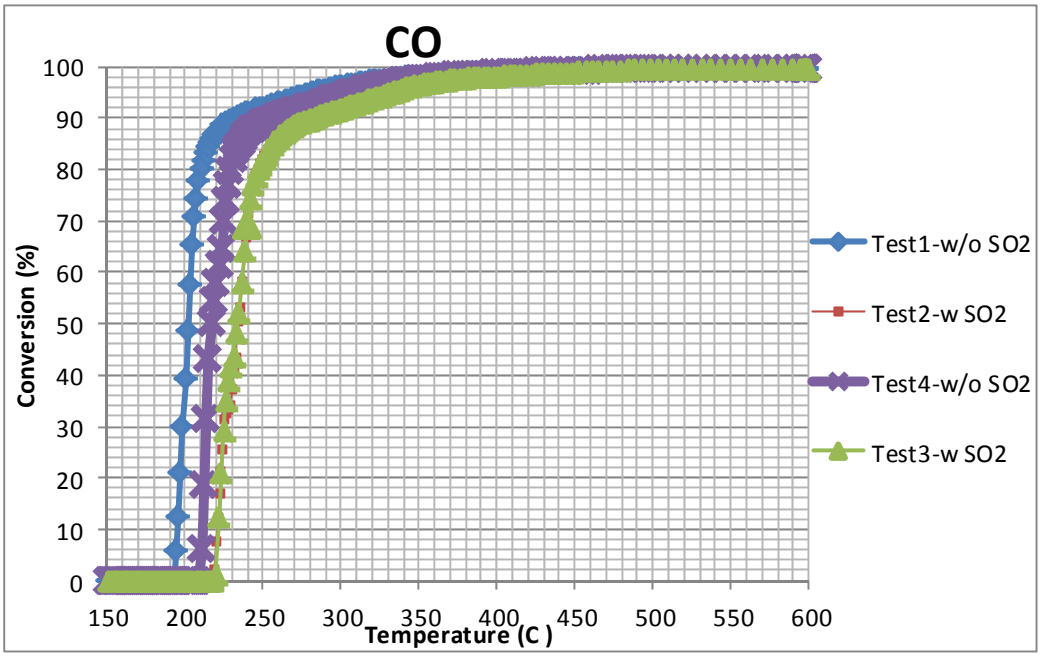

Figure 5. 25 CO Catalytic Activity of (CZO-SI) / (AO-SI) Monolithic Catalyst During Tests 1, 2, 3 & 4

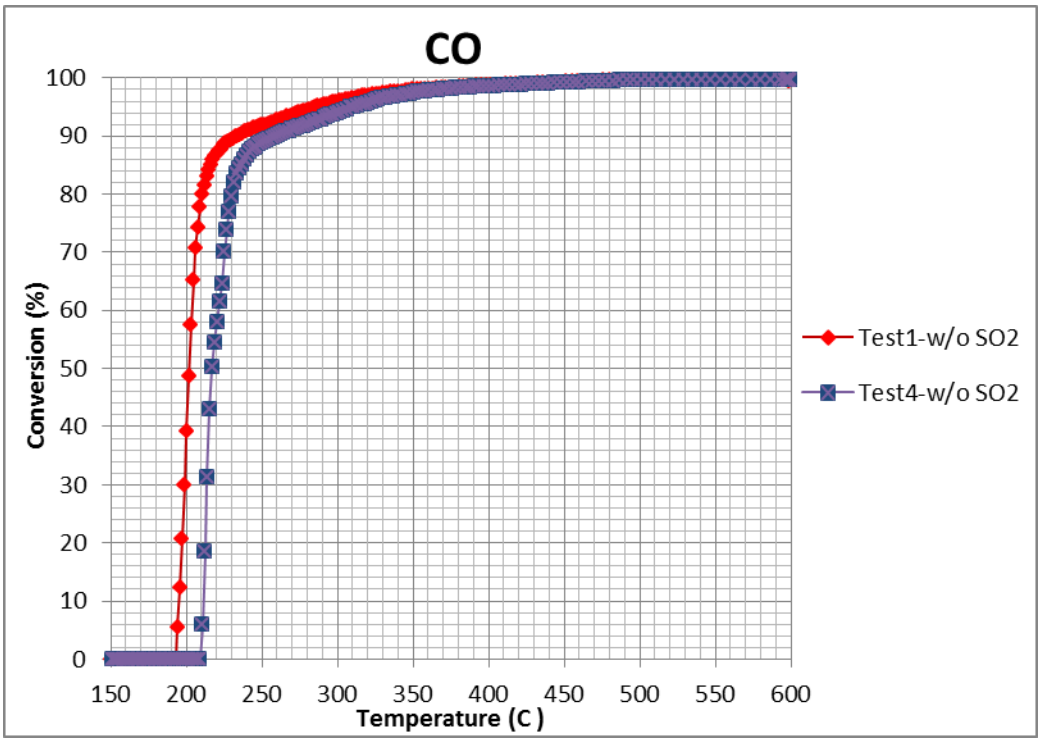

Figure 5. 26 CO Catalytic Activity of (CZO-SI) / (AO-SI) Monolithic Catalyst During Tests 1 & 4

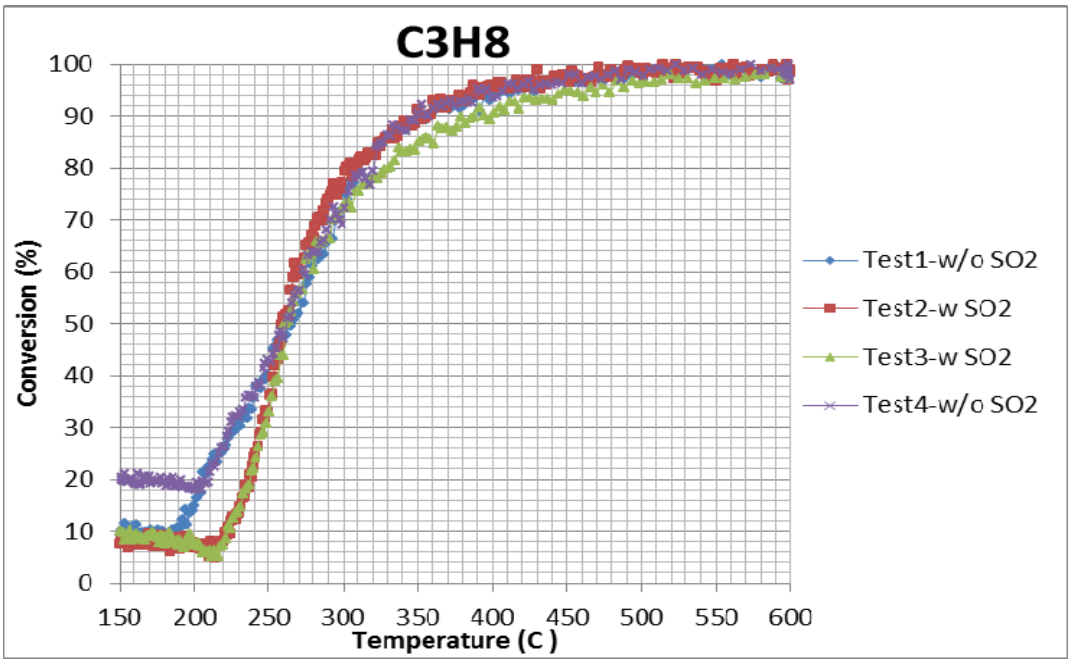

Figure 5. 27 C_3H_8 Catalytic Activity of (CZO-SI) / (AO-SI) Monolithic Catalyst During Tests 1, 2, 3 & 4

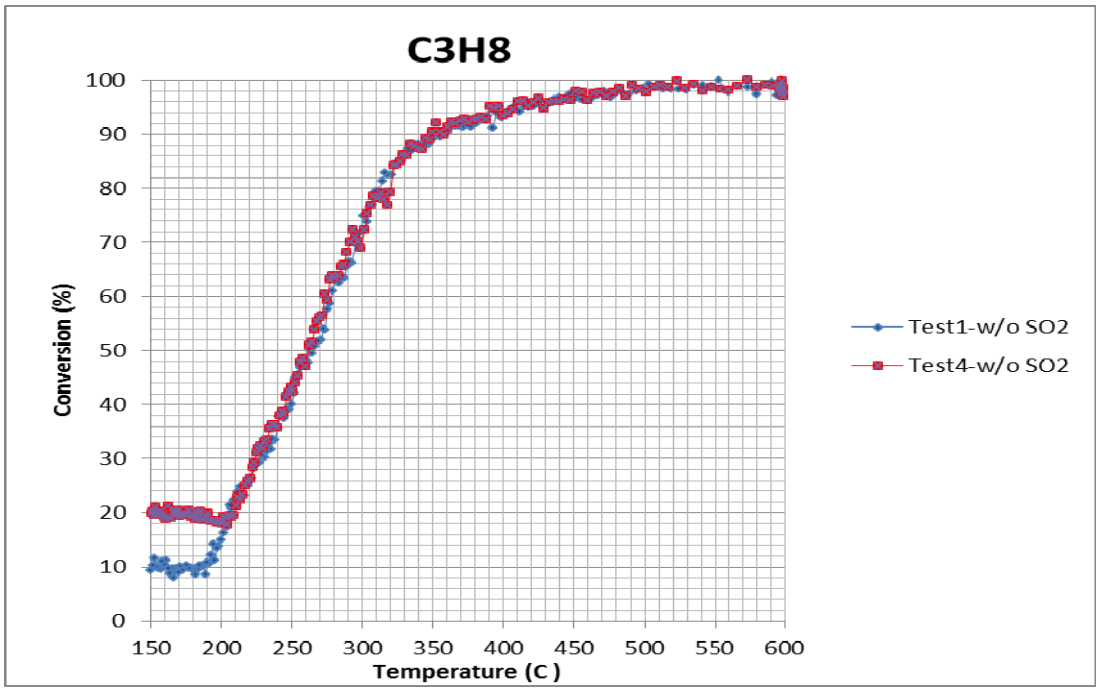

Figure 5. 28 C_3H_8 Catalytic Activity of (CZO-SI) / (AO-SI) Monolithic Catalyst During Tests 1 & 4

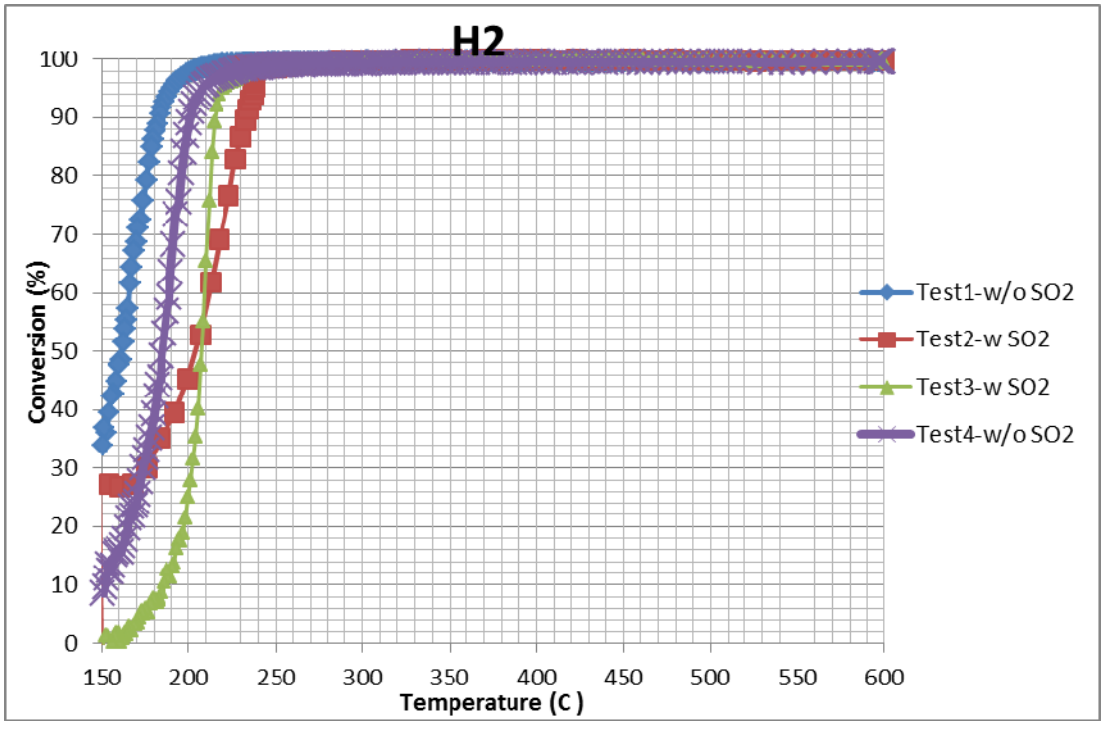

Figure 5. 29 H_2 Catalytic Activity of (CZO-SI) / (AO-SI) Monolithic Catalyst During Tests 1, 2, 3 & 4

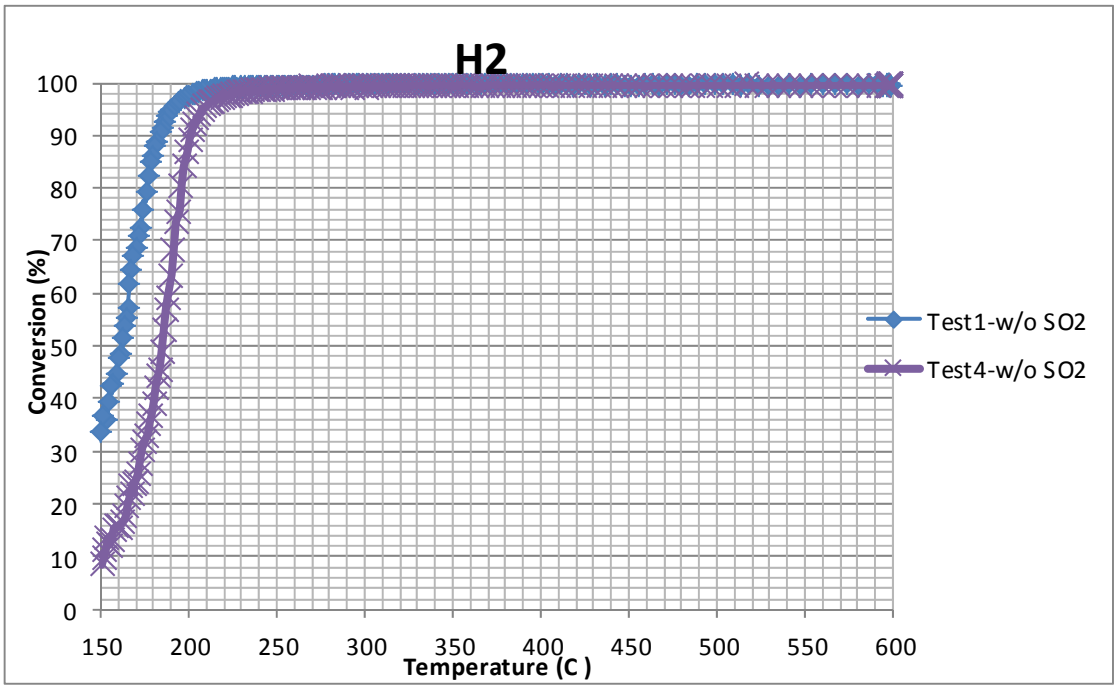

Figure 5. 30 H_2 Catalytic Activity of (CZO-SI) / (AO-SI) Monolithic Catalyst During Tests 1 & 4

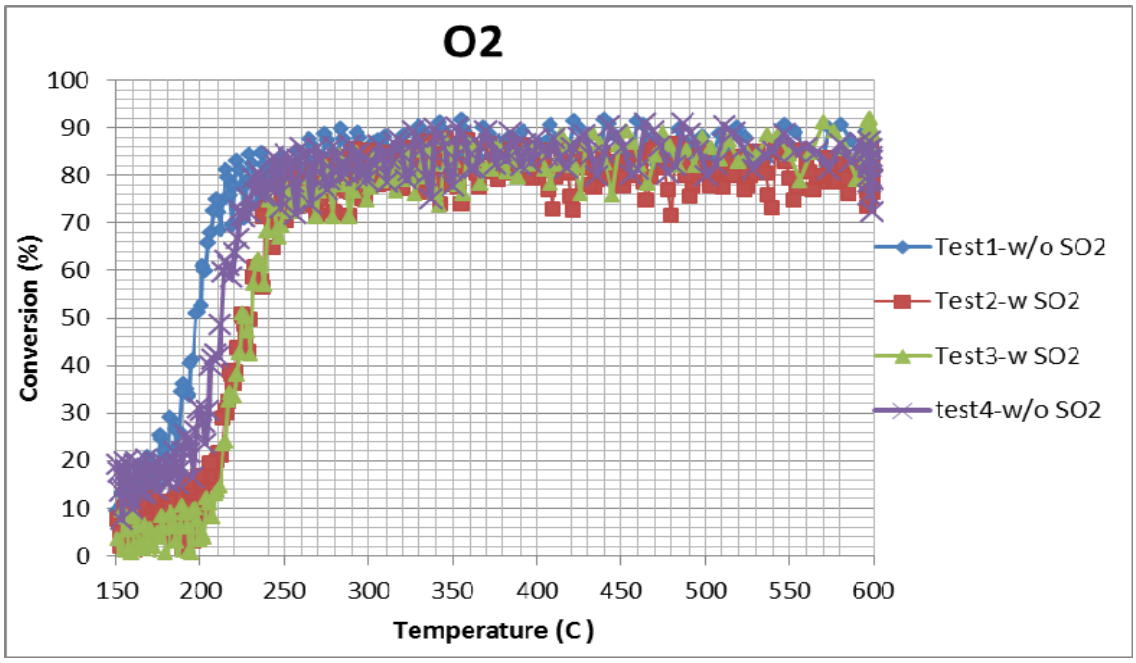

Figure 5. 31 O_2 Catalytic Activity of (CZO-SI) / (AO-SI) Monolithic Catalyst During Tests 1, 2, 3 & 4

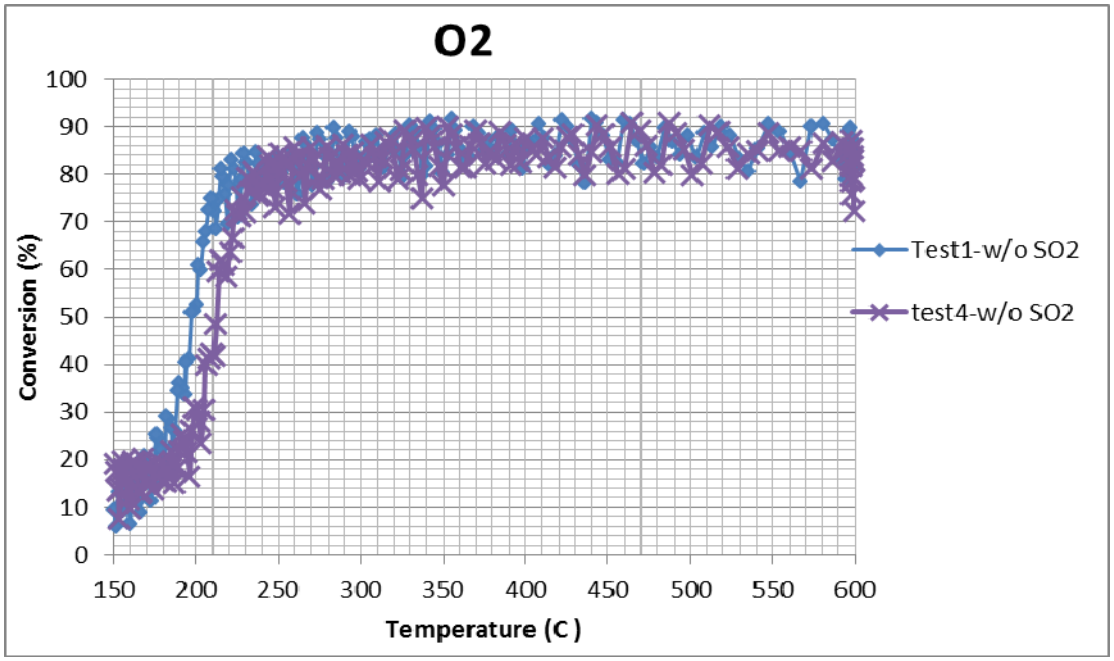

Figure 5. 32 O_2 Catalytic Activity of (CZO-SI) / (AO-SI) Monolithic Catalyst During Tests 1 & 4

$$\Delta T50 = T50(Test\,4) - T50(Test\,1) \qquad (5.1)$$

According to ΔT50 results, the negative values of ΔT50 shows that there is an improvement in the catalytic activity for NO and C_3H_6 during SO_2 exposure. The effect SO_2 on C_3H_8 conversion is temporary, T50 of C_3H_8 is constant at Test 1 and Test 4. CO, H_2 and O_2 conversions are reduced during SO_2 exposure.

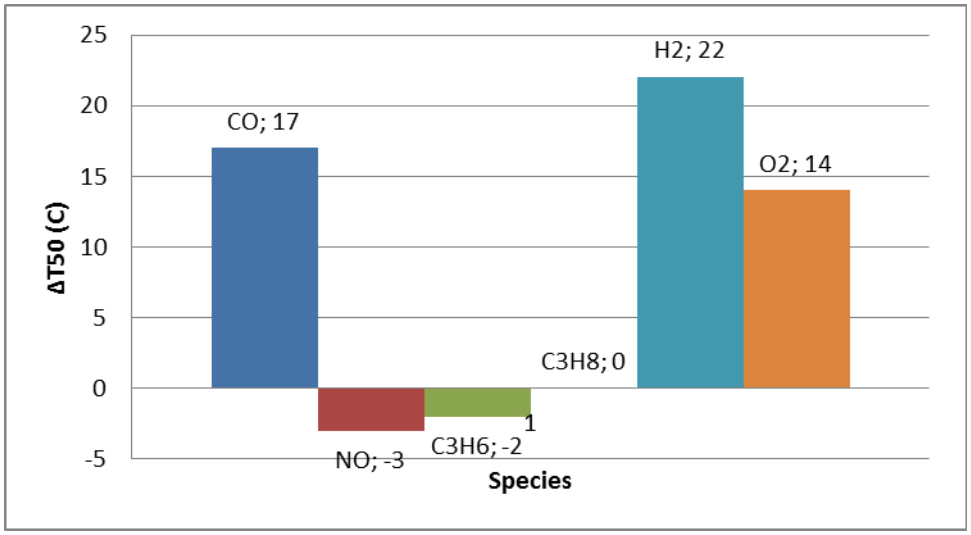

Figure 5. 33 ΔT50 (˚C) of (CZO-SI) / (AO-SI) Monolithic Catalyst During Tests 1 & 4

Three way catalysts contains noble metals as Pt, Pd and Rh. For reduction of NOx Rh is used, and for oxidations of CO and HCs Pd is used (Ulla, 2003) [29]. During the SO_2 exposure, Rh is more resistant than Pd. Because sulphur reversibly adsorbed on Rh surface. Rh would gain again catalytic activity when SO_2 is removed from system. On the other hand, Pd is poisoned by SO_2 and lost catalytic activity due to the migration of sulphur into bulk Pd Torbati (2009) [28].

According to these background information, Pd is poisoned by sulphur. Thus, catalytic activity of monolithic catalyst is reduced for CO. On the other hand, Rh is more resistant to sulphur than Pd, so NOx conversion is increased .

Tofas commercial monolithic catalyst with the same dimensions of laboratory scale monoliths, is analyzed with the same catalytic activity test procedures with research monolithic catalyst. The catalytic activity data during Test 1 and Test 4 are given in Table 5.6 .

Table 5. 6 Catalytic Activity Data of Tofas COM Monolith Catalyst During Test1 & Test 4

Species	Test1			Test4		
	T50 (˚C)	Max. Con. (%)	Tmax (˚C)	T50 (˚C)	Max. Con. (%)	Tmax (˚C)
CO	154	100	209	232	100	600
NO	232	89	408	261	89	419
C_3H_6	224	100	300	230	100	398
C_3H_8	265	98	600	327	100	597
H_2	-	100	150	180	100	230
O_2	-	95	525	230	90	550

The light-off temperature differences for all species after SO_2 exposure are higher although amount of nobel metal is higher. In Figure 5.34 $\Delta T50$ values of each species are plotted.

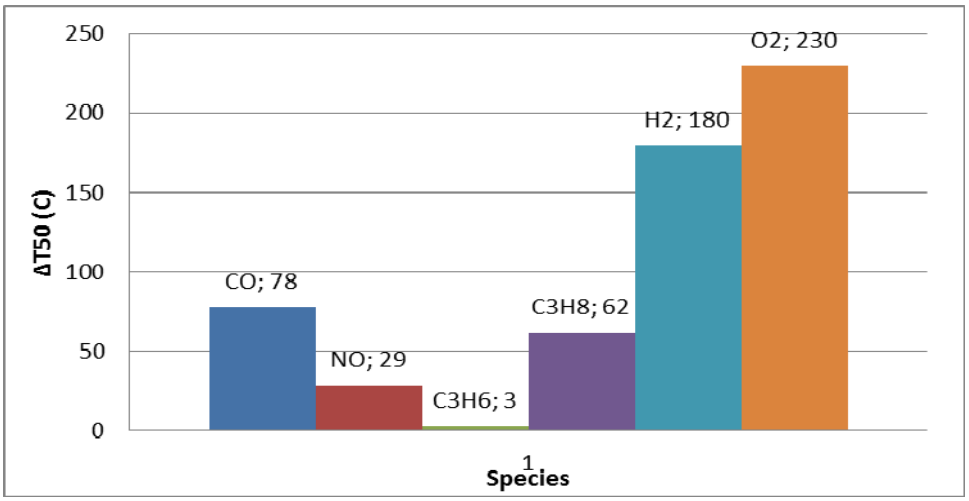

Figure 5. 34 ΔT50 (˚C) of Tofas Monolithic Catalyst During Tests 1 & 4

The four catalytic activity tests of Tofas monolithic catalyst are shown on the same graph in Figure 5.33, Figure 5.35, Figure 5.37, Figure 5.39, Figure 5.41 and Figure 5.43. The SO_2 effect on catalytic activity performance during the Test 1 and Test 4 is also plotted in Figure 5.34, Figure 5.36, Figure 5.38, Figure 5.40 and Figure 5.42 below. According to graph, Tofas catalyst is more sensitive to SO_2 poisoning.

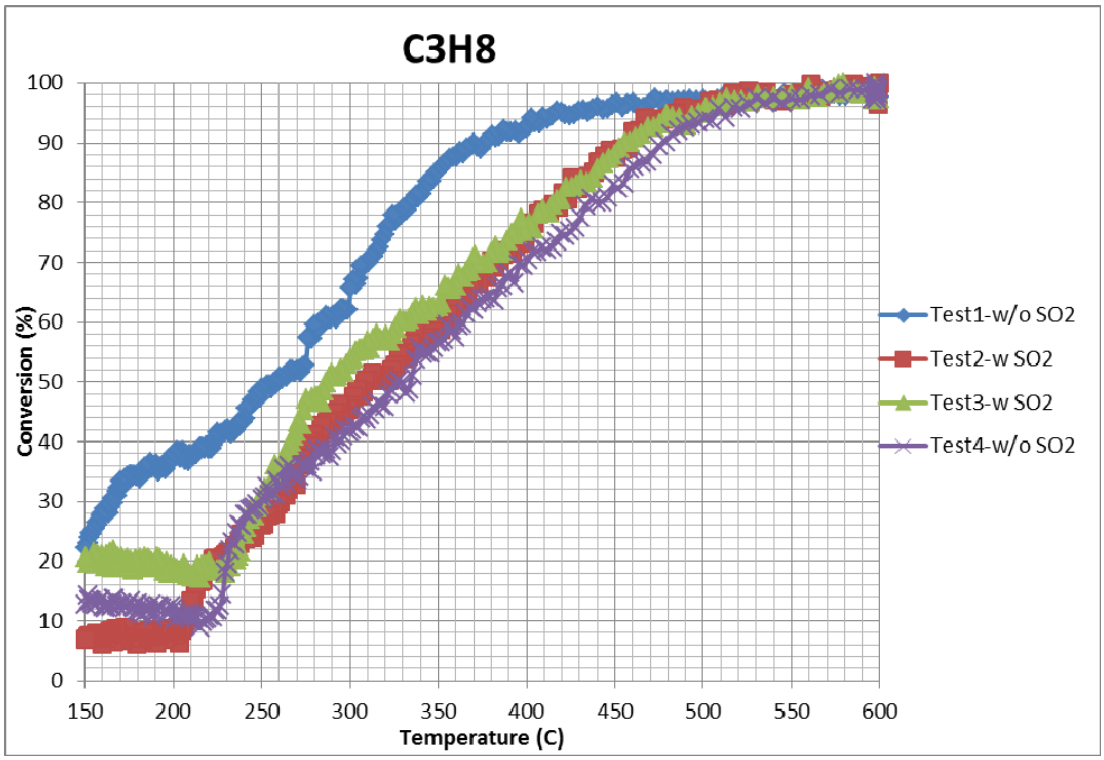

Figure 5. 35 C_3H_8 Catalytic Activity of Tofas COM Monolithic Catalyst During Tests 1, 2, 3 & 4

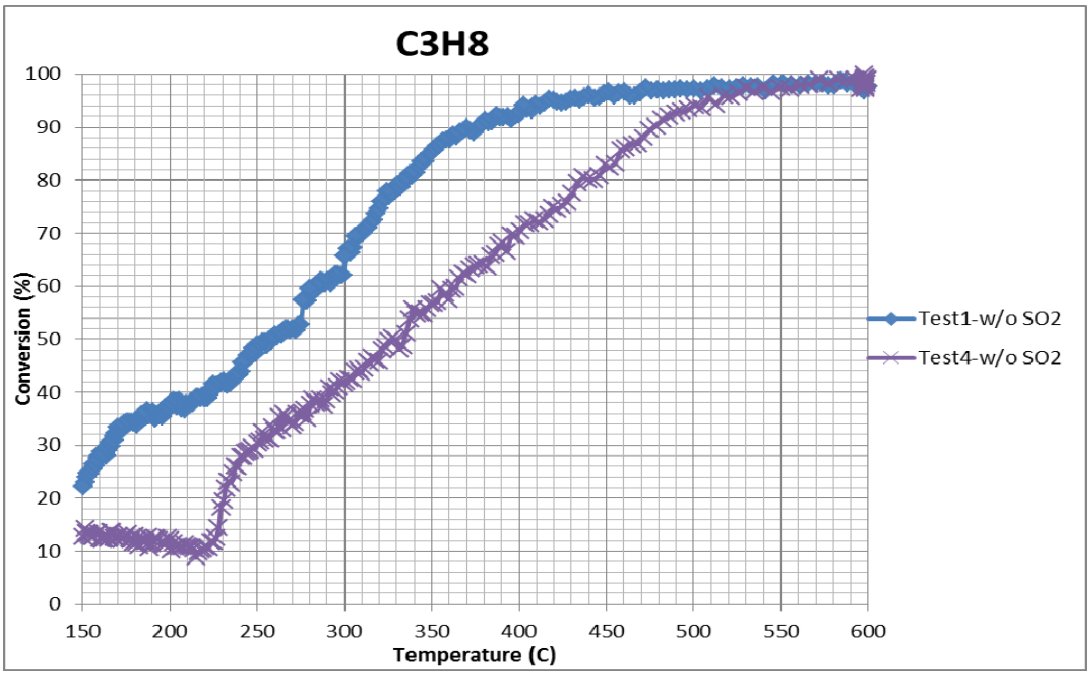

Figure 5. 36 C_3H_8 Catalytic Activity of Tofas COM Monolithic Catalyst During Tests 1 & 4

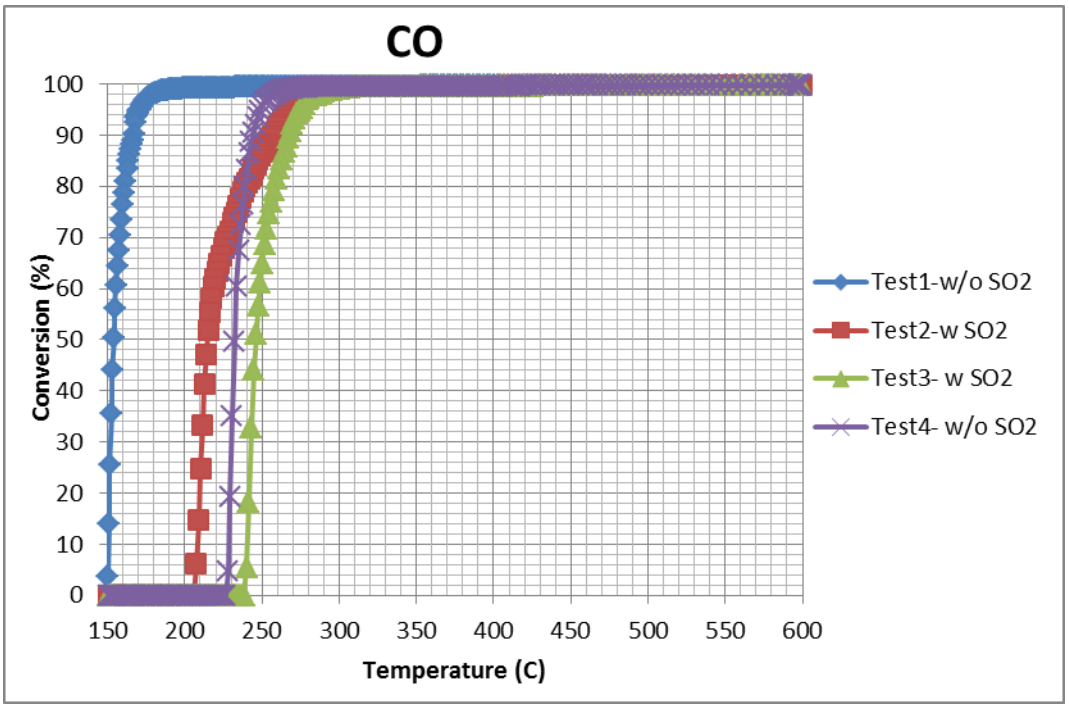

Figure 5. 37 CO Catalytic Activity of Tofas COM Monolithic Catalyst During Tests 1, 2, 3 & 4

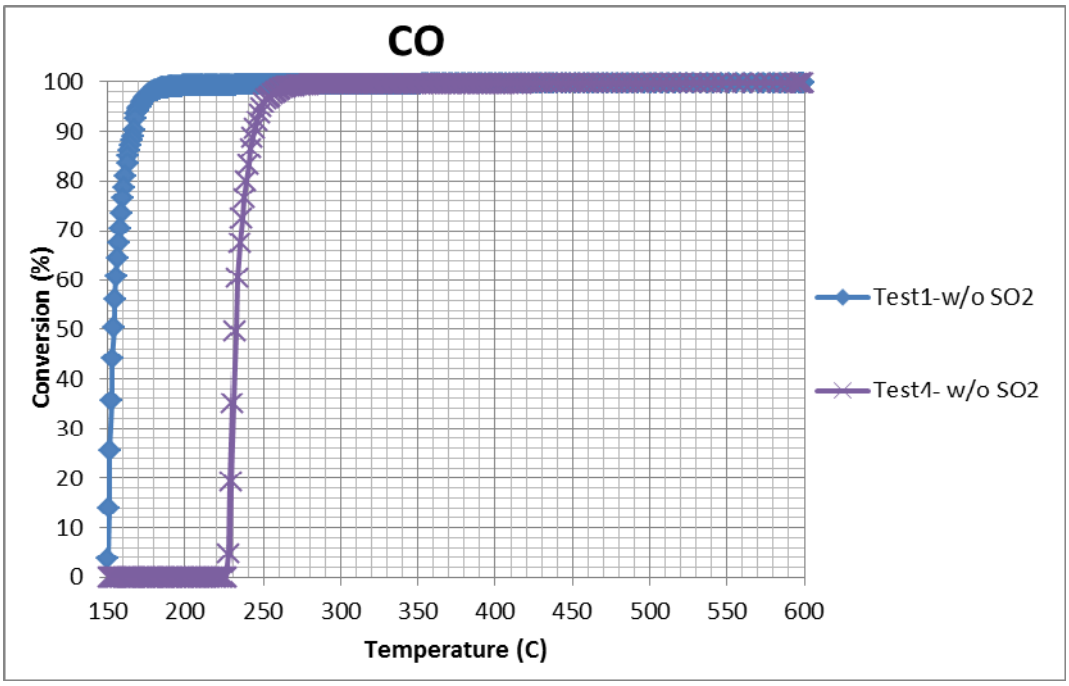

Figure 5. 38 CO Catalytic Activity of Tofas COM Monolithic Catalyst During Tests 1 & 4

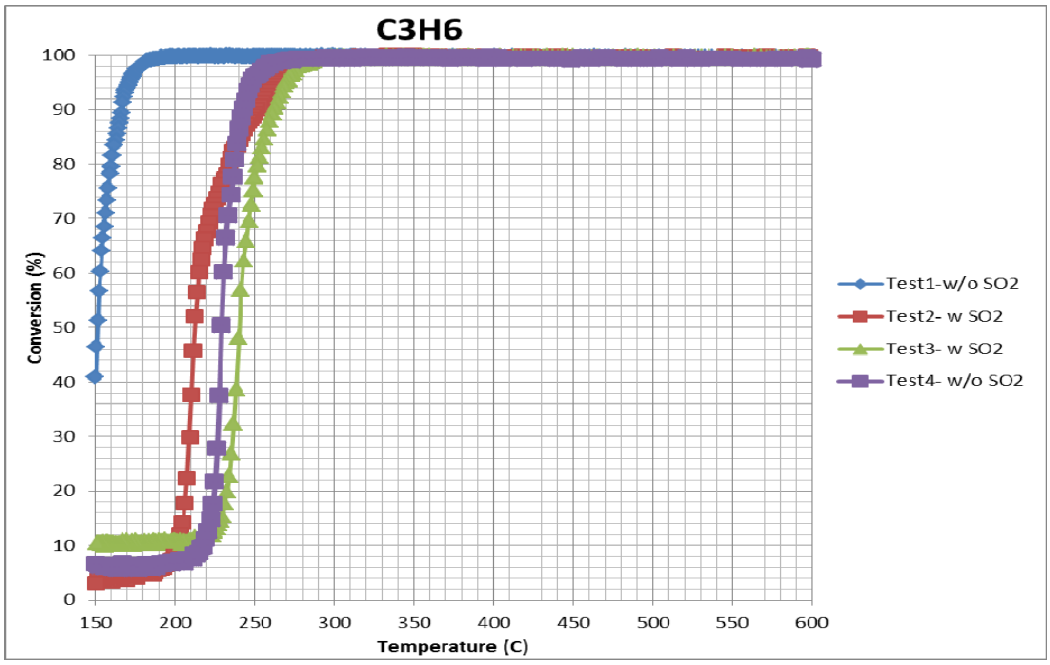

Figure 5. 39 C_3H_6 Catalytic Activity of Tofas COM Monolithic Catalyst During Tests 1, 2, 3 & 4

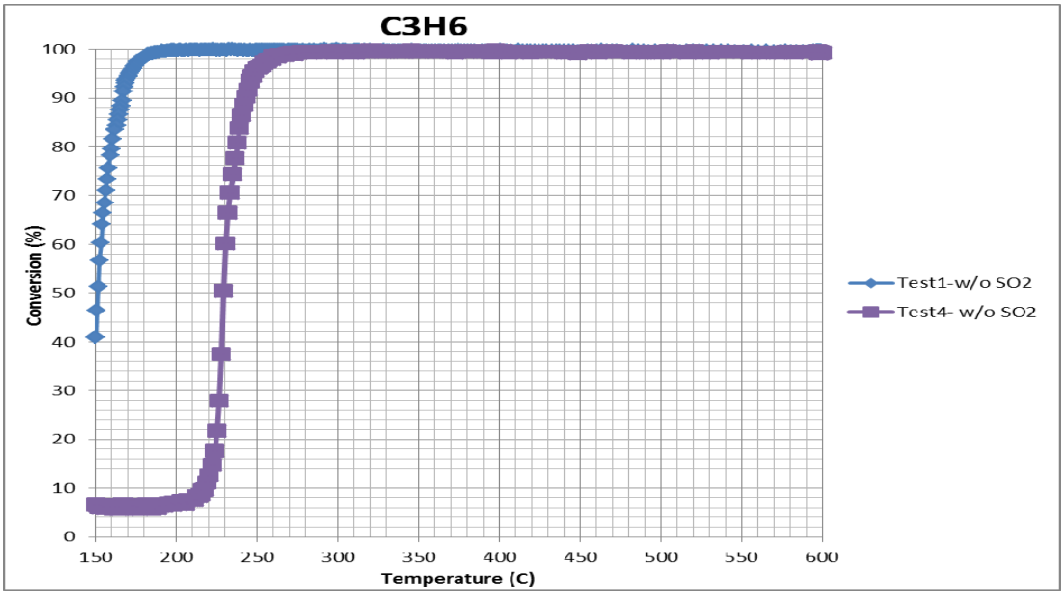

Figure 5. 40 C_3H_6 Catalytic Activity of Tofas COM Monolithic Catalyst During Tests 1 & 4

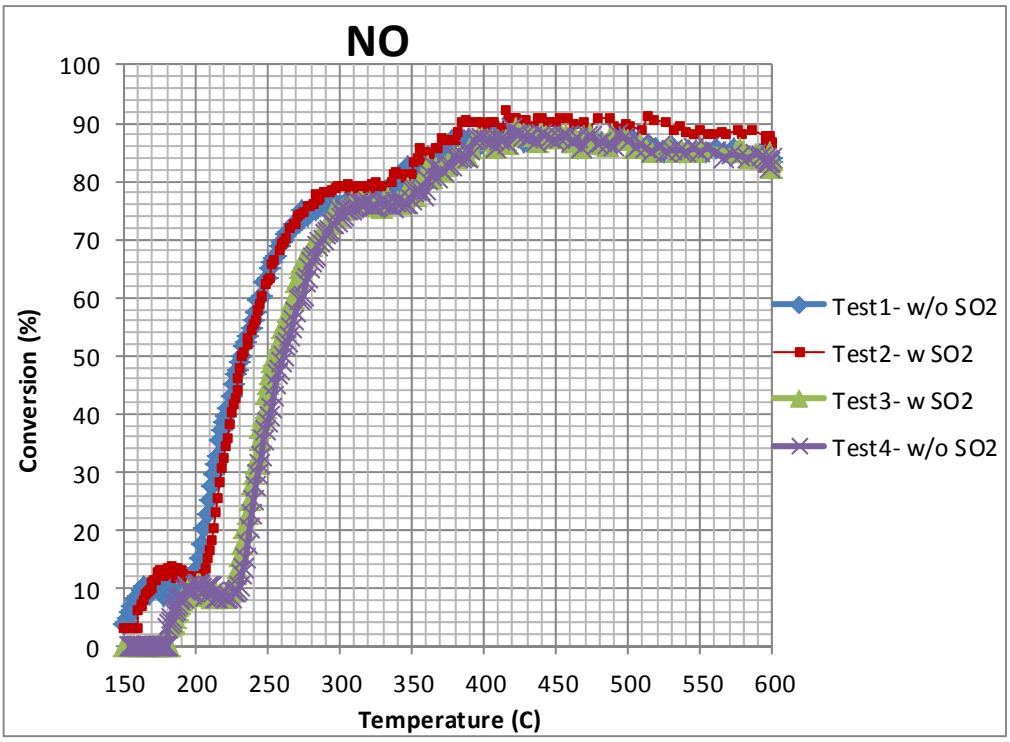

Figure 5. 41 NO Catalytic Activity of Tofas COM Monolithic Catalyst During Tests 1, 2, 3 & 4

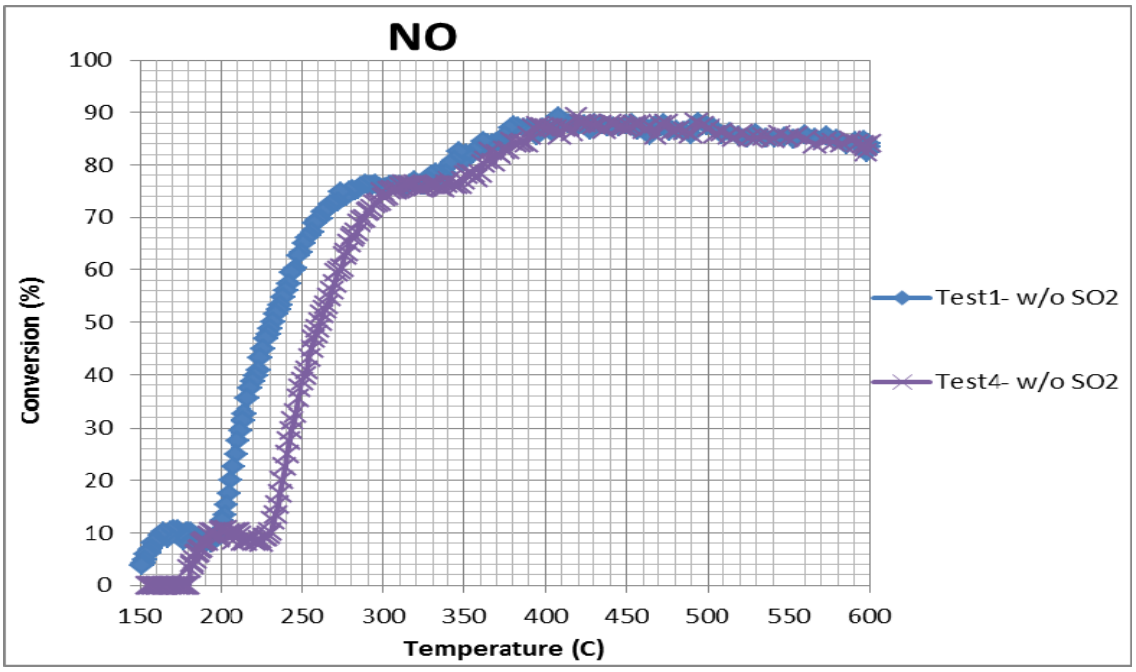

Figure 5. 42 NO Catalytic Activity of Tofas COM Monolithic Catalyst During Tests 1 & 4

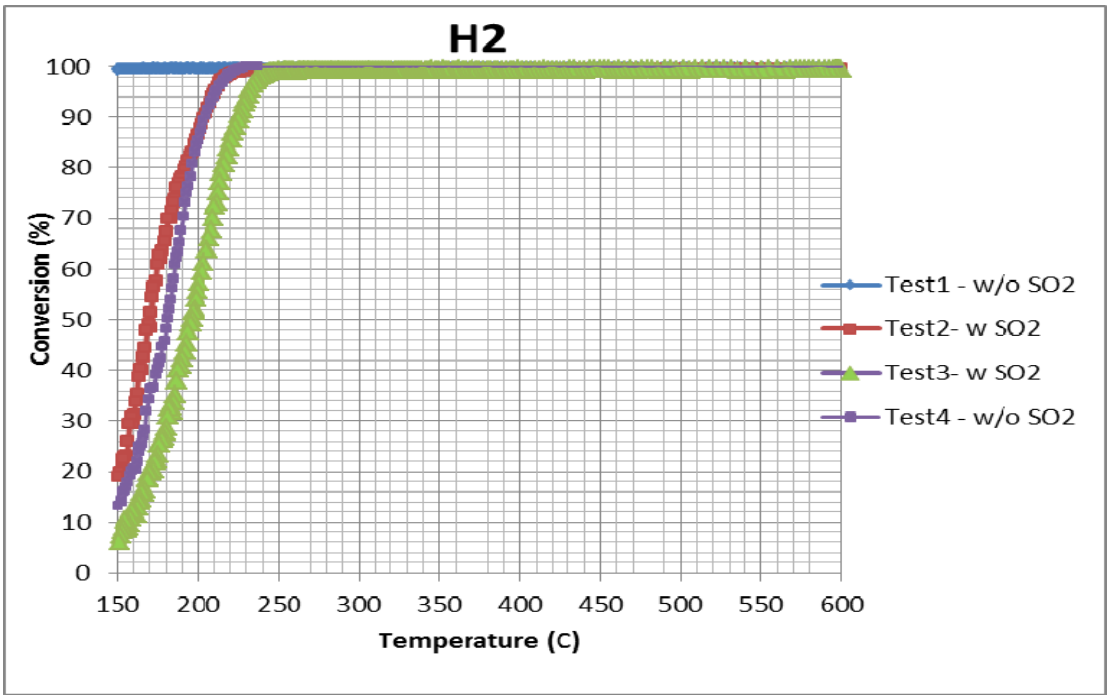

Figure 5. 43 H_2 Catalytic Activity of Tofas COM Monolithic Catalyst During Tests 1, 2, 3 & 4

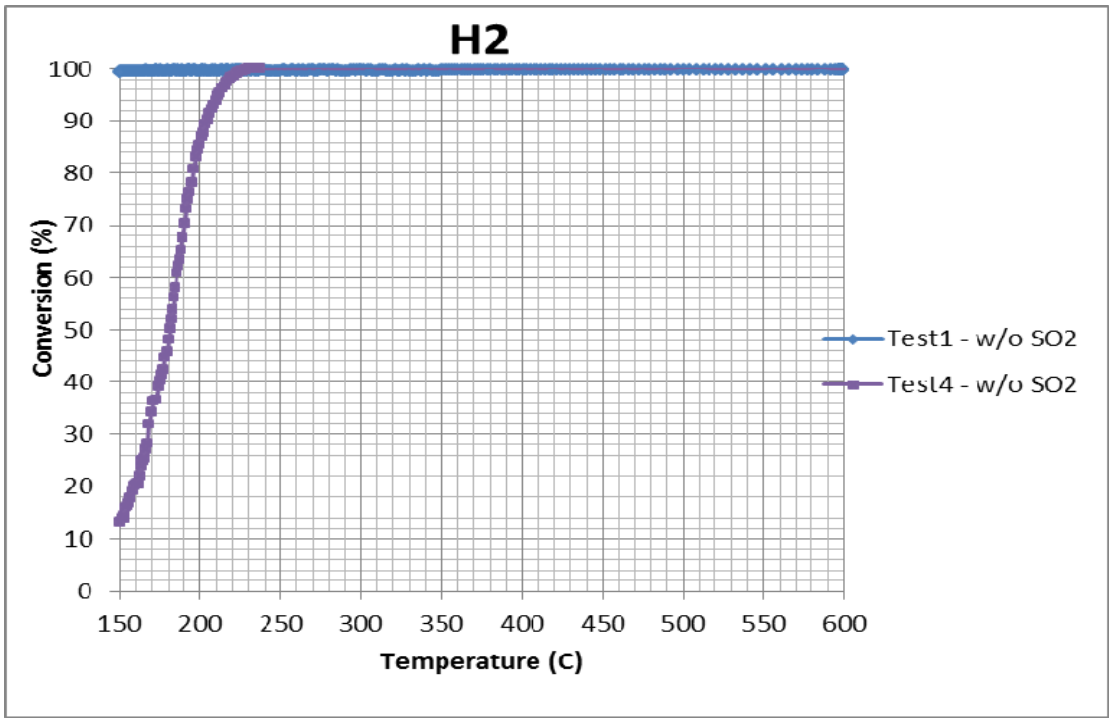

Figure 5. 44 H_2 Catalytic Activity of Tofas COM Monolithic Catalyst During Tests 1 & 4

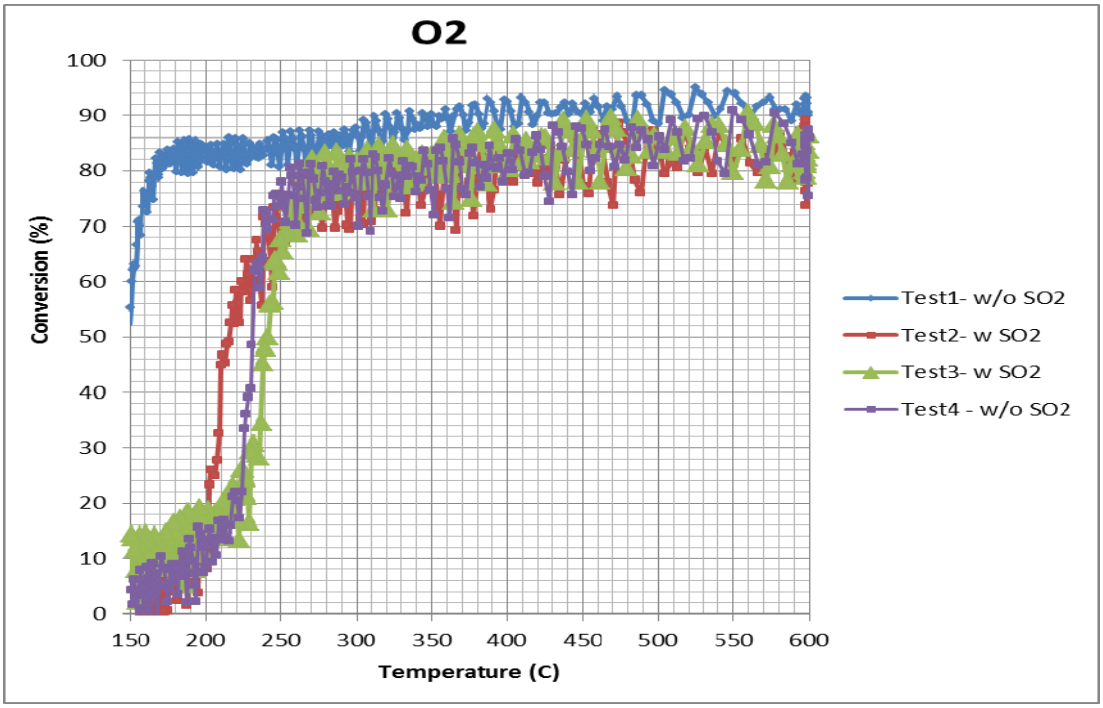

Figure 5. 45 O_2 Catalytic Activity of Tofas COM Monolithic Catalyst During Tests 1, 2, 3 & 4

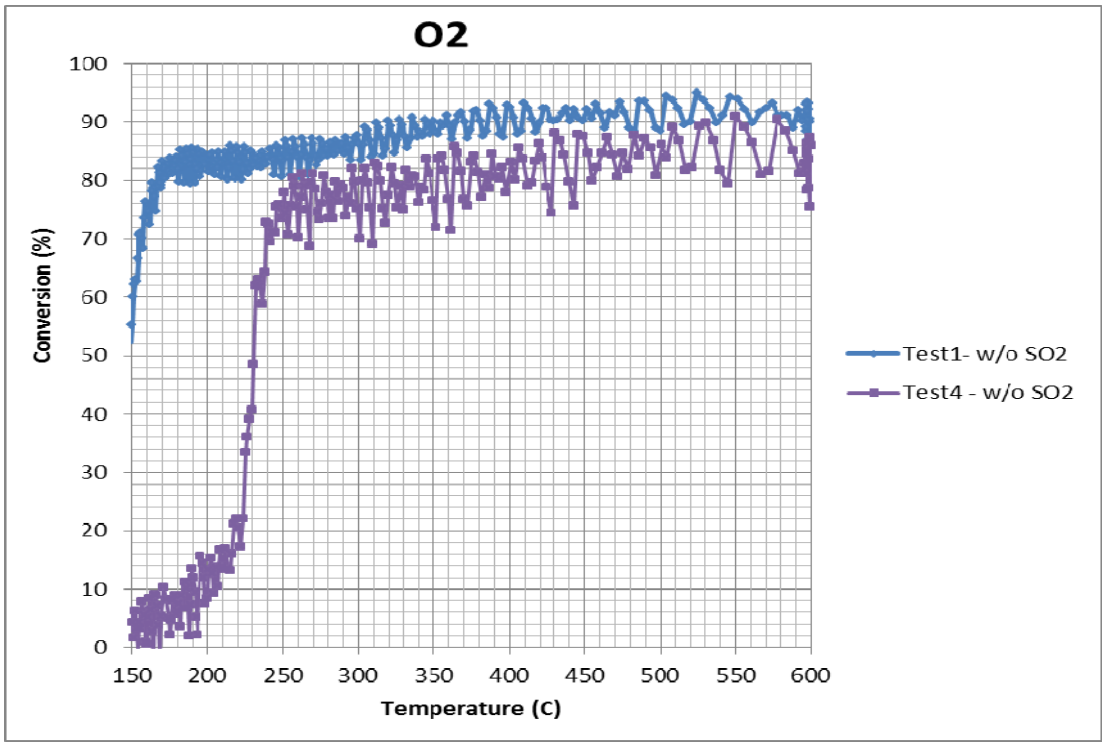

Figure 5. 46 O_2 Catalytic Activity of Tofas COM Monolithic Catalyst During Tests 1 & 4

The change in T50 data during Test 1 and Test 4 are evaluated. After the four tests, a permanent loss of catalytic performance occurred for CO, H_2 and O_2. The (CZO-SI) / (AO-SI) research monolithic catalyst has the lowest level of catalytic performance loss for these species, whereas Tofas monolithic catalyst has the highest level of catalytic performance loss. For the research monolithic catalyst activity for NO and C_3H_6, it shows better catalytic activity for NO and C_3H_6 during the Test 4 than during the Test 1. There is not any improvement in catalytic activity of research monolithic catalysts for C_3H_8. It can be stated that the research catalyst do not lose their catalytic activity for C_3H_8 during the four tests. However, Tofas monolithic catalyst shows decrease in the catalytic activity of NO which indicates the highest loss in catalytic activity for NO. This results will depend on their noble metal impregnation method. Tofas commercial catalysts will be washcoated by co-impregnated method.

The research monolithic catalyst and Tofas commercial monolithic catalyst are compared according to their performances during the Test 2 and Test 3. Tofas monolithic catalyst contains highest total metal as 30.0 g/ft^3, it shows the higher catalytic performance than the research monolithic catalyst with total metal content of 22.9 g/ft^3, except C_3H_8 conversion. It is expected that higher catalytic performance are obtained by the higher amounts of metals. Both research monolithic catalyst and Tofas monolithic catalyst reach to higher than 90% conversion of C_3H_8. The research monolithic catalyst activity is higher than Tofas monolithic catalyst. On the other hand research monolithic catalyst with lowest total metal content of 22.9 g/ft^3 shows the lowest T50 values for CO, NO, C_3H_6, C_3H_8 H_2 and O_2. As a result, research monolithic catalyst with lower total metal content shows higher catalytic performance in general.

The research monolithic catalysts do not lose their catalytic activity as much as Tofas commercial monolithic catalyst. The research monolithic catalyst has lower total metal content than Tofas commercial monolithic catalyst. Thus, the catalytic activity of this catalyst can be accepted better than Tofas commercial monolithic catalyst. In addition to this, the research monolithic catalyst is more resistant against exposure to SO_2. In consequence of these studies, research monolithic catalysts are decided to be studied further.

Monolithic catalytic activity depends on washcoat homogeneity and amount, total metal contents and many other properties. Therefore, each monolithic catalysts have specific activity performance. For these reasons, the catalytic activity tests are evaluated and compared with two Tofas commercial monolithic catalyst pieces to see reliability of dynamic test. Commercial catalyst is chosen for the reliability test due to homogeneous washcoating and being more identical. The catalytic activity data of two Tofas commercial catalyst pieces are given in Table 5.7 and the conversion vs. temperature curves for each species are combined in Figures 5.47, 5.48, 5.49, 5.50, 5.51 and 5.52.

Table 5. 7 Catalytic Activity Data of Tofas COM1 and COM2 Monolithic Catalysts

Species	Test1			Test4		
	T50 (˚C)	Max. Con. (%)	Tmax (˚C)	T50 (˚C)	Max. Con. (%)	Tmax (˚C)
CO	212	100	364	220	100	368
NO	189	467	98	231	437	90
C_3H_6	219	374	100	226	385	100
C_3H_8	236	597	100	262	590	100
H_2	-	240	100	-	236	100
O_2	211	540	100	202	544	100

According to comparison of two Tofas commercial catalysts catalytic activity curves are very similar. This result shows that the reliability of the catalytic activity tests.

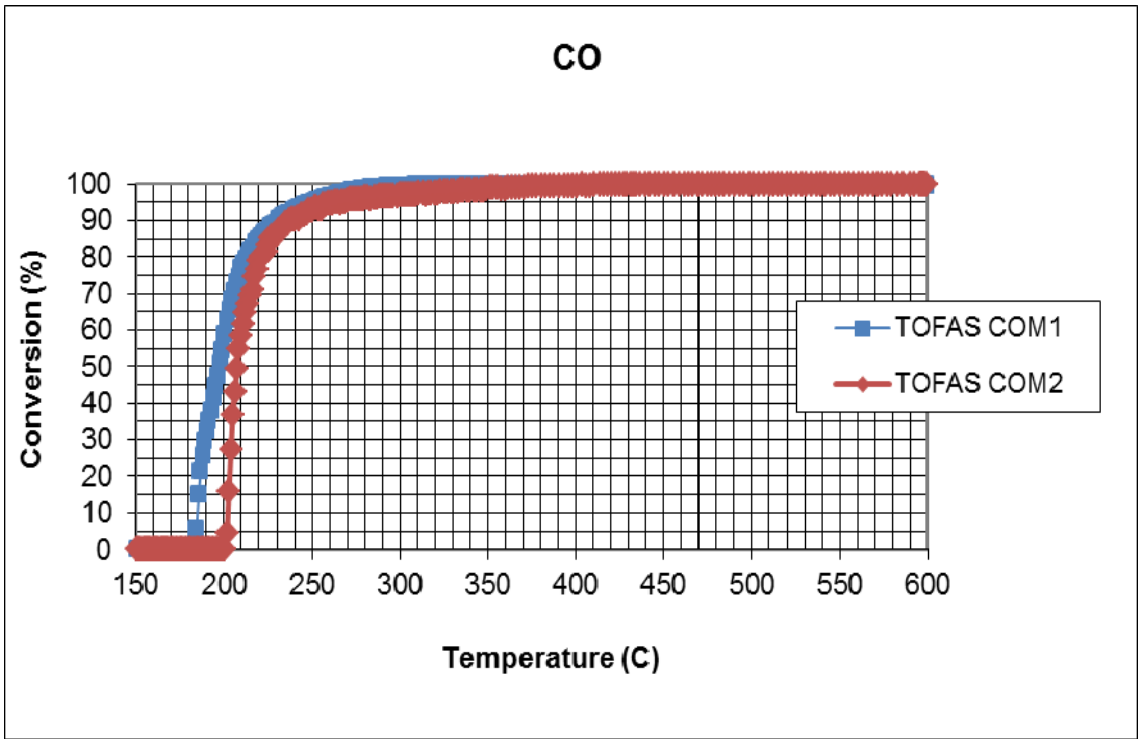

Figure 5. 47 CO Catalytic Activity of Tofas COM1 & Tofas COM2 Monolithic Catalyst

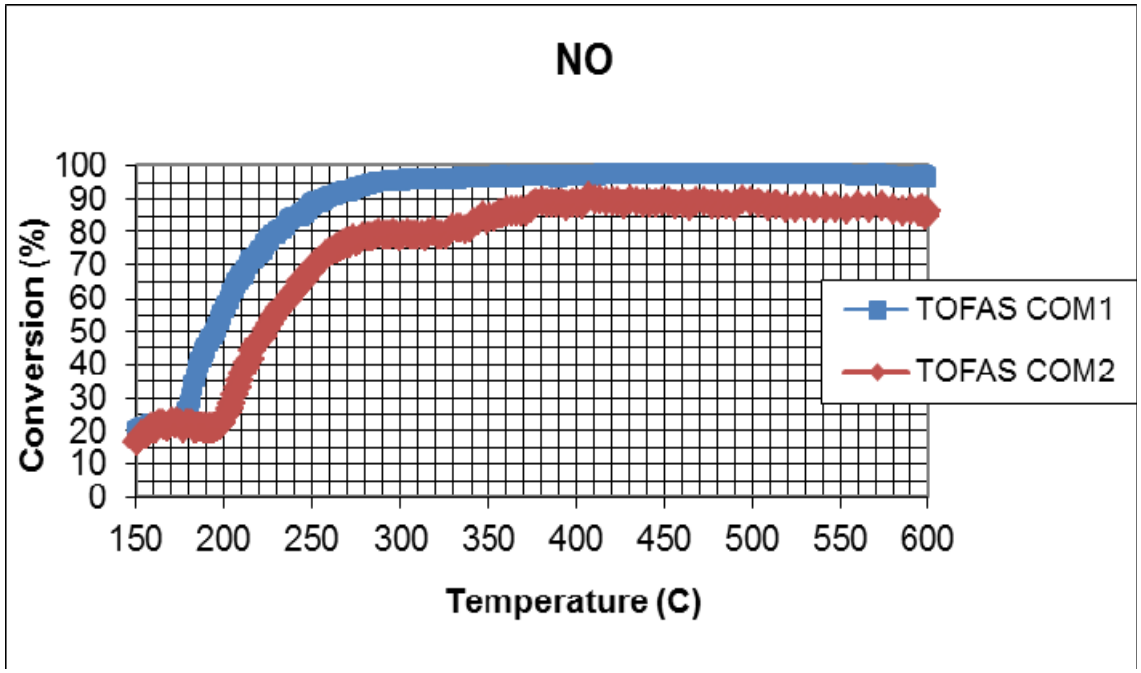

Figure 5. 48 NO Catalytic Activity of Tofas COM1 & Tofas COM2 Monolithic Catalyst

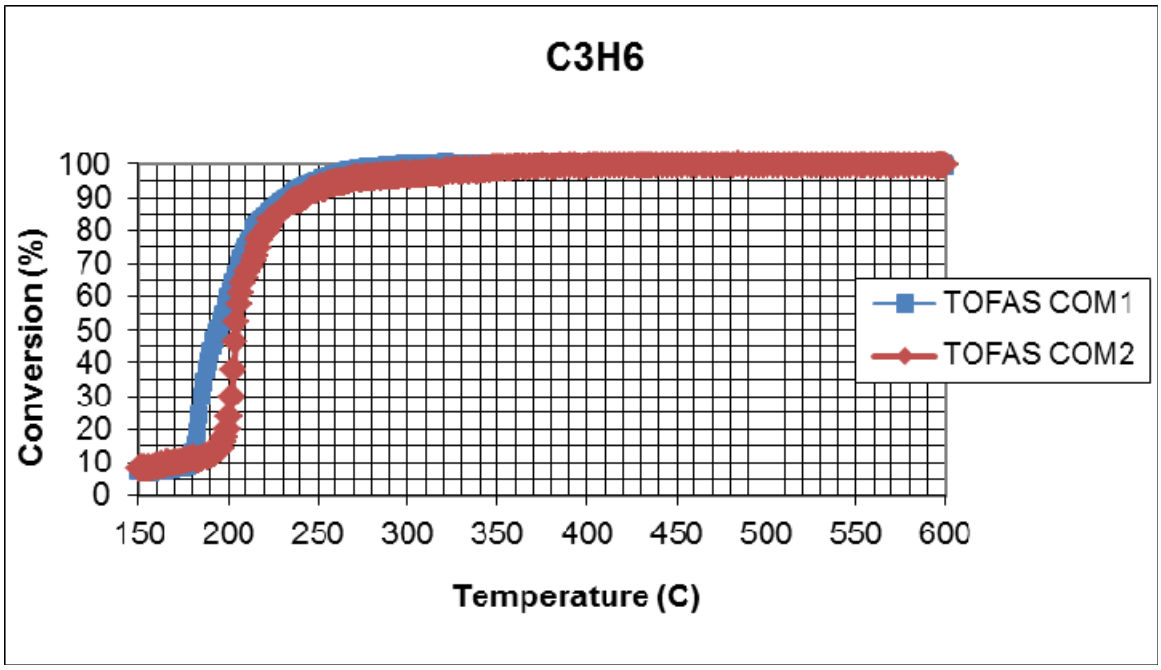

Figure 5. 49 C_3H_6 Catalytic Activity of Tofas COM1 & Tofas COM2 Monolithic Catalyst

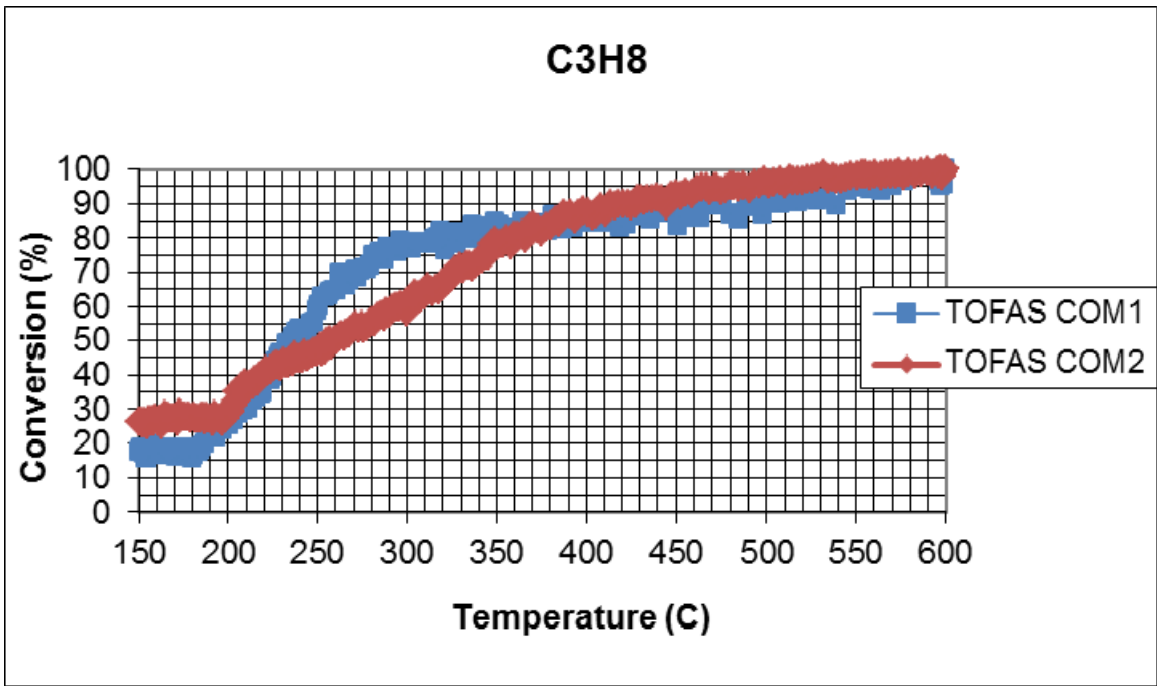

Figure 5. 50 C_3H_8 Catalytic Activity of Tofas COM 1 & Tofas COM2 Monolithic Catalyst

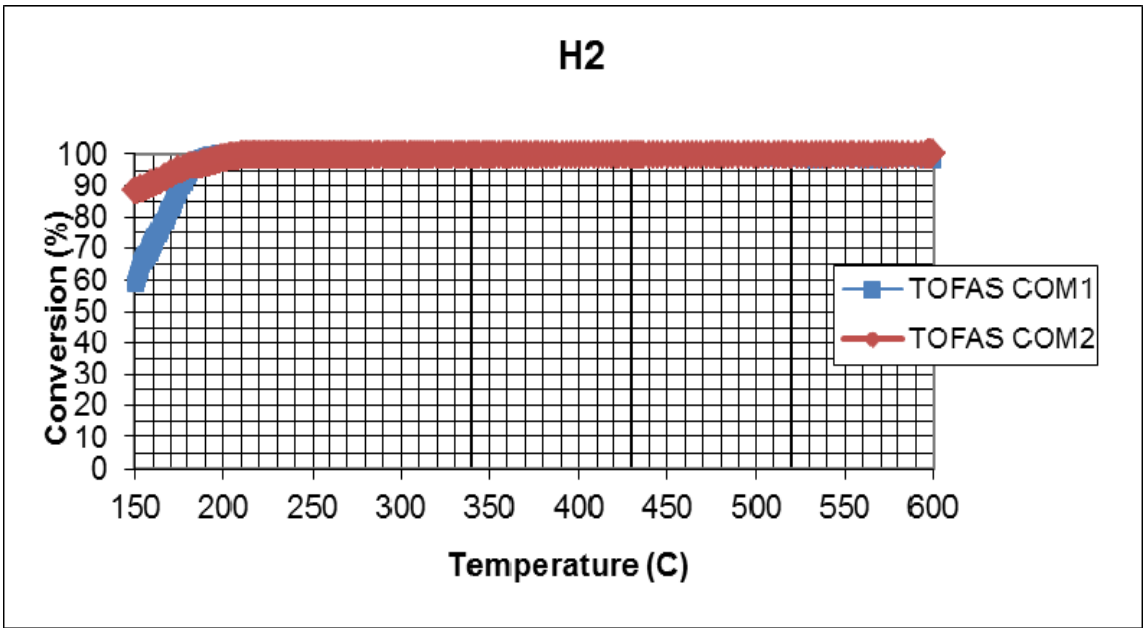

Figure 5. 51 H_2 Catalytic Activity of Tofas COM1 & Tofas COM2 Monolithic Catalyst

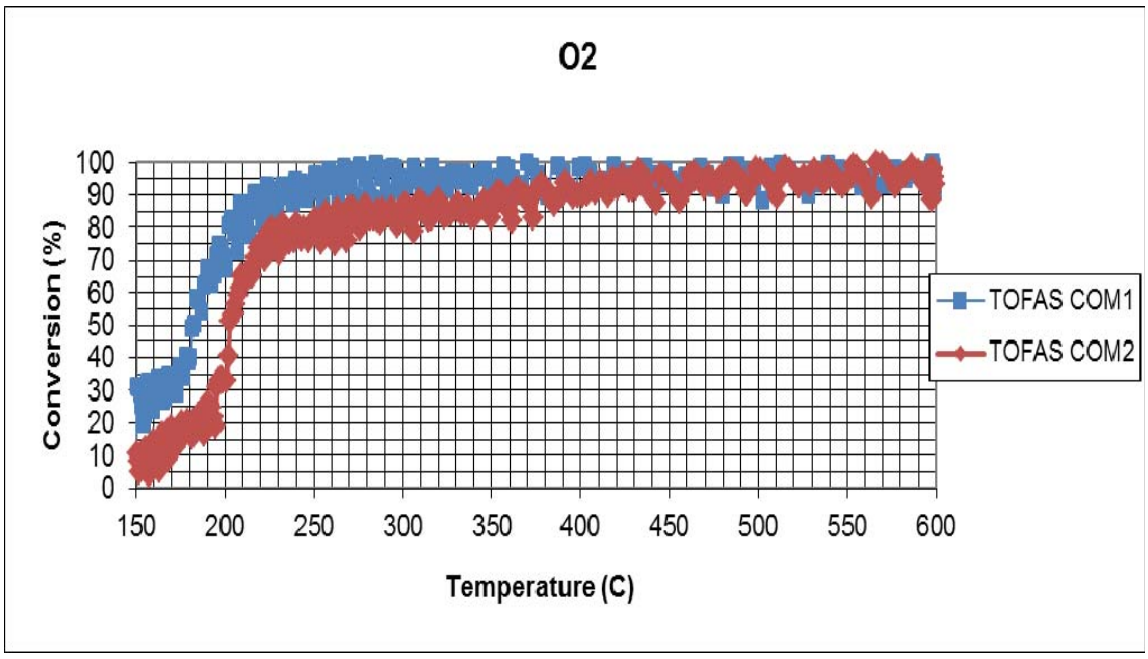

Figure 5. 52 O_2 Catalytic Activity of Tofas COM1 & Tofas COM2 Monolithic Catalyst

CHAPTER 6

CONCLUSIONS

In this study mixed oxides of CeO_2 and ZrO_2 ($Ce_{0.8}Zr_{0.2}O_2$) are synthesized by co-precipitation method. Nobel metals in catalyst are 0.65 wt% Pd and 0.1 wt% Rh metals with a Pd/Rh ratio of 6.5. Nobel metals are coated to monolithic catalysts by washcoating. After calcination process at 500°C for 3h the monolithic catalysts are exposured the simulated exhaust gas compositions in dynamic test system. According to conversion of mixture gases catalytic activities are evaluated.

The support materials of catalysts are characterized by BET surface area and XRD. BET surface area of CZO and CZAO is 145.3 and 320.3 m^2/g, respectively. Aluminum oxide is the main component of the support materials of catalysts. It provides a high surface area.

Metal loaded powder catalysts are also characterized by BET and XRD. CZO surface area is decreased from 145.3 m^2/g to nearly 80.0 m^2/g. CZAO surface area is reduced from 320.6 m^2/g to 83.3 m^2/g. This surface area decreased is due to one more calcination for noble metal impregnations on support material.

The monolithic catalytic activity tests of conversion results are compared during the heating and cooling period. The higher conversions are reached at lower temperature during the cooling period. This improvement is related to the catalytic reduction during the heating period. According to the this, all catalysts activity results are evaluated the cooling steps.

Conversions of CO, C_3H_6, H_2 and O_2 are obtained easier than conversion of NO and C_3H_8 by monolithic three way catalyst.

These monolithic catalysts are prepared by impregnating with Rh and Pd. The catalytic activity performance of monolithic catalysts are studied without SO_2 and with SO_2 during the dynamic test. Four catalytic activity tests of monolithic catalysts are performed. During the first test the fresh monolithic catalysts activities are evaluated. The simulated exhaust gas mixture during the first test does not contain SO_2. After first test, 20 ppm SO_2 is added into the simulated gas mixture during the second and the third. Lastly, the monolithic catalyst are tested with simulated exhaust gas without SO_2. By this test program the effect of SO_2 is analyzed. As a results, the monolithic catalyst is reduced catalytic activity with SO_2 exposure and the monolithic catalyst recover its activity again after SO_2 removal from dynamic system.

The catalyst conversion behaviors are affected by both thermal aging (high temperature induced sintering and precious metal coagulation effects) as well as chemical aging (e.g. deposition of phosphorous, sulphur) of the active surface. In this study only chemical aging effect is analyzed.

After SO_2 exposure, the 50% conversions of NO and C_3H_6 are done at lower light-off temperature. Better conversion of NO is related to the Rh resistance of sulphur poisoning. In addition to this, the promoting effect of sulphur is increased C_3H_6 oxidation and catalytic

activity. On the other hand, catalytic activities are reduced for conversion of H_2, CO and O_2. Pd is poisoned by the sulphur, thus conversion of CO are lost.

The commercial catalyst activity is also affected by SO_2 exposure. The 50% conversions of all species are done at higher light-off temperature.
As a result, although the research monolithic catalysts has lower noble metal than Tofas commercial monolithic catalyst, the catalytic activity of this catalyst is better than Tofas commercial monolithic catalyst. Moreover, the research monolithic catalysts has strong resistance against exposure to SO_2. According to these studies data, the research monolithic catalysts are found promising and decided to be studied further.

In addition to this, by this dynamic test program the catalytic activity of (Pd + Rh) + (CZAO) and (CZO + Rh) / (CZO + Pd) + AO will be analyzed to understand importance of impregnation method of nobel metal. Thus, the best method of impregnation method will be determined. Study of modelling TWCs are started to understand catalytic activity more clearly.

REFERENCES

1. Addiego, W.P. et al. High surface area washcoated substrate and method for producing same. US Patent 5212130. 18 May 1993.

2. Agrafiotis, C., Tsetsekou, A., Stournaras, C. J., Julbe, A., Dalmazio, L., Guizard, C. et al. (2001). Evaluation of sol–gel methods for the synthesis of doped-ceria environmental catalysis systems Part II. Catalytic activity and resistance to thermal aging. Applied Catalysis B: Environmental, 34, 149 - 159.

3. Beck, D.D., Sommers, J.W., DiMaggio, C.L. (1994). Impact of sulfur on model palladium-only catalysts under simulated three-way operation. Applied Catalysis B: Environmental, 3, 205 – 227.

4. Ciambelli, P., Sannino, D., Palma, V., & Russo, P. (2003). Experimental methods for activity measurements in environmental catalysis. Catalysis Today, 77, 347 - 358.

5. Cullity, B. P., & Stock, S.R. (2001). Elements of X-ray Diffraction (3rd. Ed.). New York: Prentice Hall.

6. Di Monte, R., Fornasiero, P., Graziani, M., & Kaspar, J. (1998). Oxygen storage and catalytic NO removal promoted by CeO2 -containing mixed oxides. Journal of Alloys and Compounds, 275–277, 877–885.

7. Di Monte, R., Kaspar, J., Fornasiero, P., Graziani, M., Paze, C., & Gubitosa, G. (2002). NO reduction by CO over Pd/Ce0.6Zr0.4O2 - Al2O3 catalysts: in situ FT-IR studies of NO and CO adsorption. Inorganica Chimica Acta, 334, 318 - 326.

8. Farrauto, R. J., & Heck, R. M. (1999). Catalytic converters: state of the art and perspectives. Catalysis Today, 51, 351 - 360.

9. Fogler, H. S. (2006). Elements of chemical reaction engineering (4th. Ed.). Massachusetts: Prentice Hall.

10. Fornasiero, P., Montini, T., Graziani, M., Zilio, S., & Succi, M. (2008). Development of functionalized Fe–Al–Cr alloy fibers as innovative catalytic oxidation devices. Catalysis Today, 137, 475 - 482.

11. Gas Correction Factors. Retrieved December 24, 2008 from Teledyne Hastings Instruments Web Site: http://www.teledyne-hi.com/tech-papers/GasDataTables.xls

12. Gennari, F.C., Montini, T., Fornasiero, P., & Gamboa, J.J.A. (2008). Reduction behavior of nanoparticles of Ce0.8Zr0.2O2 produced by different approaches. Int J Hydrogen Energy, doi:10.1016/j.ijhydene.2007.12.006.

13. Gonzales – Velasco, J.R., Gutierrez-Ortiz, M.A., Marc, J.L., Gonzales-Marcos, M.P., & Blanchard, G. (2001). Selectivity of high surface area Ce0.68Zr0.32O2 for the new

generation of TWC under environments with different redox character. Applied Catalysis B: Environmental, 33, 303 – 314.

14. Granados, M.L., Larese, C., Galisteo, F.C., Mariscal, R., Fierro, J.L.G., & Fernandez – Ruiz, R. et al. (2005). Effect of mileage on the deactivation of vehicle-aged three-way catalysts. Catalysis Today, 107 – 108, 77 – 85.
15. Kaspar, J., & Fornasiero, P. (2003). Nanostructured materials for advanced automotive de-pollution catalysts. Journal of Solid State Chemistry, 171, 19 – 29.

16. Kaspar, J., Fornasiero, P., & Hickey, N. (2003a). Automotive catalytic converters: current status and some perspectives. Catalysis Today, 77, 419 - 449.

17. Lambrou, P.S., Costa, C.N., Christou, S.Y & Efstathiou, A.M (2004). Dynamics of
18. oxygen storage and release on commercial aged Pd-Rh three-way catalysts and their
19. characterization by transient experiments. Applied Catalysis B: Environmental 54
20. (2004), 237–250.

21. Lassi, U., Hietikko, M., Rahkamaa-Tolonen, K., Kallinen, K., Savimaki, A., Harkonen, M., Laitinenb, R. & Keiskia, R.L. Deactivation correlations over Pd/Rh monoliths: the role of gas phase composition. Topics in Catalysis Vols.30/31, July 2004.

22. Nguefack, M., Popa, A.F., Rossignol, S., & Kappenstein, C. (2003). Preparation of alumina through a sol–gel process. Synthesis, characterization, thermal evolution and model of intermediate boehmite. Phys. Chem., 5, 4279–4289.

23. Nijhuis, T.A., Beers, A.E.W., Vergunst, T., Hoek, I., Kapteijn, F., & Moulijn, J.A. (2001). Preparation of monolithic catalysts. Catalysis Reviews, 43, 4, 345 – 380.

24. Noh, J., Yang, O., Kim, D. H., & Woo, S. I. (1999). Characteristics of the Pd-only three-way catalysts prepared by sol–gel method. Catalysis Today, 53, 575 – 582.

25. Perry, R. H., & Green, D. W. (1997). Perry's chemical engineers' handbook (7th. Ed.). New York: Mc Graw Hill.

26. Rajasree, R. , Hoebink, J.H.B.J. & Schouten, J.C. (2004). Transient kinetics of carbon monoxide oxidation by oxygen over supported palladium/ceria/zirconia three-way catalysts in the absence and presence of water and carbon dioxide. Journal of Catalysis 223, 36–43.

27. Rossignol, G., Gerard, F., & Duprez, D. (1999a). Effect of the preparation method on the properties of zirconia–ceria materials. Journal of Materials Chemistry, 9, 1615 – 1620.

28. Rossignol, G., Madier, Y., & Duprez, D. (1999b). Preparation of zirconia–ceria materials by soft chemistry. Catalysis Today, 50, 261 – 270.

29. Shinjoh, H., Tanabe, T., Yokota, K. & Sugiura, M.(2004). Comparative NOx reduction behavior of Pt, Pd, and Rh supported catalysts in simulated exhaust gases as a function of oxygen concentration. Topics in Catalysis Vols.30/31, July 2004.

30. Suopanki, A., Polvinen, R., Valden, M., & Harkonen, M. (2005). Rh oxide reducibility and catalytic activity of model Pt–Rh catalysts. Catalysis Today, 100, 327 – 330.

31. Torbati, R. (2009). Advanced catalytic systems for the partial oxidation of hydrocarbons: Improving sulphur tolerance of Rh based catalysts (Doctoral dissertation). Retrieved from http://www.fedoa.unina.it/3845/

32. Ulla, L. (2003). Deactivation correlations of Pd/Rh three way catalysts designed for Euro IV emission limits. Effects of ageing atmosphere, temperature and time (Academic dissertation). University of Oulu, Oulu.

33. Yao, M. H., Baird, R. J., Kunz, F. W., & Hoosty, T. E. (1997). An XRD and TEM investigation of the structure of alumina-supported ceria–zirconia. Journal of Catalysis, 166, 67 – 74.

34. Yingying, G., Shengsheng, F., Jinlin, L., Xiangkui, G., & Manjuan, W. (2007). Preparation of mesoporous Ce0.5Zr0.5O2 mixed oxide by hydrothermal templating method. Journal of Rare Earths, 25, 710 – 714.

35. Yucai, H. (2006). Hydrothermal synthesis of nano Ce-Zr-Y oxide solid solution for automotive three way catalyst. J. Am. Ceram. Soc., 89 [9], 2949 - 2951. doi:10.1111/j.1551-2916.2006.01130.x

APPENDIX A

CATALYST PREPARATION

A.1 Preparation of Ceria – Zirconia Mixed Oxide

- ✓ 100.00 g of $CeN_3O_9.6H_2O$ and 19.34 g of $N_2O_7Zr.aq$ are dissolved in 1L of deionized water and stirred for 30 min.
- ✓ 333 mL of H_2O_2 is added into the mixture and stirred for 1h.
- ✓ The mixture is added into 250 mL NH_4OH solution drop wisely and kept for 12h.
- ✓ The product is filtered with $CH_3CHOHCH_3$ and refluxed in 250 mL $CH_3CHOHCH_3$ for 6h.
- ✓ The refluxed product is dried at 150 ºC for 12 h.
- ✓ The powder sample is grounded and calcined in an oven at 500 ºC for 3h under dry air.

A.2 Preparation of Pseudoboehmite

- ✓ 50 g of $Al(OC_4H_9)_3$ is hydrolyzed with 365 mL of deionized water at 60 ºC under vigorous stirring for 2 h.
- ✓ 1.7 mL of HCl is added into the mixture.
- ✓ The mixture is heated to 80 ºC and stirred vigorously for 1h.
- ✓ The resulting gel product is dried at 150 ºC for 48 h.
- ✓ The powder sample is grounded and calcined in an oven at 300 ºC for 5h with a heating rate of 5 ºC/min under dry air.

A.3 Addition of Metals

- ✓ 0.01 g of $Rh(NO_3)_3$ and 0.217 g of $PdCl_2$ solution are added for 1 g of support material.
- ✓ For 1 g of Ceria – Zirconia Mixed Oxide as support material metal precursor or solution is dissolved in 633 µL of deionized water.
- ✓ For 1 g of Ceria – Zirconia – Alumina Mixed Oxide as support material metal precursor or solution is dissolved in 840 µL of deionized water.
- ✓ The mixture is rotated in rotary vacuum evaporator for 15 min. without vacuum and heating.
- ✓ The support material is added into the mixture and rotated in water bath at 80 ºC under vacuum (-280 mbar) to evaporate the liquid.
- ✓ The product is dried at 150 ºC for 12h.
- ✓ The powder sample is grounded and calcined in an oven under dry air at 500 ºC for 3h.

A.4 Preparation of Washcoating Slurry

- ✓ 50 g of impregnated ceria-zirconia mixed oxide, 117.5 g of γ-Al_2O_3 and 12.85 g of pseudoboehmite is mixed with 270 mL of deionized water in a 1250 mL HDPE mortar.
- ✓ 3 mm alumina mills are added occupying 33V% of the mixture.
- ✓ The mixture is ball-milled for 30 min at 275 rpm.
- ✓ 11890 µL HNO_3 solution is added into the slurry and ball-milled again for 3h at 275 rpm.

APPENDIX B

CATALYTIC ACTIVITY TEST CALCULATIONS

B.1 Mass Simulated Exhaust Gas Flow Rate Calculation

In this study all catalytic activity tests are performed at 50000 h^{-1} hourly space velocity (GHSV). The total gas flow rate is calculated using Equation B.1.1. (Fogler, 2006).

$$GHSV = \frac{\nu_0}{V_{eff}} \tag{B.1.1}$$

Monolith effective volume is calculated using Equation B.1.2. The frontal area in ceramic monolith is 69% open (31% closed) (Kaspar et al., 2003).

$$V_{eff} = \left(\pi \times \left(\frac{(d)^2}{4} \right) \times (h) \right) \times (0.69) \tag{B.1.2}$$

Monolith of diameter is 2.2 cm and height is 1.3 cm in this study. Effective volume of monolith is calculated as B.1.3.

$$V_{eff} = \left(\pi \times \left(\frac{(2.2\,cm)^2}{4} \right) \times (1.3\,cm) \right) \times (0.69) = 3.4097\,cm^3 \tag{B.1.3}$$

According to Equations B.1.3 and B.1.1 the gas flow rate is calculated as 2841.5 mL/min Equation in B.1.4.

$$50.000\,h^{-1} = \frac{\nu_0 (L/h)}{(3.4097 cm^3) \times (1L/1000\,cm^3)}$$

$$\nu_0 = 170.4850\,L/h \tag{B.1.4}$$

$$\nu_0 = (170.5850 L/h) \times (1000\,mL/1L) \times (1h/60\,\text{min}) = 2841.4167\,mL/\text{min}$$

B.2 Exhaust Gas Composition

In this study all catalyst activity test are performed with using simulated exhaust gas compositions. All catalytic activity tests are done at stoichiometric condition. Thus, the composition of oxygen is determined to have 1.0 stoichiometry. In Table B.2.1 the simulated exhaust gas composition is given as ppm and %.

Table B.2. 1 Simulated Exhaust Gas Mixture Composition

Species	Gas Mixture Composition (ppm)	Gas Mixture Composition (%)
C_3H_6	375	0.0375
C_3H_8	125	0.0125
CO	10000	1.0000
H_2	2300	0.2300
CO_2	100000	10.0000
NO	1500	0.1500
SO_2	20	0.0020
O_2	7700	0.7700
N_2	Balance	Balance

The composition of oxygen is calculated as 0.7700% with Equation B.2.1.

$$S = \frac{2[O_2]+[NO]}{[H_2]+[CO]+9[C_3H_6]+10[C_3H_8]}$$

$$1.0 = \frac{2[O_2]+[0.1500]}{[0.2300]+[1.0000]+9[0.0375]+10[0.0125]} \qquad \text{(B.2.1)}$$

$$[O_2] = 0.7700\,\%$$

The simulated exhaust gas composition is prepared with five different gas cylinders. The first cylinder contains C_3H_6, C_3H_8, CO, H_2 and CO_2 as mixture. The second cylinder contains NO, the third cylinder contains SO_2 and balance N_2.The fourth cylinder contains O_2 and the fifth cylinder contains N_2. The compositions of cylinders are tabulated as % and ppm in Table B.2.2

Table B.2. 2 Cylinder Compositions

Cylinder	Species	Cylinder Composition (%)	Cylinder Composition (ppm)
1	C_3H_6	0.3300	3300
	C_3H_8	0.1100	1100
	CO	8.8700	88700
	H_2	2.0400	20400
	CO_2	88.6500	886500
2	NO	50.0000	500000
	N_2	50.0000	500000
3	SO_2	0.0100	100
	N_2	99.9900	999900
4	O_2	99.5000	995000
5	N_2	99.9980	999980

The flow rate from each cylinder is calculated by using the data of the cylinder compositions. Flow rate composition of C_3H_8 is calculated as an example in B.2.2.

$$FlowRate = v_0(mL/\min) x GasMixtureComposition(\%)$$

(B.2.2)

$$C_3H_8\ MixtureFlowRate = \frac{2841.5(mL/\min)\times(0.0125)}{(100)} = 0.3552 mL/\min$$

All activity tests are done around the stoichiometric number of 1.0. The exhaust gas compositions are around the reducing and oxidation conditions by adding the 10.5 mL/min oxygen with a frequency of 1 Hz. The flow rates of five cylinders are given in Table B.2.3.

Table B.2. 3 Flow Rates of Cylinders Gas Compositions for Reducing, Stoichiometric and Oxidizing Conditions

Cylinder	Flow Rate (mL/min)		
	Reducing	Stoichiometric	Oxidizing
1	320.5118	320.5118	320.5118
2	8.5243	8.5243	8.5243
3	568.3000	568.3000	568.3000
4	16.6289	16.6289	27.1287
5	1638.0601	1638.0601	1638.0601
water	284.1417	284.1417	284.1417
Total	2836.1667	2841.4165	2846.6667

The gas composition of the simulated exhaust gas for reducing, stoichiometric and oxidizing conditions are tabulated as % in Table B.2.4

Table B.2. 4 Simulated Gas Mixture Composition for Reducing, Stoichiometric and Oxidizing Conditions

Species	Gas Mixture Composition (%)		
	Reducing	**Stoichiometric**	**Oxidizing**
C_3H_6	0.0376	0.0375	0.0374
C_3H_8	0.0125	0.0125	0.0125
CO	1.0019	1.0000	0.9982
H_2	0.2304	0.2300	0.2296
CO_2	10.0185	10.0000	9.9816
NO	0.1503	0.1500	0.1497
SO_2	0.0020	0.0020	0.0020
O_2	0.5863	0.7700	0.9530
N_2	57.7561	57.6494	57.5431

The stoichiometric condition number for three different condition is calculated with Equations B.2.3 and B.2.4.

The composition of oxygen for reducing condition is calculated as 0.7801%.

$$S = \frac{2[O_2]+[NO]}{[H_2]+[CO]+9[C_3H_6]+10[C_3H_8]}$$

$$S = \frac{2[0.5863]+[0.1503]}{[0.2304]+[1.0019]+9[0.0376]+10[0.0125]} \quad \text{(B.2.3)}$$

$$S = 0.7801\%$$

The composition of oxygen for oxidizing condition is calculated as 1.2169 %.

$$S = \frac{2[O_2]+[NO]}{[H_2]+[CO]+9[C_3H_6]+10[C_3H_8]}$$

$$S = \frac{2[0.9530]+[0.1497]}{[0.2296]+[0.9982]+9[0.0374]+10[0.0125]} \quad \text{(B.2.4)}$$

$$S = 1.2169\%$$

B.3 Water Content in The Simulated Exhaust Gas Composition

Using Antoine Equation (Perry & Green, 1997) the saturation temperature of the water vapor of N_2 in the system is calculated. This equation is valid between 1-100 ºC temperature of water with the constants.

$$\log P^{sat} = A - \frac{B}{C+T} \qquad \text{(B.3.1)}$$

$$T = \frac{B}{A - \log P^{sat}} - C$$

Where;

$$A = 8.07131$$

$$B = 1730.63$$

$$C = 233.426$$

The atmosphere pressure is assumed as 1 atm. The fraction of the necessary flow rate of the water vapor and N_2 gas is assumed as the partial pressure.

$$\frac{H_2O}{N_2 + H_2O} = \frac{284.1417}{1638.0601 + 284.1417} = 0.1478$$

$$P^{sat} = (1\,atm) \times 0.1478 = 0.1478\,atm$$

$$P^{sat} = (0.1478\,atm) \times \frac{760\,torr}{1\,atm} = 112.3439\,torr$$

As a result, the saturation pressure is found as 54.0178 ºC.

$$T = \frac{1730.63}{8.07131 - \log(112.3439)} - 233.426$$

$$T = 54.0178°C$$

B.4 Analysis of Catalytic Activity Test Data

B.4.1 Mass CO Analyzer Data Calculations

The data from CO analyzer are in ppm unit. Thus, CO conversion is directly calculated using Equation B.4.1 (Fogler, 2006).

$$X = \frac{C_{A0} - C_A}{C_{A0}} \times 100\% \qquad \text{(B.4.1)}$$

As an example,

$$C_{A0} = 9999\,ppm$$

$$C_A = 123\,ppm$$

$$X = \frac{C_{A0} - C_A}{C_{A0}} = \frac{9999 - 123}{9999} \times 100\% = 98.7699\%$$

B.4.2 MS Data Calculations

The MS system is calibrated for each species and calibration equations are plotted for each one to convert data to concentration. Then, concentration values are used to calculate conversions with Equation B.4.1.

As an example,

$$C_3H_8\ Calibration\,Equation : y = (1E+13)x - 26638$$

$$y = C_3H_8\ Species\,Concentration(ppm)$$

$$x = C_3H_8\ MS\,Sinyal$$

$$x_0 = 1.24E-08$$

$$x_f = 2.74E-09$$

$$C_{A0} = 19E+13) \times (1.24E-08) - 26638 = 97362.0000\,ppm$$

$$C_A = (1E+13) \times (2.74E-09) - 26638 = 762.0000\,ppm$$

$$X = \frac{C_{A0} - C_A}{C_{A0}} = \frac{97362.0000 - 762.0000}{97362.0000} \times 100\% = 99.2174\%$$

APPENDIX C

CALIBRATIONS

C.1 Mass Flow Controller Calibrations

Calibration of all MFCs are done with nitrogen. MFC gas correction factor is used for each gas mixture in the cylinders. These correction factors are taken from Teledyne for 200 series of MFCs (Gas Correction Factors, 2008). In Table C.1 gas correction factors are given for each cylinders.

Table C.1. 1 MFC Gas Correction Factors

Cylinder	MFC	Species	Gas Correction Factor
1	Mix MFC	C_3H_6	0.743
		C_3H_8	
		CO	
		H_2	
		CO_2	
2	NO MFC	NO	0.98975
		N_2	
3	SO_2 MFC	SO_2	1
		N_2	
4	O_2 MFC	O_2	0.981
5	N_2 MFC	N_2	1

Table C.1. 2 Calibration Data for Mix MFC

Set Flow Rate (ml/min)	Calibration Volume (mL)	Measured Time (sec)	Measured Time (min)	Measured Nitrogen Flow Rate (ml/min)	Corrected Gas Flow Rate (ml/min)
150	30	7.06	0.1176	254.9575	189.4334
200	30	5.35	0.0892	336.4486	249.9813
250	30	4.32	0.0720	416.6667	309.5833
300	30	3.51	0.0585	512.8205	381.0256
350	30	2.97	0.0495	606.0606	450.3030
400	30	2.56	0.0427	703.1250	522.4219
450	30	2.25	0.0375	800.0000	594.4000
500	30	1.98	0.0330	909.0909	675.4545
550	30	1.8	0.0300	1000.0000	743.0000
600	30	1.66	0.0276	1084.3370	805.6627

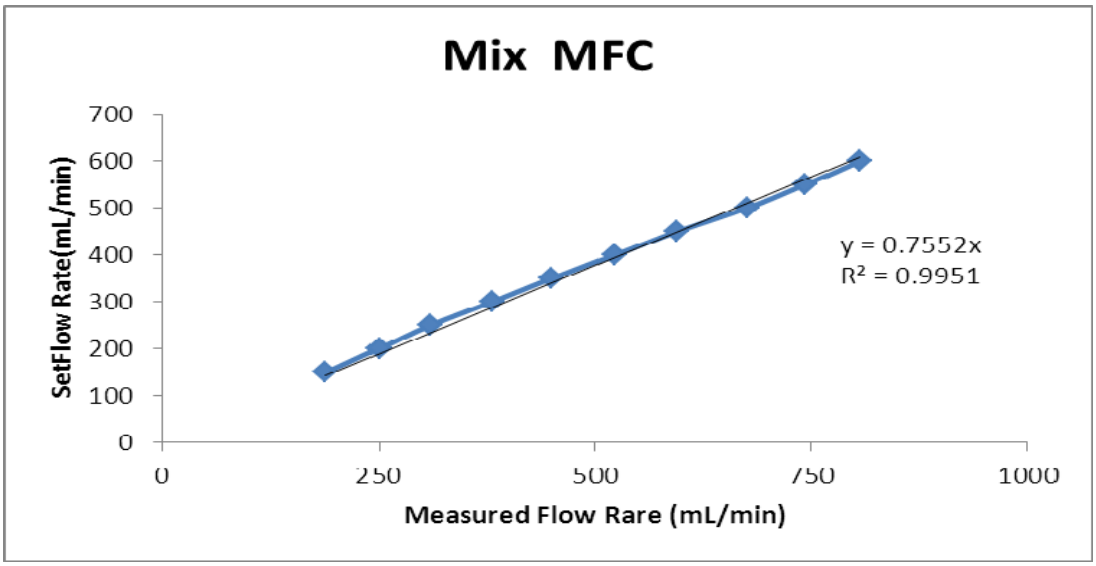

Figure C.1. 1 Calibration Graph for Mix MFC

Table C.1. 3 Calibration Data for NO MFC

Set Flow Rate (ml/min)	Calibration Volume (mL)	Measured Time (sec)	Measured Time (min)	Measured Nitrogen Flow Rate (ml/min)	Corrected Gas Flow Rate (ml/min)
5	10	88.33	1.472	6.7927	6.7231
10	10	45.22	0.754	13.2685	13.1325
15	10	30.28	0.505	19.8151	19.6120
20	10	22.77	0.380	26.3505	26.0804
25	10	18.31	0.305	32.7690	32.4331
30	10	15.3	0.255	39.2157	38.8137
35	10	13.09	0.218	45.8365	45.3667
40	10	11.43	0.191	52.4934	51.9554
45	10	10.17	0.170	58.9971	58.3923

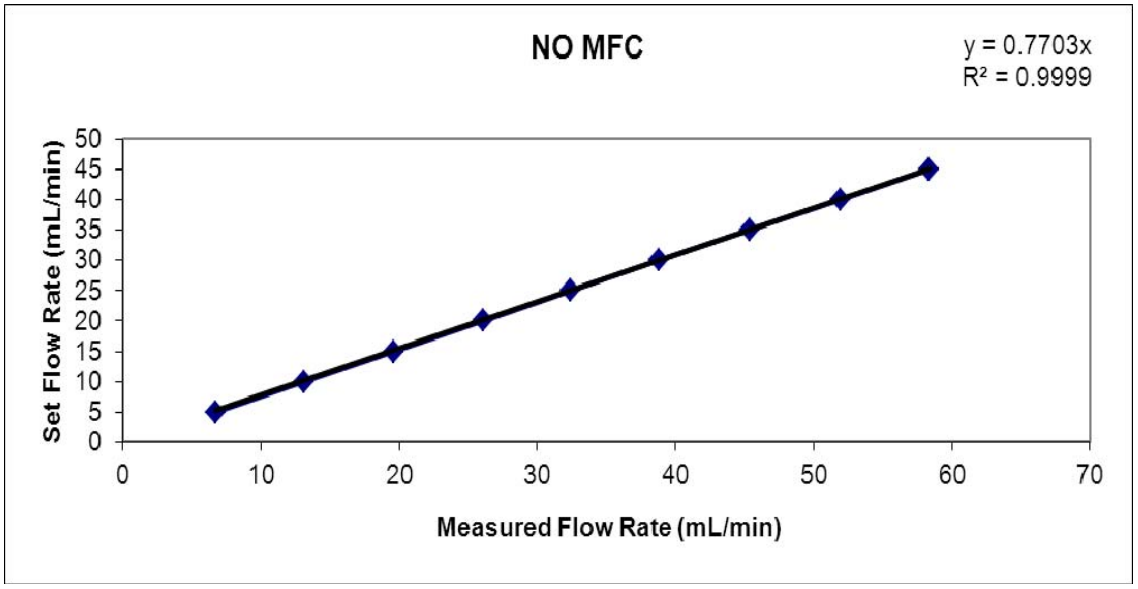

Figure C.1. 2 Calibration Graph for NO MFC

Table C.1. 4 Calibration Data for SO_2 MFC

Set Flow Rate (ml/min)	Calibration Volume (mL)	Measured Time (sec)	Measured Time (min)	Measured Nitrogen Flow Rate (ml/min)
250	30	5.8	0.097	310.3448
500	30	2.74	0.046	656.9343
750	30	1.71	0.029	1052.6316

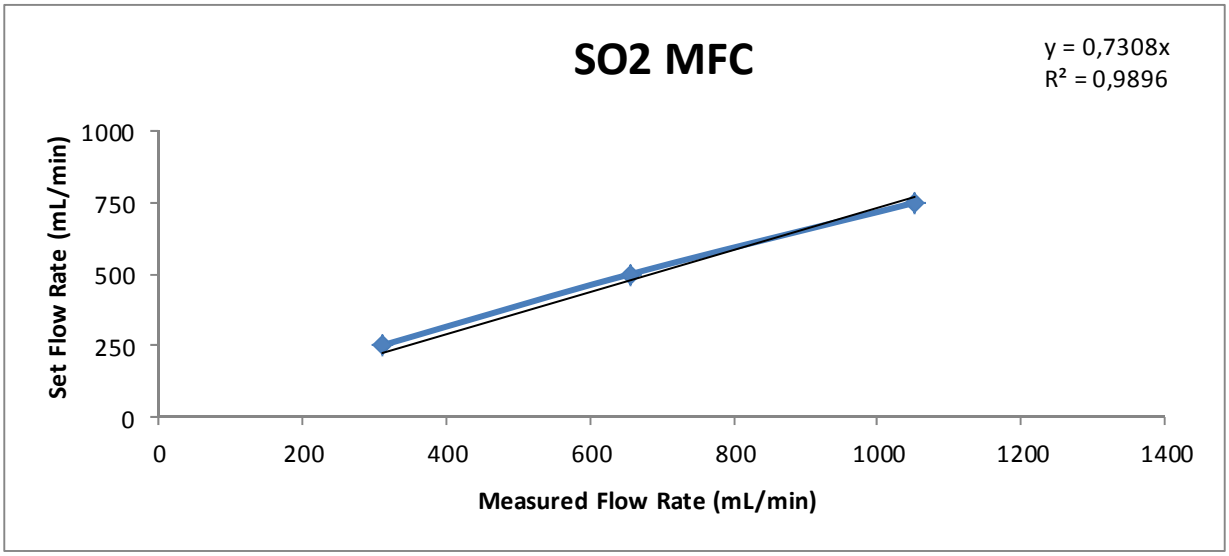

Figure C.1. 3 Calibration Graph for SO_2 MFC

Table C.1. 5 Calibration Data for O_2 MFC

Set Flow Rate (ml/min)	Calibration Volume (mL)	Measured Time (sec)	Measured Time (min)	Measured Nitrogen Flow Rate (ml/min)	Corrected Gas Flow Rate (ml/min)
10	10	46.57	0.776	12.8838	12.6390
15	10	30.87	0.515	19.4363	19.0671
20	10	23.13	0.386	25.9403	25.4475
25	10	18.54	0.309	32.3625	31.7476
30	10	15.48	0.258	38.7597	38.0233
35	10	13.14	0.219	45.6621	44.7945
40	10	11.74	0.196	51.1073	50.1363

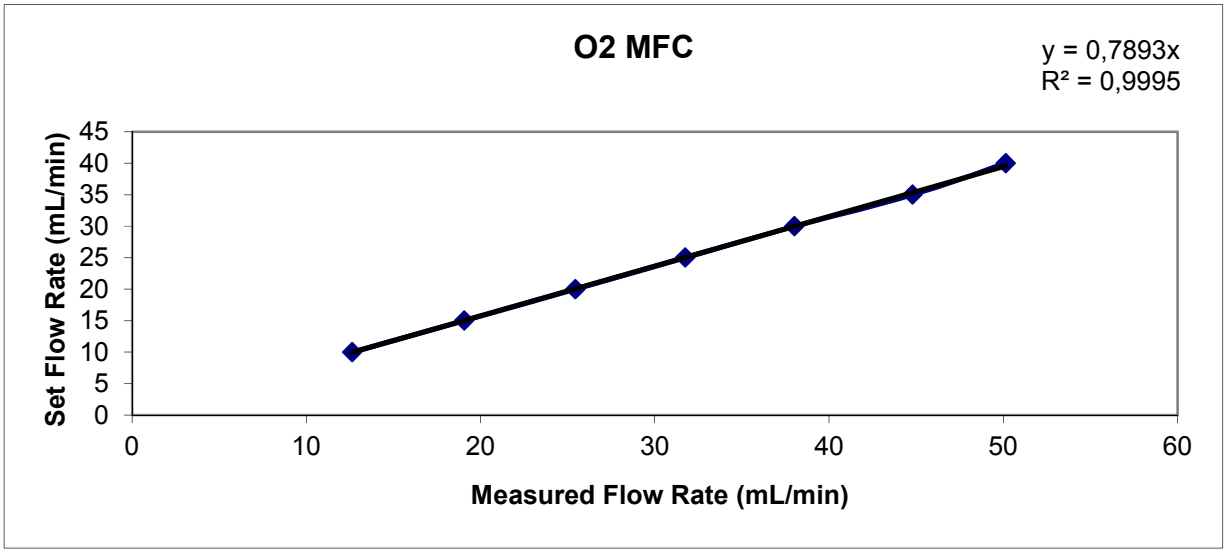

Figure C.1. 4 Calibration Graph for O_2 MFC

Table C.1. 6 Calibration Data for N_2 MFC

Set Flow Rate (ml/min)	Calibration Volume (mL)	Measured Time (sec)	Measured Time (min)	Measured Nitrogen Flow Rate (ml/min)
250	30	5.85	0.0975	307.6923
500	30	2.74	0.0456	656.9343
750	30	1.71	0.0285	1052.6316
1000	30	1.21	0.0201	1487.6033
1250	30	0.94	0.0157	1914.8936

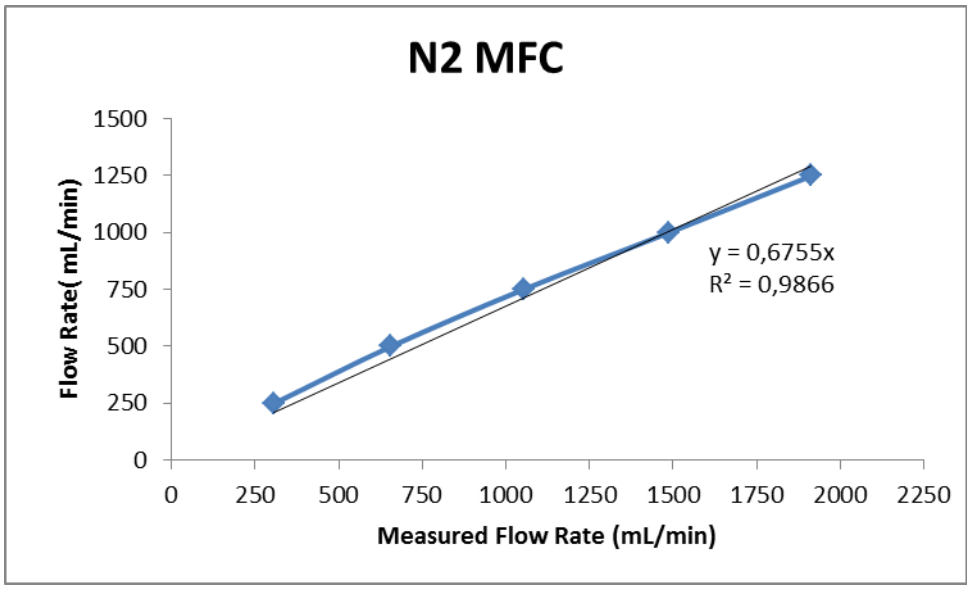

Figure C.1. 5 Calibration Graph for N_2 MFC

C.2 Mass Spectrometer Calibrations

In the catalytic activity test MS calibration is done periodic. An example of MS calibration data and graphs for each species are given below.

C.2.1 Mass Spectrometer Calibration

Table C.2. 1 O_2 MS Calibration Data

O_2 MS Calibration Data	
Concentration (ppm)	**MS Signal**
0	1.70E-07
1842	2.21E-07
3684	2.70E-07
5527	3.30E-07
7369	3.70E-07
9211	4.20E-07

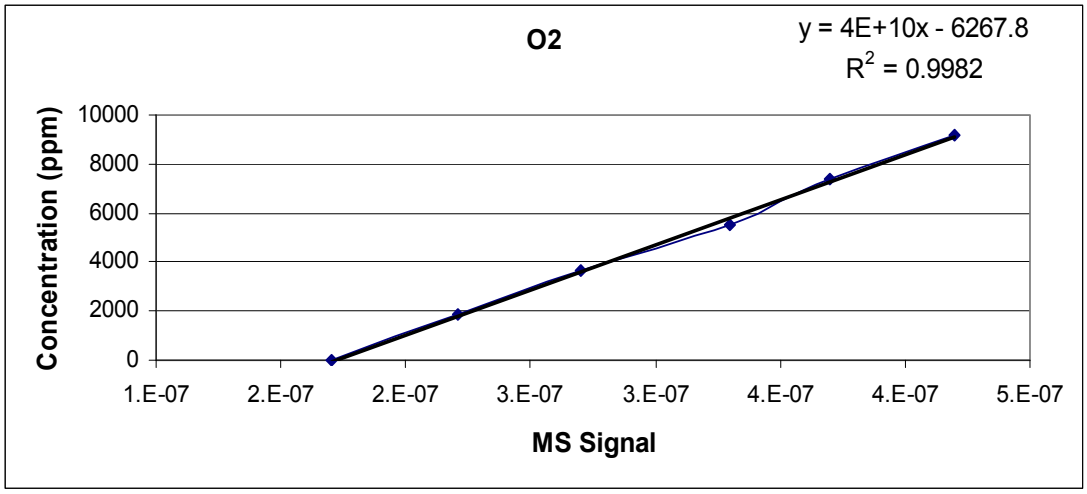

Figure C.2. 1 O_2 MS Calibration Graph

Table C.2. 2 NO MS Calibration Data

NO MS Calibration Data	
Concentration (ppm)	**MS Signal**
0	2.78E-08
360	3.82E-08
720	5.14E-08
1080	6.48E-08
1440	7.80E-08
1800	9.13E-08

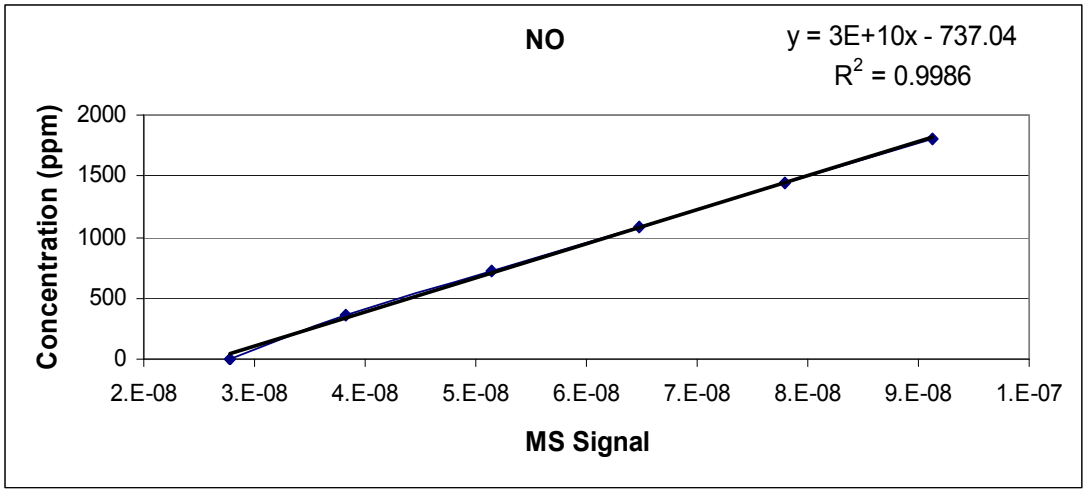

Figure C.2.2 NO MS Calibration Graph

Table C.2. 3 C_3H_6 MS Calibration Data

C_3H_6 MS Calibration Data	
Concentration (ppm)	**MS Signal**
0	1.37E-10
24024	3.94E-09
48047	7.47E-09
72071	1.09E-08
96094	1.42E-08
120118	1.72E-08

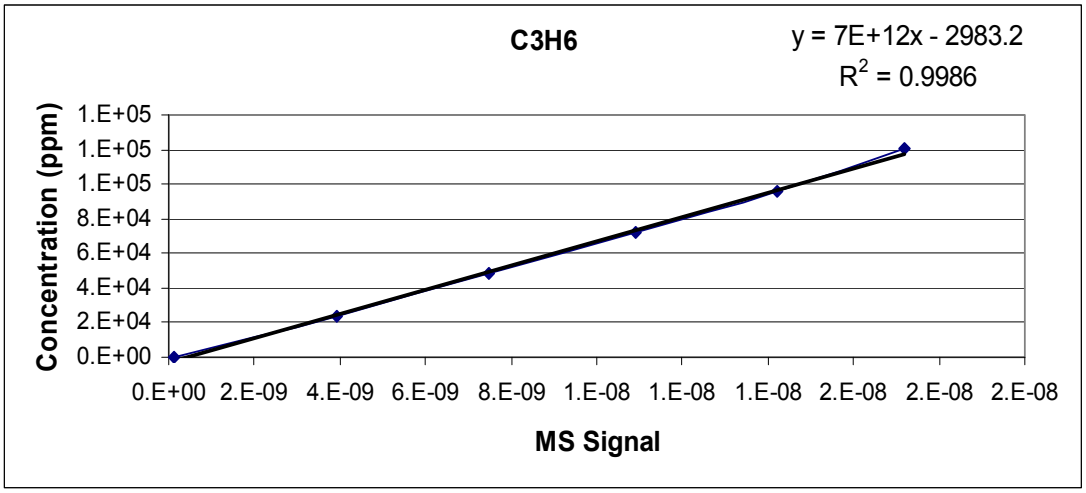

Figure C.2. 3 C_3H_6 MS Calibration Graph

Table C.2. 4 C_3H_8 MS Calibration Data

C_3H_8 MS Calibration Data	
Concentration (ppm)	**MS Signal**
0	2.21E-09
24024	4.17E-09
48047	6.00E-09
72071	8.16E-09
96094	1.01E-08
120118	1.20E-08

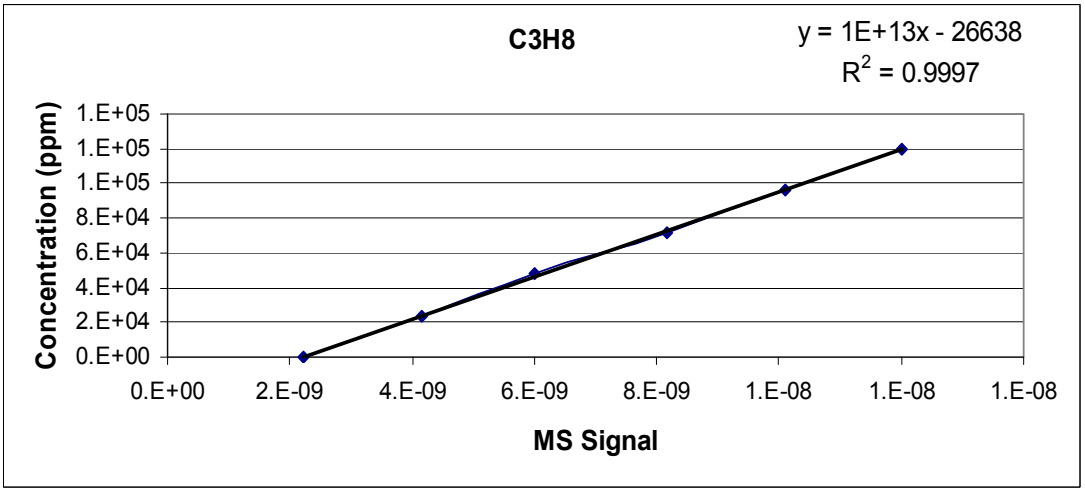

Figure C.2. 4 C_3H_8 MS Calibration Graph

Table C.2. 5 H_2 MS Calibration Data

H_2 MS Calibration Data	
Concentration (ppm)	**MS Signal**
0	2.44E-09
24024	1.23E-08
48047	2.20E-08
72071	3.13E-08
96094	3.98E-08
120118	4.85E-08

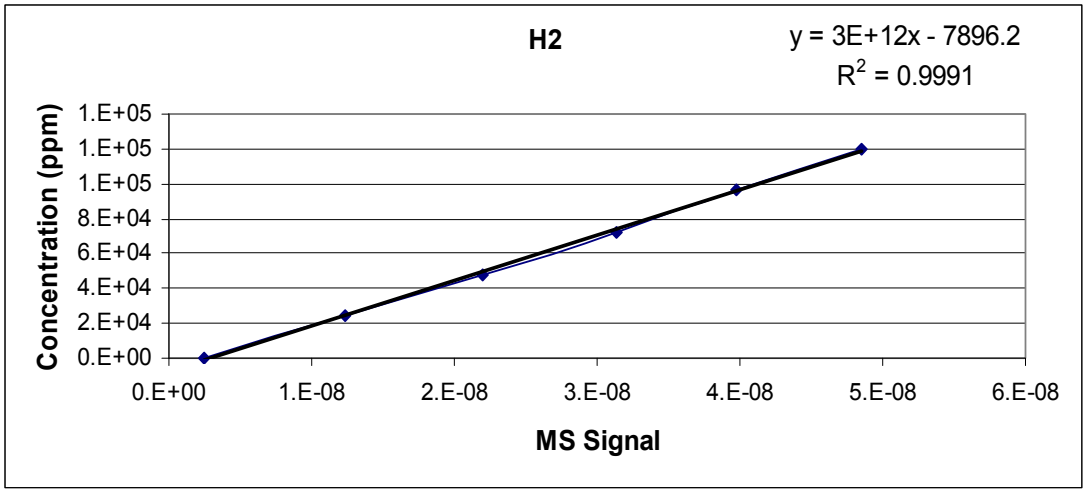

Figure C.2. 5 H_2 MS Calibration Graph

Table C.2. 6 Calibration Equations for MS Calibration

Species	**Calibration Equation**
O_2	4E+10x – 6267.8
NO	3E+10x – 737.04
C3H6	7E+12x – 2983.2
C3H8	1E+13x – 26638
H2	3E+12x – 7896.2

APPENDIX D

CATALYTIC ACTIVITY TEST RESULTS

D.1 Catalytic Activity Tests Without SO2, Research Monolithic Catalyst

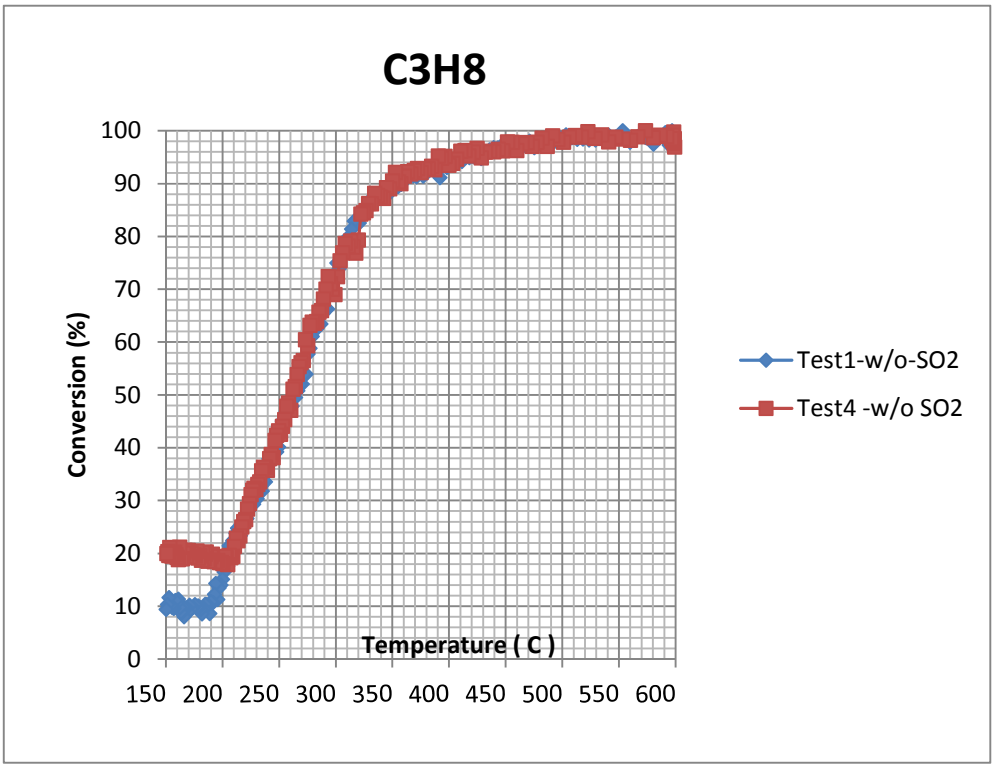

Figure D.1.1 C_3H_8 Catalytic Activity of Research Monolithic Catalyst During Tests 1 & 4

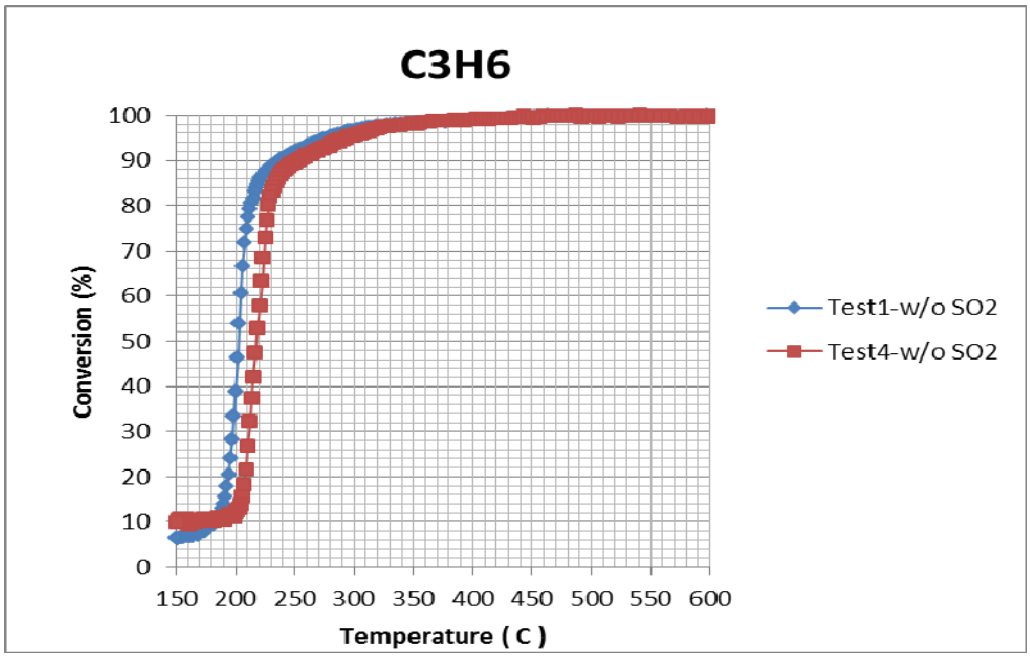

Figure D.1. 2 C_3H_6 Catalytic Activity of Research Monolithic Catalyst During Tests 1 & 4

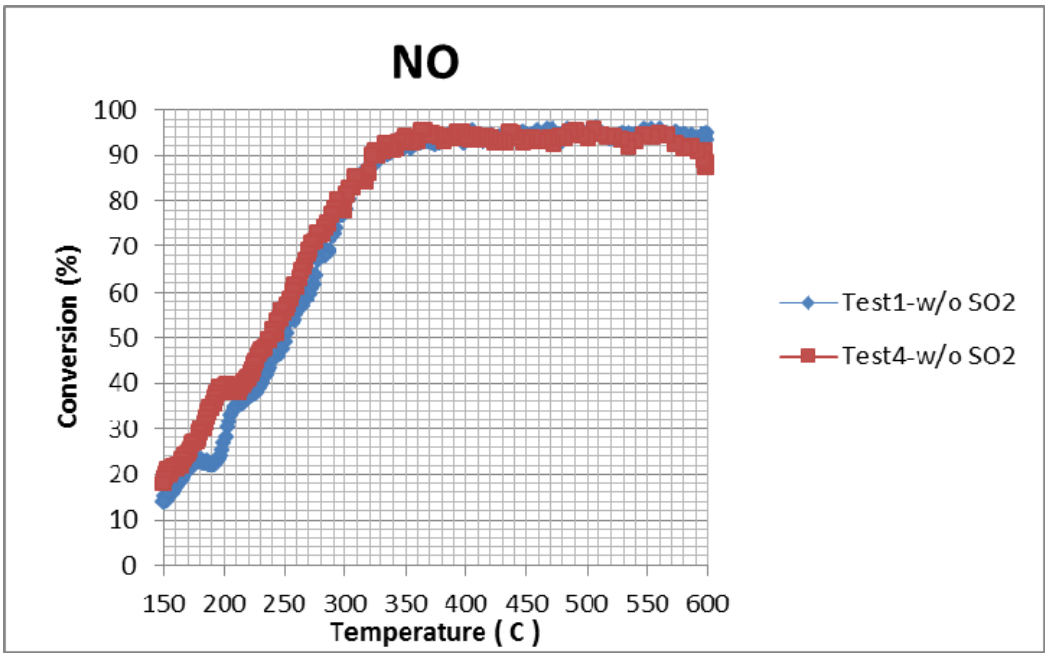

Figure D.1. 3 NO Catalytic Activity of Research Monolithic Catalyst During Tests 1 & 4

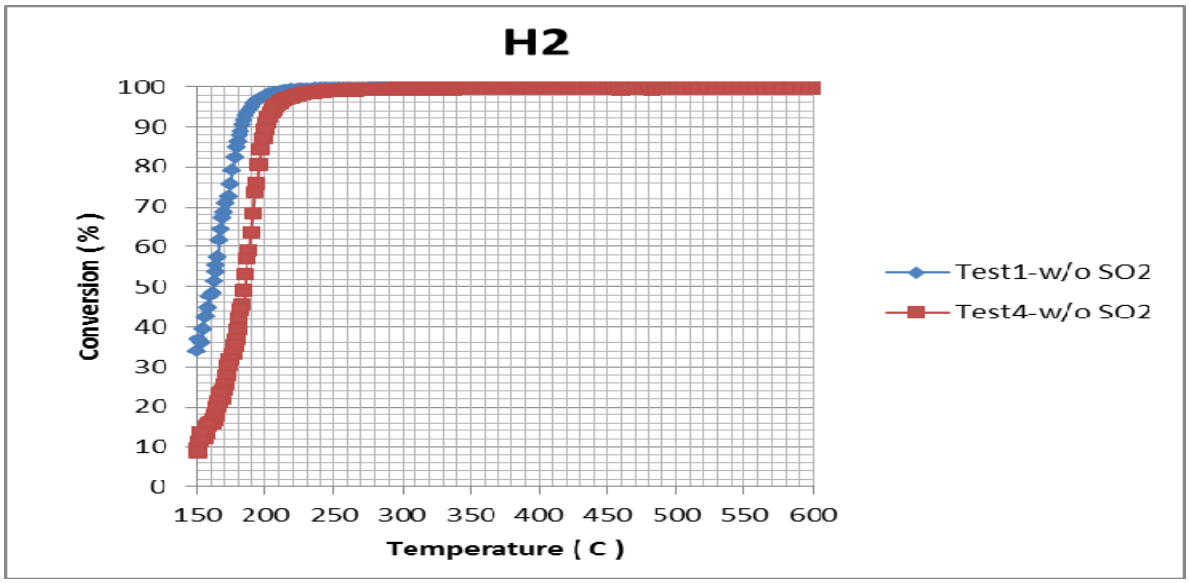

Figure D.1. 4 H_2 Catalytic Activity of Research Monolithic Catalyst During Tests 1 & 4

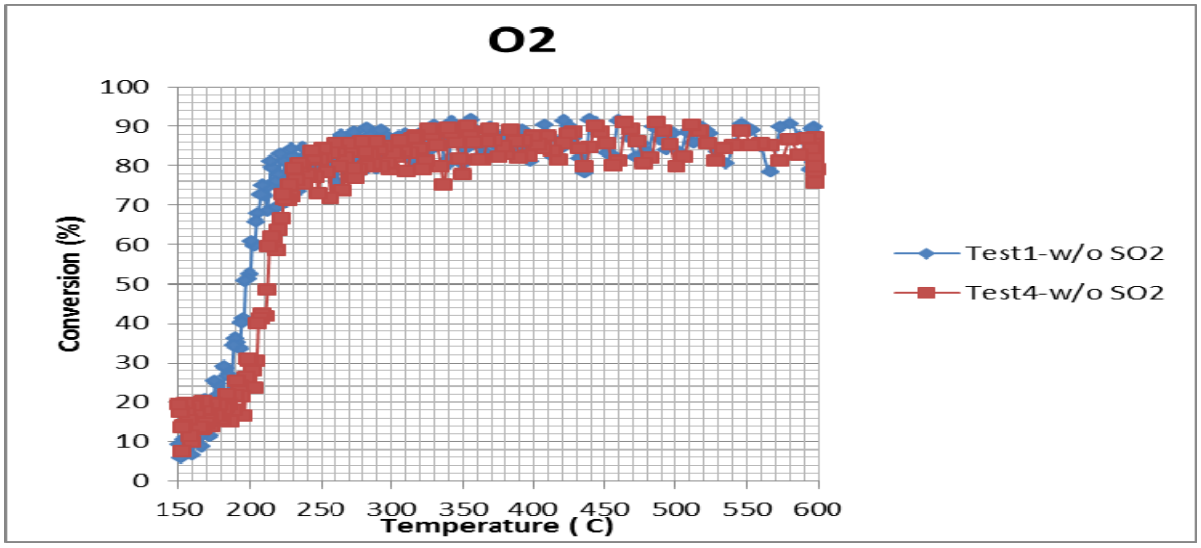

Figure D.1. 5 O_2 Catalytic Activity of Research Monolithic Catalyst During Tests 1 & 4

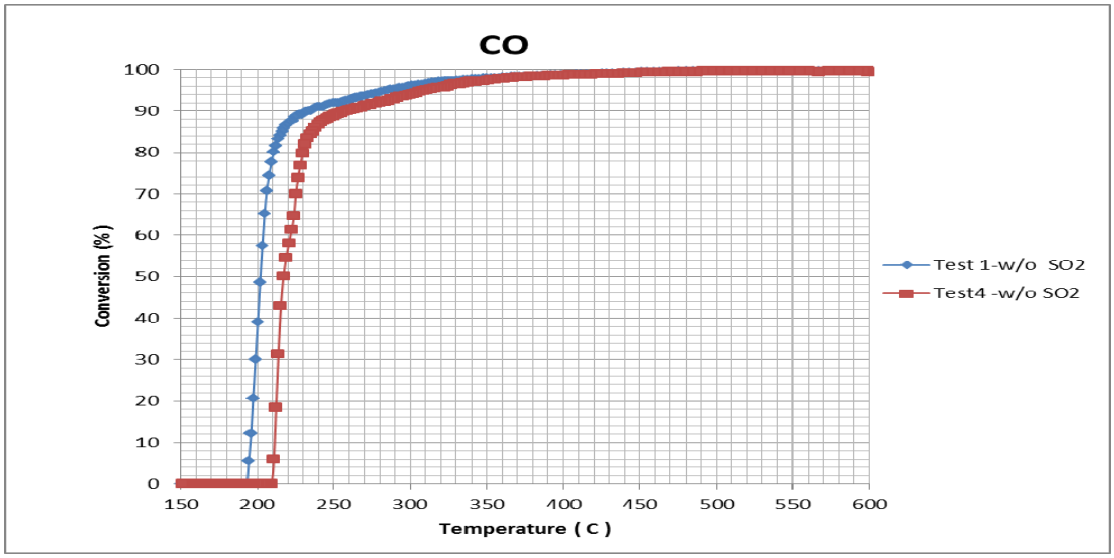

Figure D.1. 6 CO Catalytic Activity of Research Monolithic Catalyst During Tests 1 & 4

D.2 Catalytic Activity Tests With SO2, Research Monolithic Catalyst

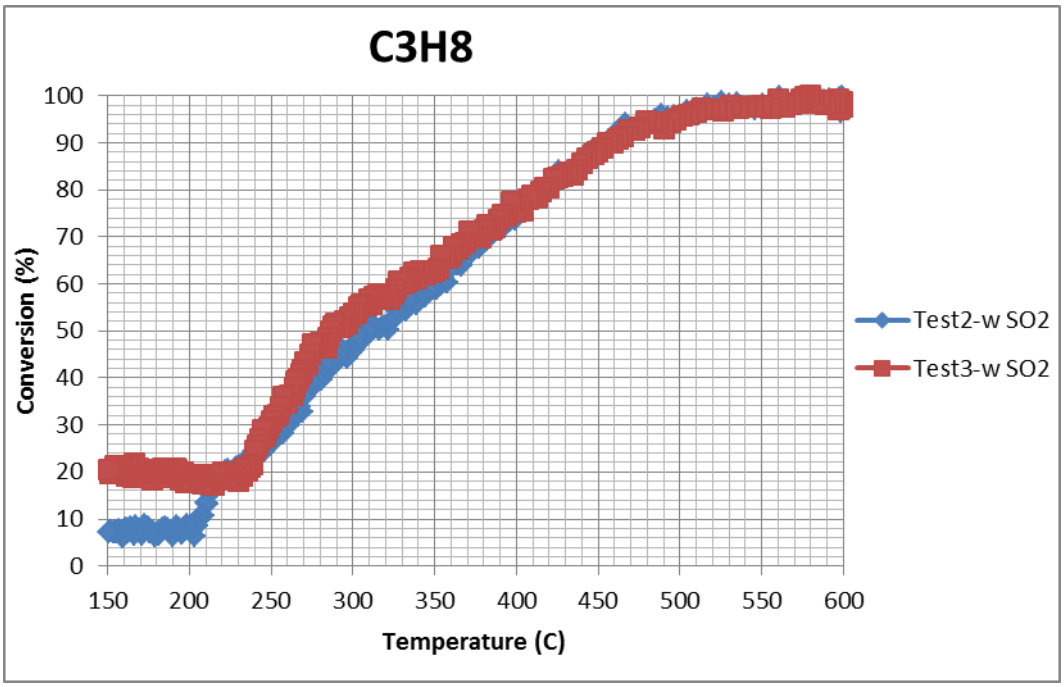

Figure D.2. 1 C_3H_8 Catalytic Activity of Research Monolithic Catalyst During Tests 2 & 3

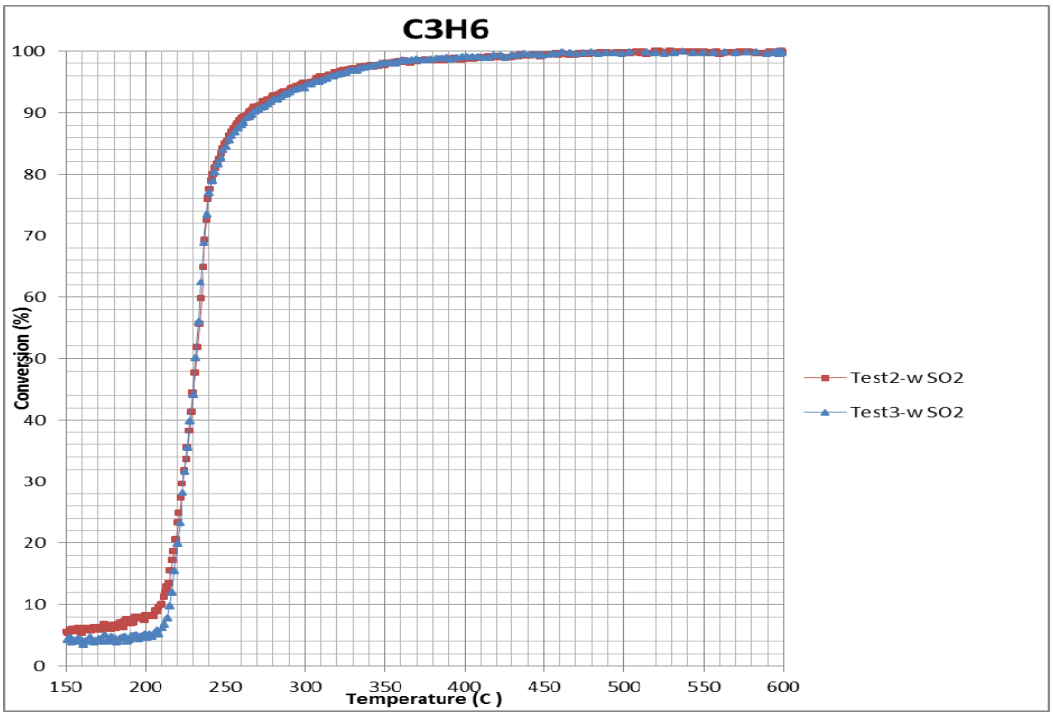

Figure D.2. 2 C_3H_6 Catalytic Activity of Research Monolithic Catalyst During Tests 2 & 3

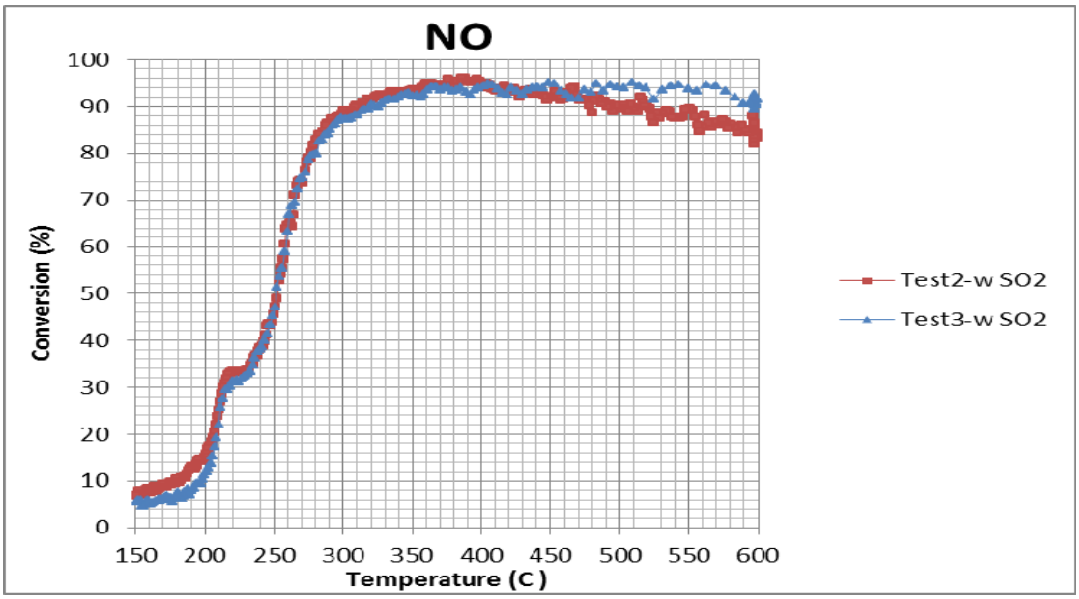

Figure D.2. 3 NO Catalytic Activity of Research Monolithic Catalyst During Tests 2 & 3

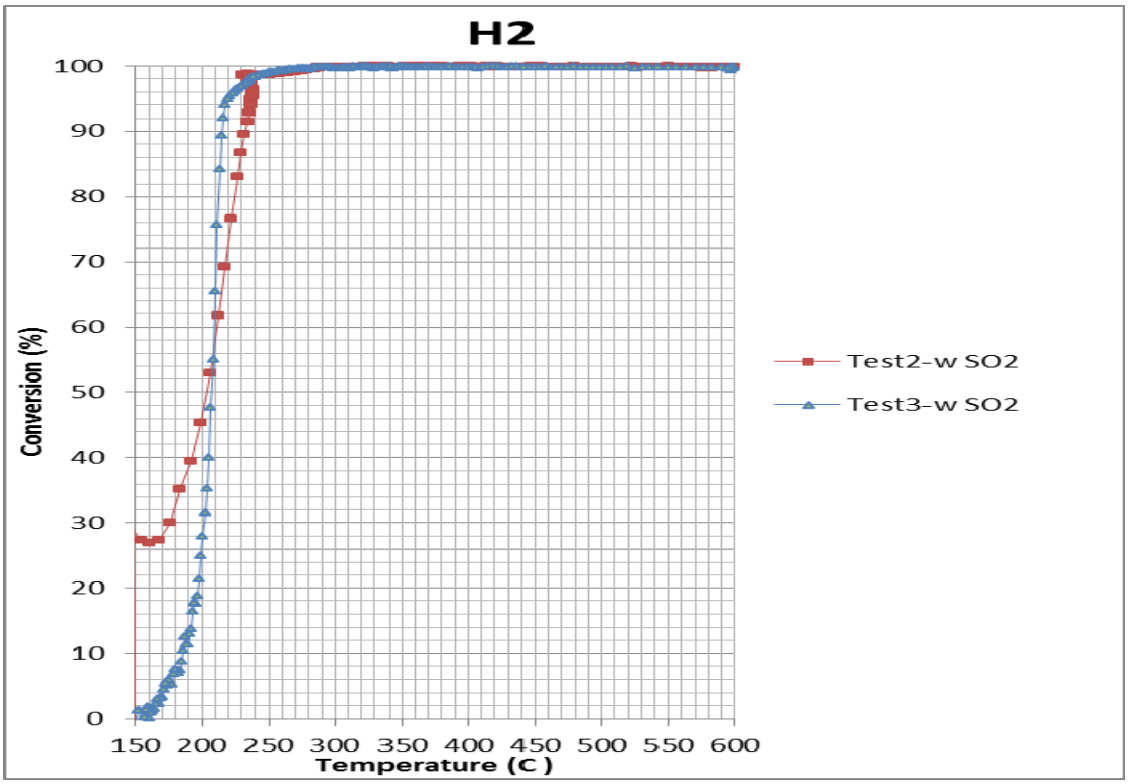

Figure D.2. 4 H_2 Catalytic Activity of Research Monolithic Catalyst During Tests 2 & 3

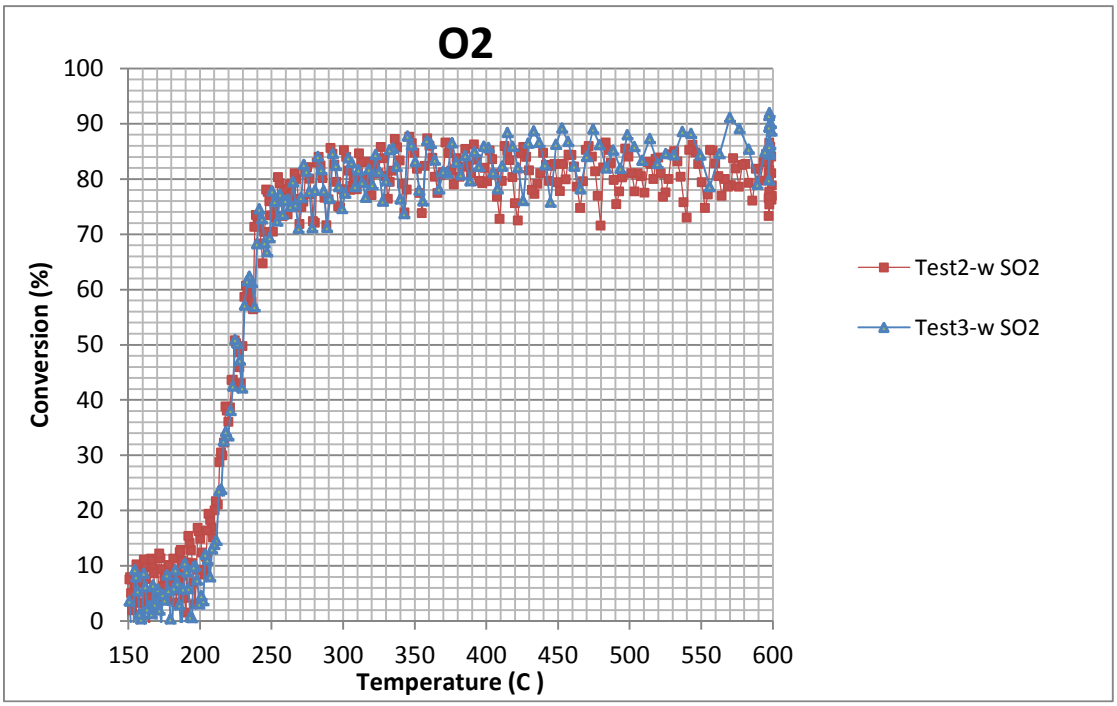

Figure D.2. 5 O_2 Catalytic Activity of Research Monolithic Catalyst During Tests 2 & 3

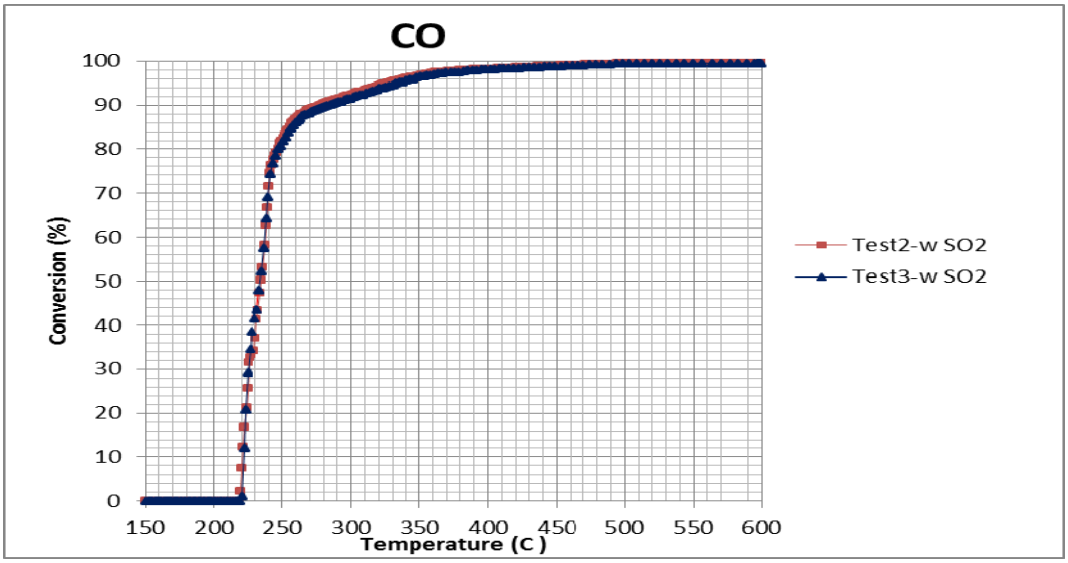

Figure D.2. 6 CO Catalytic Activity of Research Monolithic Catalyst During Tests 2 & 3

D.3 Catalytic Activity Tests Without SO2, Tofas Commercial Monolithic Catalyst

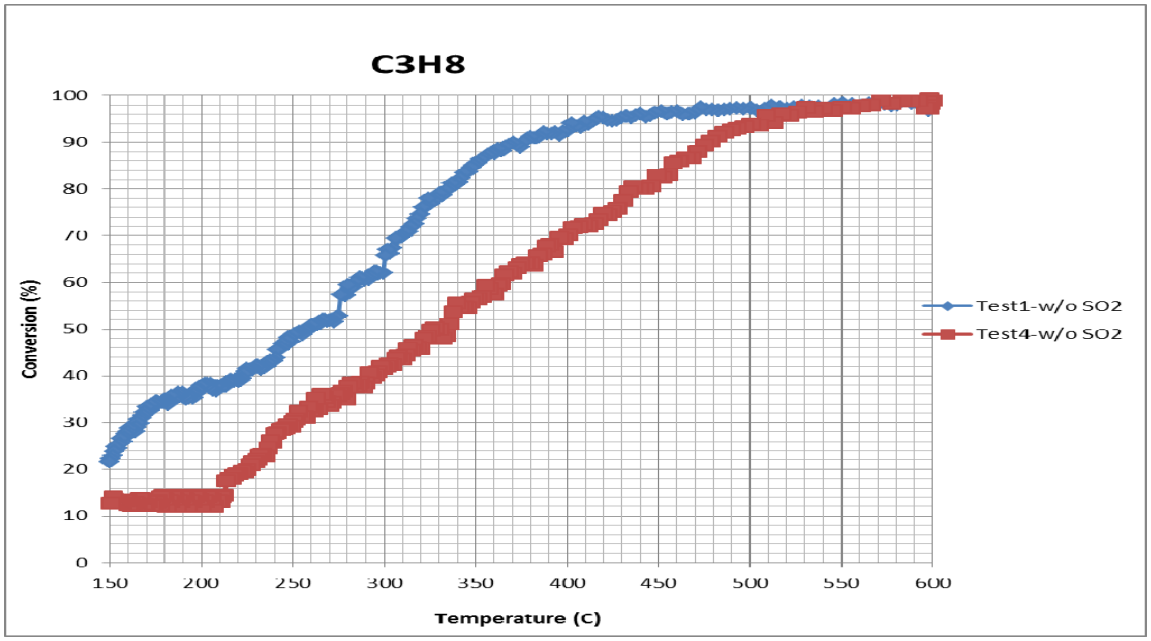

Figure D.3. 1 C_3H_8 Catalytic Activity of Tofas COM Monolithic Catalyst During Tests 1 & 4

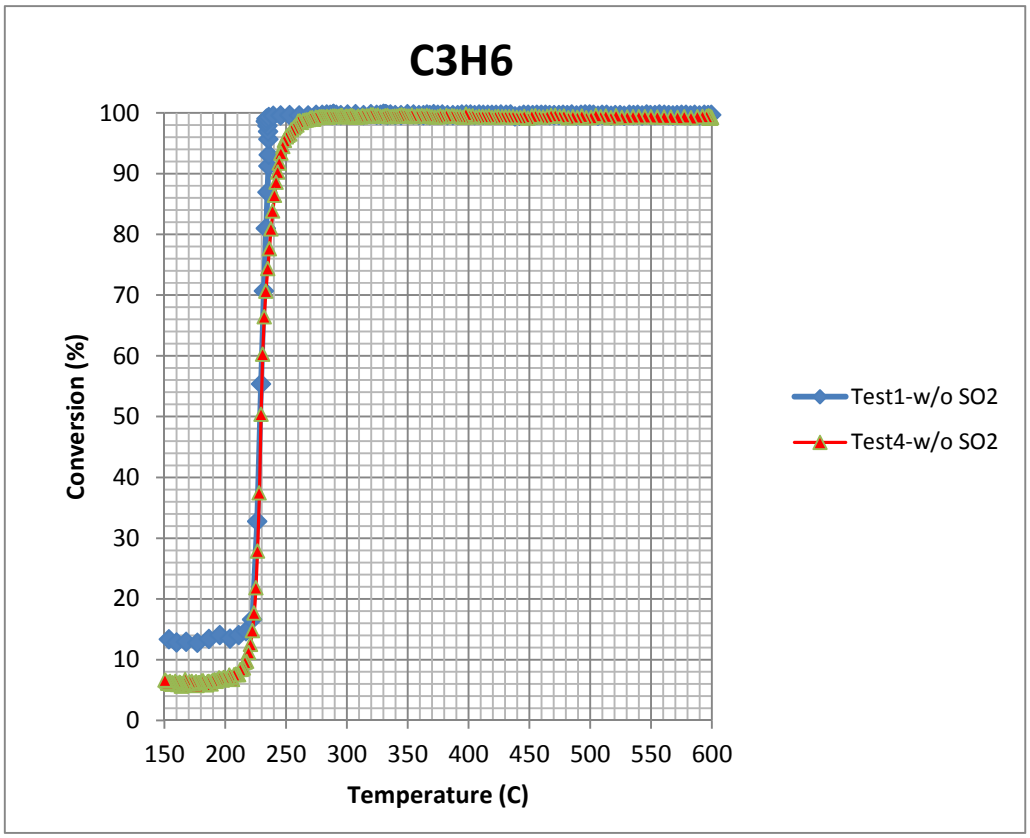

Figure D.3. 2 C_3H_6 Catalytic Activity of Tofas COM Monolithic Catalyst During Tests 1 & 4

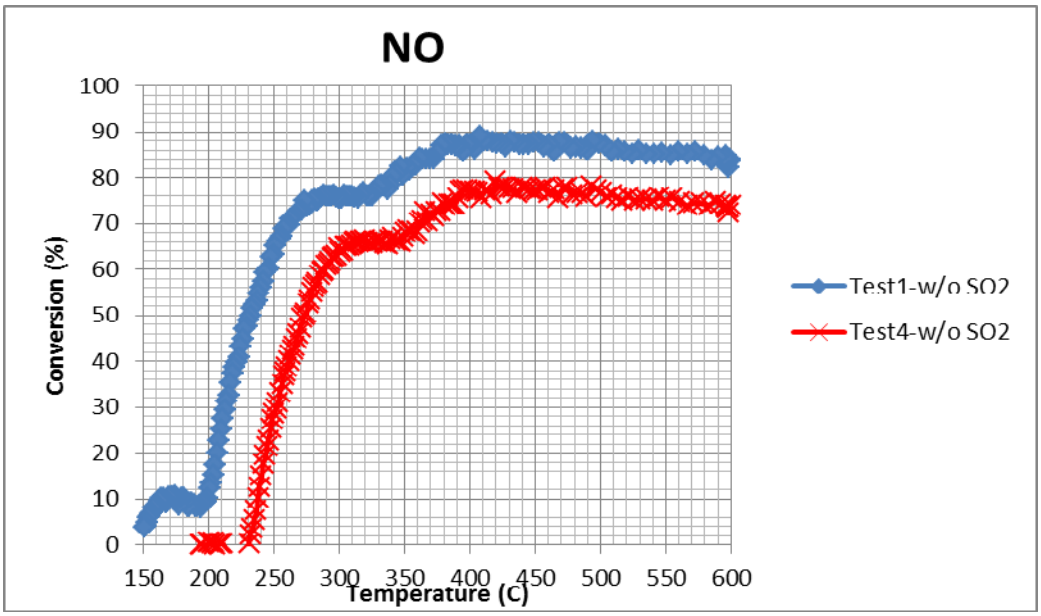

Figure D.3. 3 NO Catalytic Activity of Tofas COM Monolithic Catalyst During Tests 1 & 4

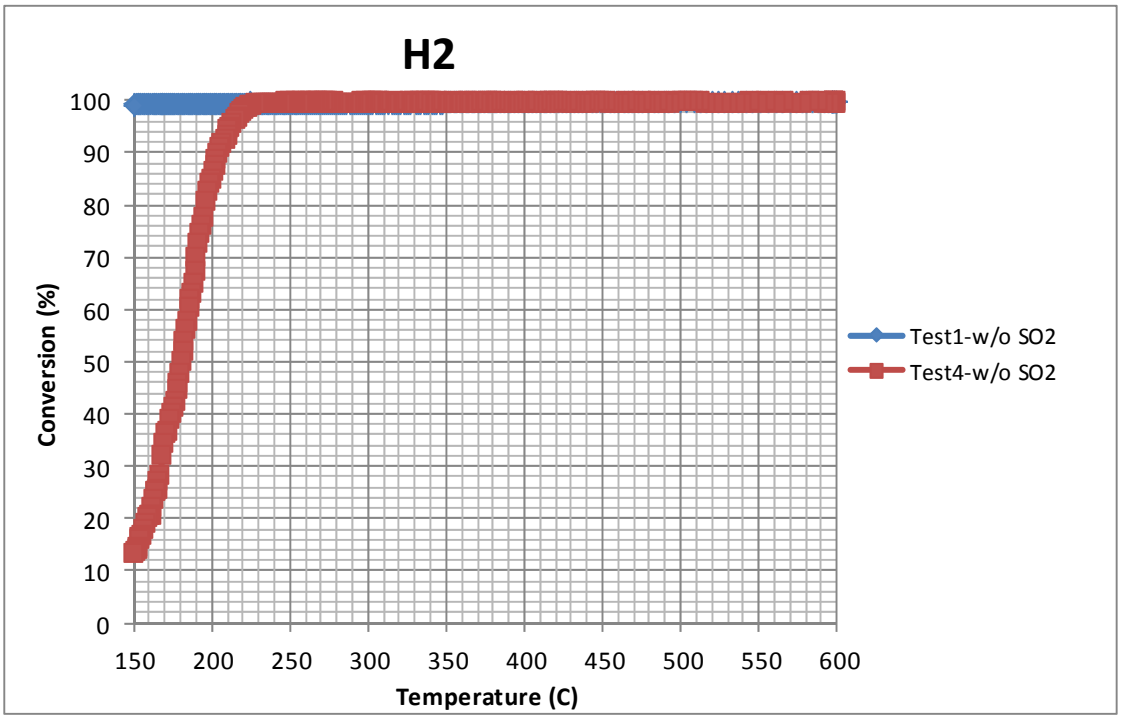

Figure D.3. 4 H_2 Catalytic Activity of Tofas COM Monolithic Catalyst During Tests 1 & 4

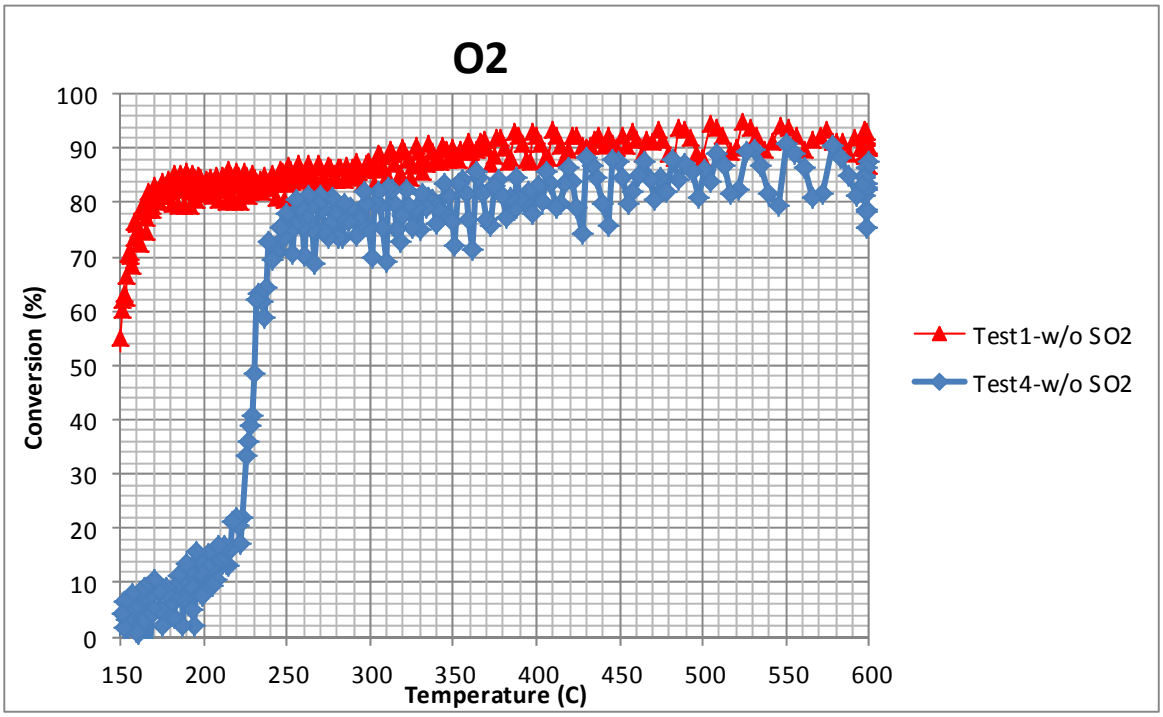

Figure D.3. 5 O_2 Catalytic Activity of Tofas COM Monolithic Catalyst During Tests 1 & 4

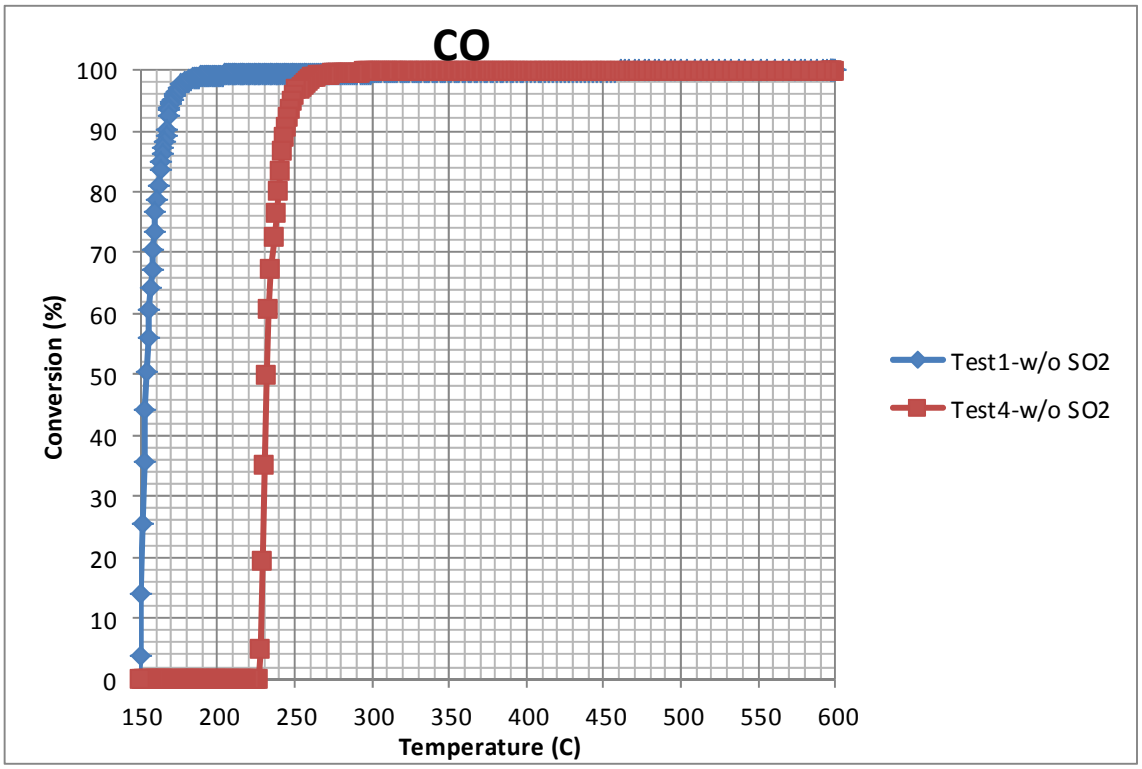

Figure D.3. 6 CO Catalytic Activity of Tofas COM Monolithic Catalyst During Tests 1 & 4

D.4 Catalytic Activity Tests With SO2, Tofas Commercial Monolithic Catalyst

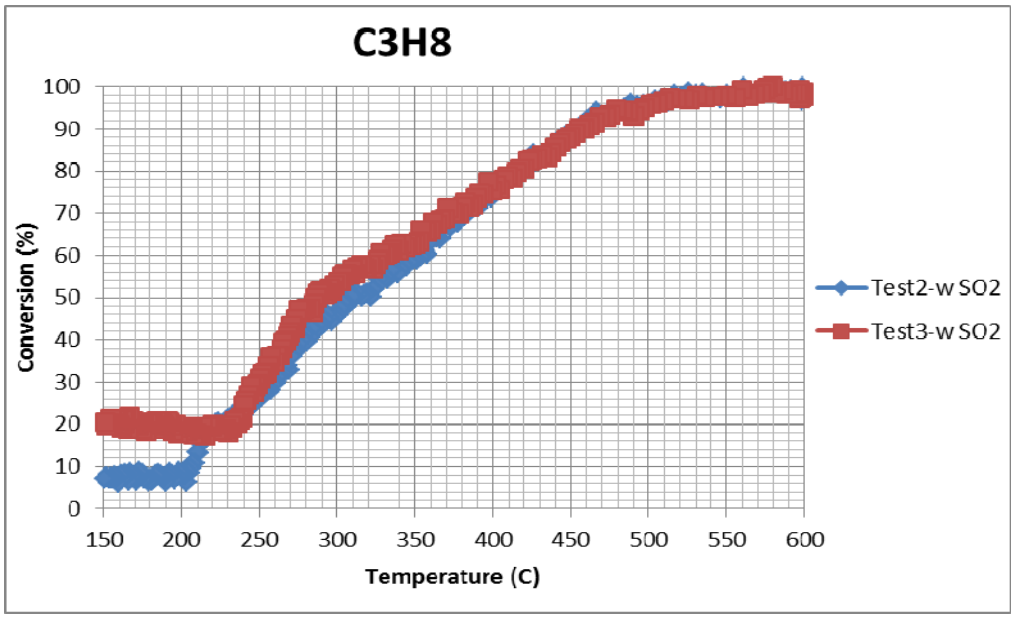

Figure D.4. 1 C_3H_8 Catalytic Activity of Tofas COM Monolithic Catalyst During Tests 2 & 3

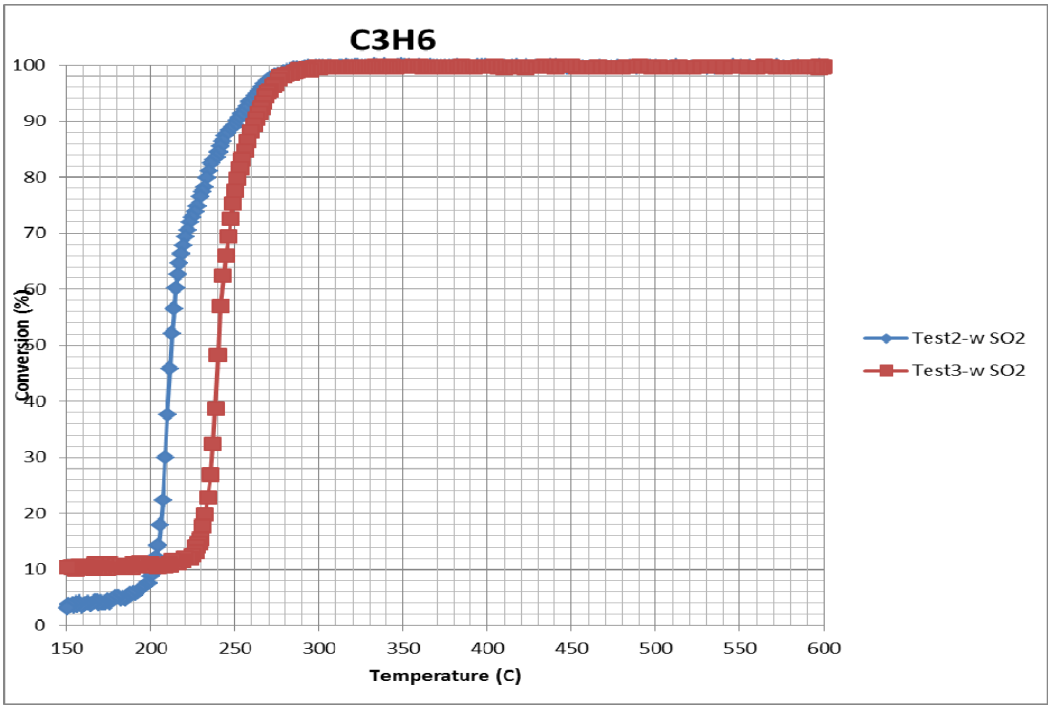

Figure D.4. 2 C_3H_6 Catalytic Activity of Tofas COM Monolithic Catalyst During Tests 2 & 3

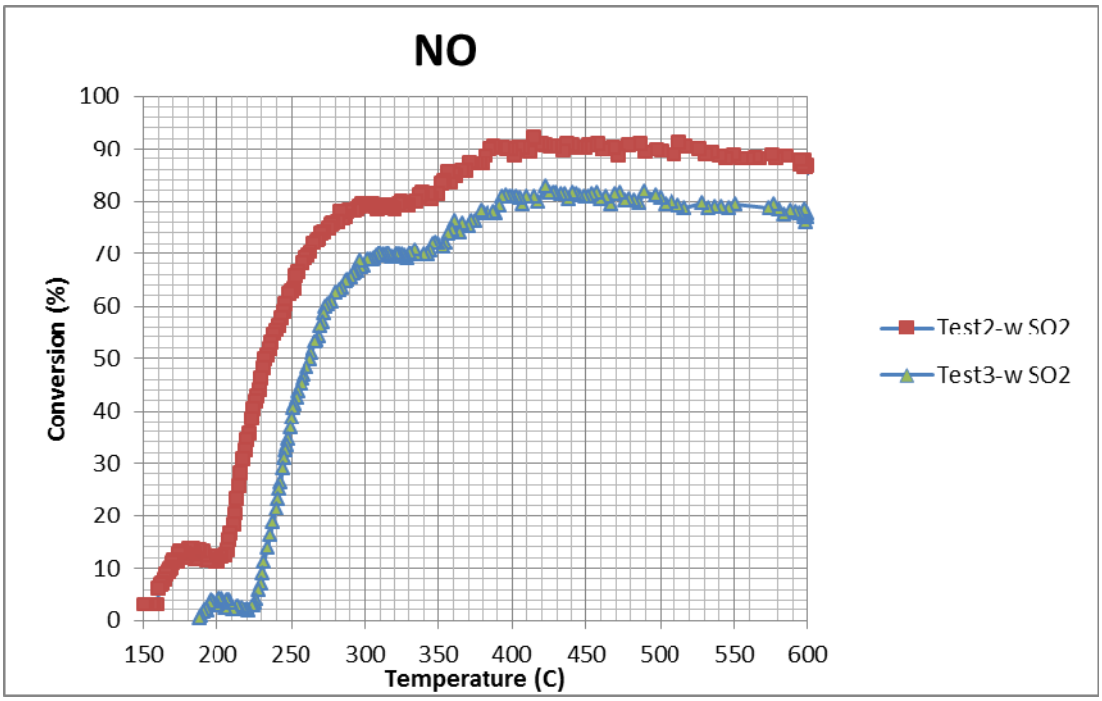

Figure D.4. 3 NO Catalytic Activity of Tofas COM Monolithic Catalyst During Tests 2 & 3

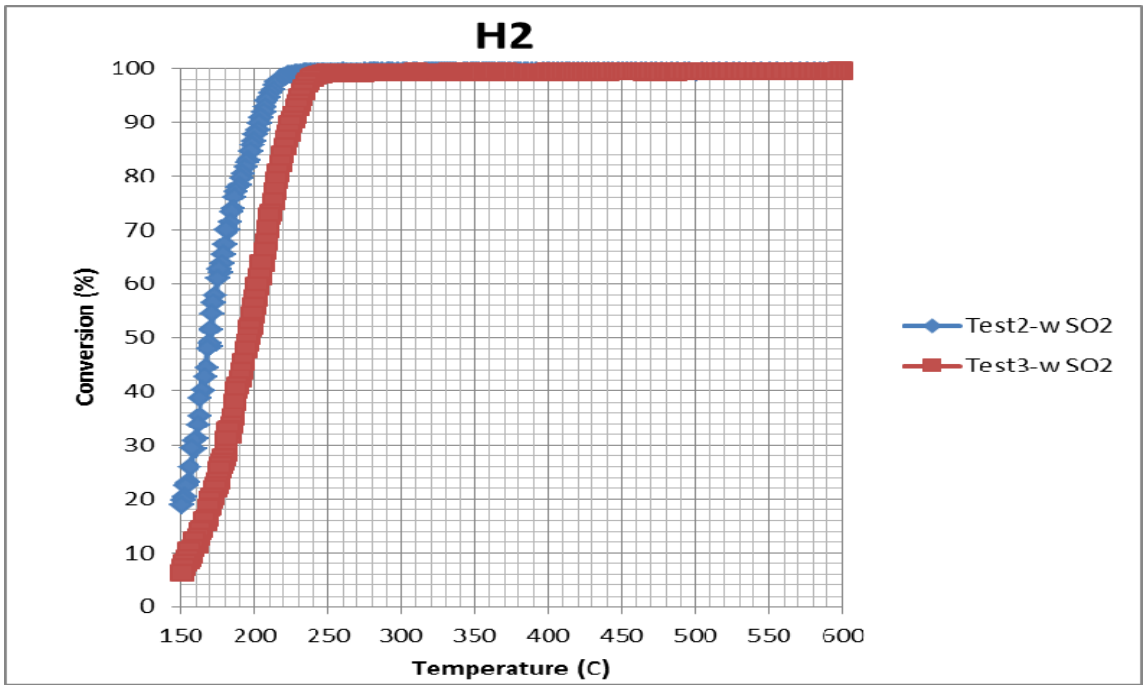

Figure D.4. 4 H_2 Catalytic Activity of Tofas COM Monolithic Catalyst During Tests 2 & 3

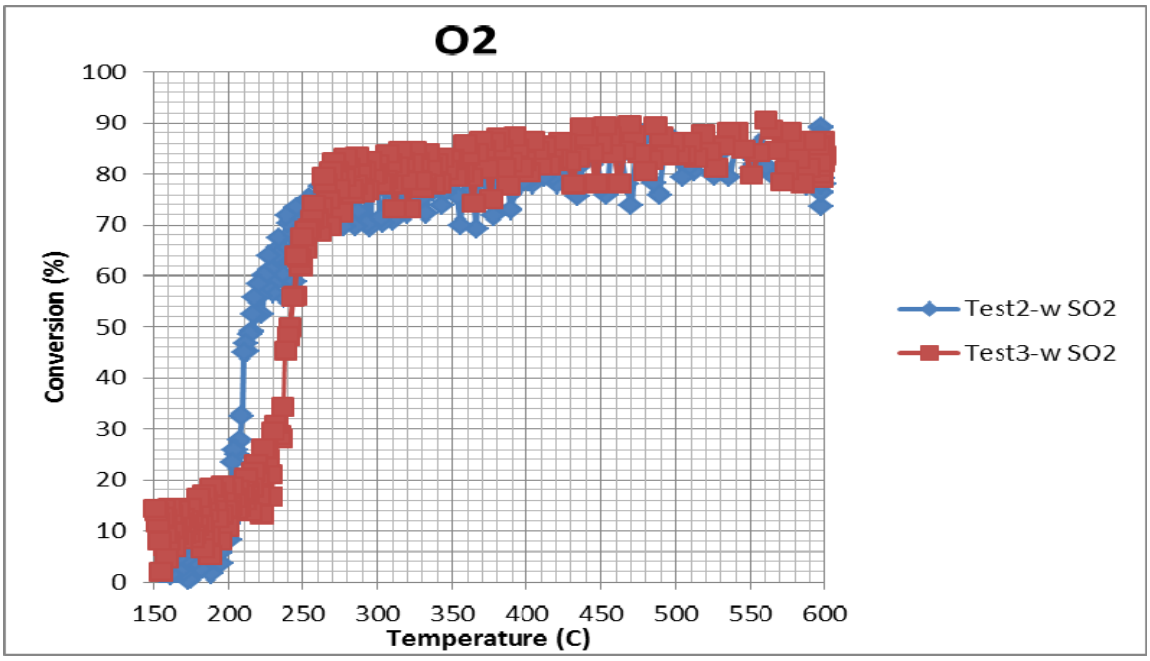

Figure D.4. 5 O_2 Catalytic Activity of Tofas COM Monolithic Catalyst During Tests 2 & 3

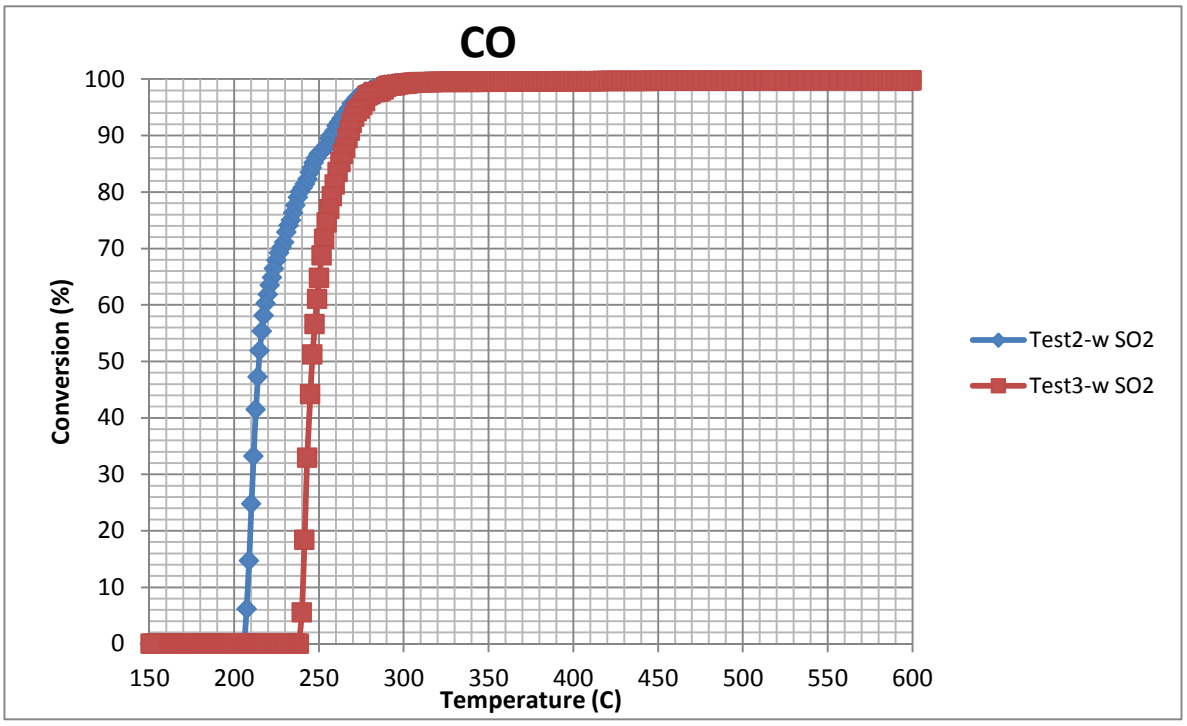

Figure D.4. 6 CO Catalytic Activity of Tofas COM Monolithic Catalyst During Tests 2 & 3

APPENDIX E

ESTIMATION OF PARTICLE SIZE AND XRD DIFFRACTOGRAMS

E.1 Particle Size

For the X-ray particles Scherrer Equation is used to determine size (Equation E.1) (Cullity & Stock, 2001).

$$t = \frac{0.9\ \lambda}{B\cos(\theta_B)} \qquad \text{(E.1)}$$

Where,
t : particle size,
λ : wavelength in nm,
B : full width of the peak at half of maximum Bragg peak in radians,
θ_B : Bragg angle

For the wavelength of the Cu Kα X-ray is 0.154 nm

B = 1.46º and $2\theta_B$ = 29.39º

$$B = 1.46° = 1.46° \times \frac{\pi}{360} = 0.0126\,radians$$

$$2\theta_B = 29.39°$$

$$\theta_B = 14.695°$$

$$t = \frac{(0.90) \times (0.154\,nm)}{(0.0126) \times \left|\cos(14.695)\right|} = 17\,nm$$

E.2 XRD Diffractograms of Fresh Powdered Slurries of Catalysts

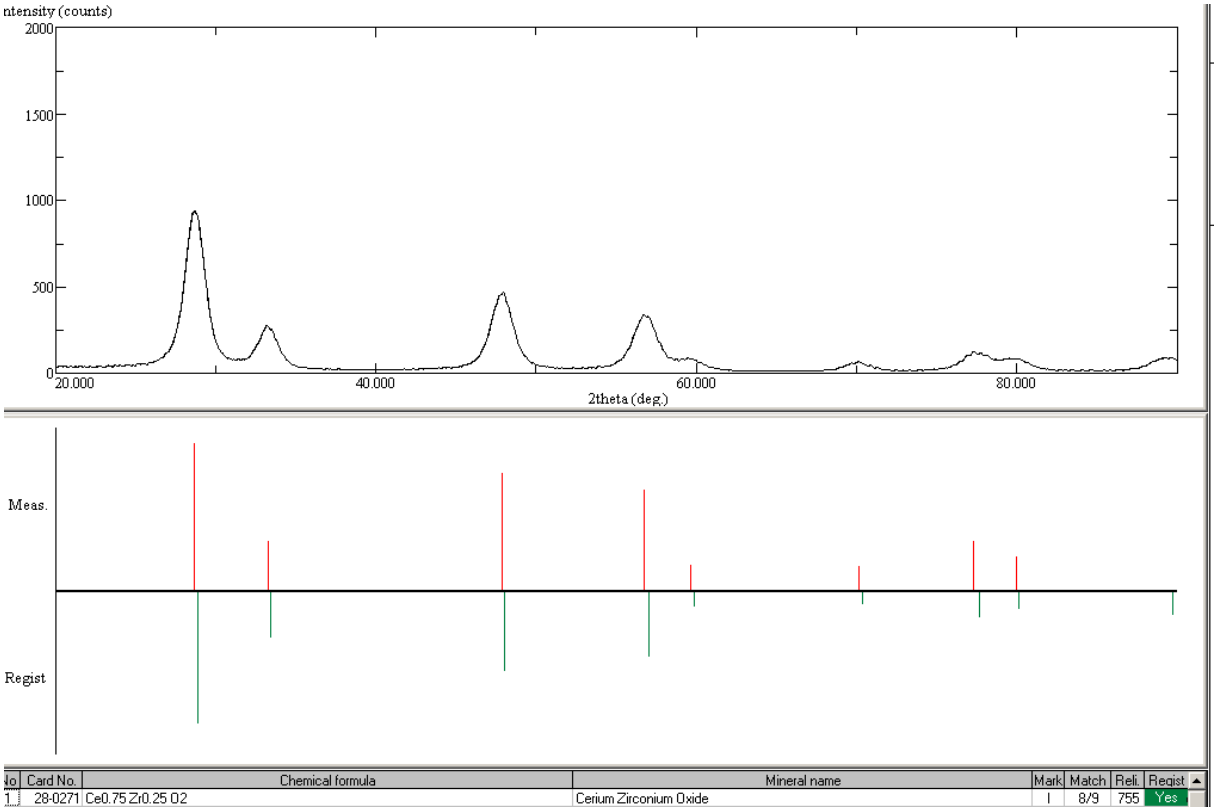

Figure E.2. 1 XRD Diffractograms of (CZO-SI) / (AO-SI) Monolithic Catalyst

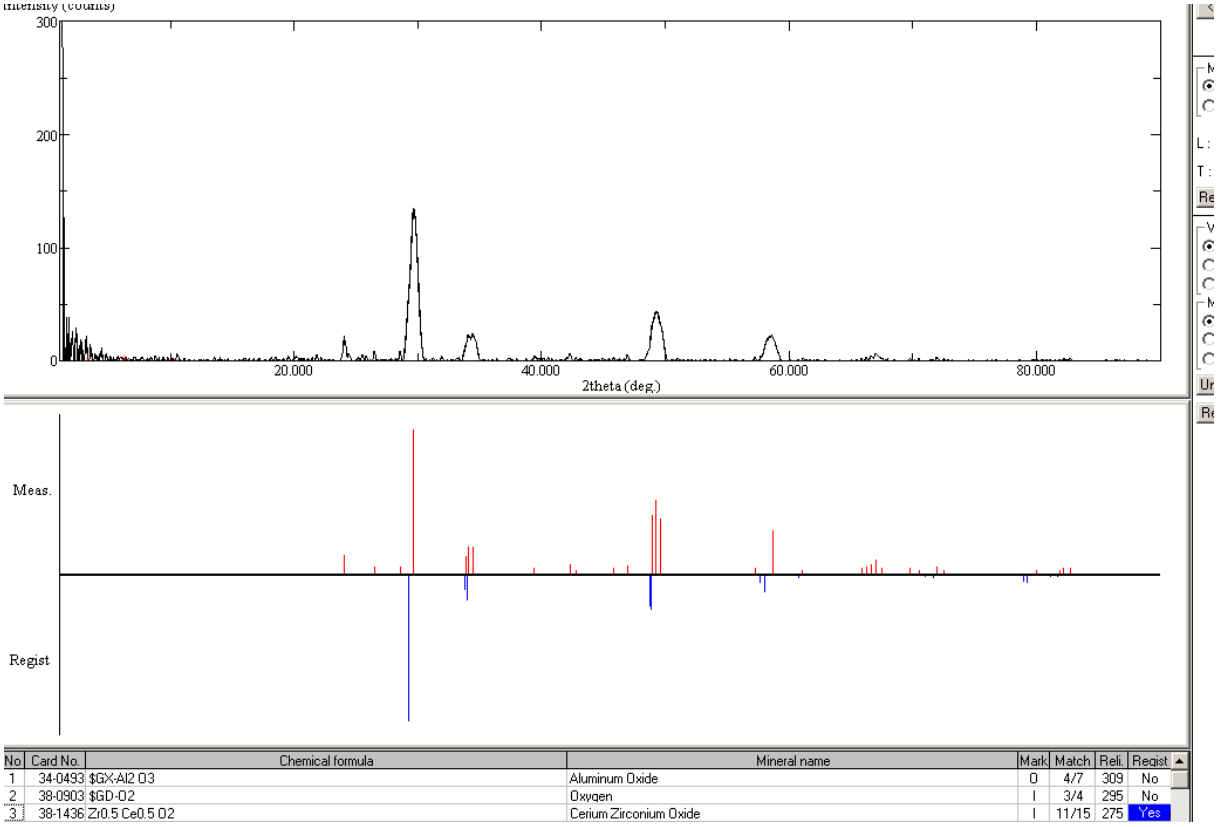

No	Card No.	Chemical formula	Mineral name	Mark	Match	Reli.	Regist
1	34-0493	$GX-Al2 O3	Aluminum Oxide	O	4/7	309	No
2	38-0903	$GD-O2	Oxygen	I	3/4	295	No
3	38-1436	Zr0.5 Ce0.5 O2	Cerium Zirconium Oxide	I	11/15	275	Yes

Figure E.2. 2 XRD Diffractogram of Tofas Commercial Monolithic Catalyst